2012

Spatial distribution and modulation of nitric oxide synthase in a hypertensive rat model

Andrew Yannaccone
Virginia Commonwealth University

School of Medicine
Virginia Commonwealth University

This is to certify that the dissertation prepared by Andrew T. Yannaccone entitled SPATIAL DISTRIBUTION AND MODULATION OF NITRIC OXIDE SYNTHASE IN A HYPERTENSIVE RAT MODEL has been approved by his or her committee as satisfactory completion of the dissertation requirement for the degree of Doctor of Philosophy.

Dr. Roland N. Pittman; VCU School of Medicine

Dr. Sheryl Finucane; VCU School of Allied Health Professions

Dr. Rakesh C. Kukreja; VCU School of Medicine

Dr. Paul H. Ratz; VCU School of Medicine

Dr. Mary S. Shall; VCU School of Allied Health Professions

Dr. Diomedes E. Logothetis; Chair, Department of Physiology & Biophysics, VCU School of Medicine

Dr. Jerome F. Strauss III; Dean, VCU School of Medicine

Dr. F. Douglas Boudinot, Dean of the Graduate School

February 6, 2012

SPATIAL DISTRIBUTION AND MODULATION OF NITRIC OXIDE SYNTHASE

IN A HYPERTENSIVE RAT MODEL

A dissertation submitted in partial fulfillment of the requirements for the degree of Doctor of Philosophy at Virginia Commonwealth University.

by

ANDREW T. YANNACCONE
BS, Health Science, Misericorida University, 2002
MSPT, Physical Therapy, Misericordia University, 2002

Director: DR. ROLAND N. PITTMAN
PROFESSOR
DEPARTMENT OF PHYSIOLOGY & BIOPHYSICS

Virginia Commonwealth University
Richmond, Virginia

February 2012

Acknowledgement

Any doctoral student would (and should!) agree that the journey to a PhD is seldom, if ever, one the student makes alone. Indeed, I would not be where I am today were it not for the tireless love, support and encouragement of my friends, family, professional peers and colleagues. Truth be told, words alone cannot express the depth of my gratitude. Fortunately, I share a connection with many of these wonderful individuals that goes beyond words. To all of you I offer a deeply heartfelt and sincere "Thank you"!

I will now endeavor to list many of those that made this unforgettable journey with me by name. First and foremost, I would like to acknowledge and thank my advisor, Dr. Roland N. Pittman, whose gentle humor, patience, generosity and devotion to the science of physiology made my experience in his laboratory unforgettable and a sincere pleasure; my parents Tom and Kay; my sister Adria; my grandparents Donald, Robert, Dorothy and Virginia; my little angel Junebug; all of my aunts, uncles, cousins and other extended family members (I love you all!); my better half Kevin Norfleet and family; steadfast and patient friends, both old and new and in no particular order, including Dr. Melissa Bednarek, Dr. Janine Firmender and family, Olivia Cornell, Gabriel Mullins, Connie Quinn, Christine Luhrs German, Jason Tuminski, Chris Scarba, Jason Polovchik, Ken Nguyen, David Measel, Jason and Kirsten (Peterson) Ditzler, Sharon Schroeder and family, Dr. Bill and Mrs. Janet Baedke, Diane Souders Martin, Dr. Michael and Mr. Robert Tian, Ann Maddox, Marshall Vogt, Dominique Sautron, James

Spencer, Amanda Claggett, Michael Ny, Dr. Danny Jaek, Matt Hupp, Alex Bonilla, Donnie Page, Allison Behm Pugh, Amy Hyser Mundis, Robert and Andrea Criswell, Austin Ratliff, Ryan White, Avanti Kollaram, Chris Corday, Chris Davis, Darrell Coffey, Field Sexton, Phoebe Dacha, Frank Kosnosky Jr., Jenny McNamara, Dr. Kelly Stinelli Lindenberg, Charlie and Kristen (Chaffins) Kelly, Laura Evelyn Spafford, Tom Winn, Mary Kay and Alex Vasold, Amanda McGuire, Michelle Bailey and family, Kristin Simmons, Mary Alice Lachman, Matt and Paulann Buczek, Michelle Pfeiffer, Miranda Walker, Norma Briggs Bear, Patricia Brameld Genet, Preston Davis, Quang Nguyen, Dr. Sam Campbell, Sarah Rome, Steven Thai, Michael and Vanessa Anderson and Dr. Will Case.

I would like to thank my physical therapy professional peers, both past and present, including (but not limited to) Mark Bouziane, the entire rehabilitation services team at Retreat Doctors' Hospital and the entire rehabilitation staff at Lancaster General Hospital (2003-2006). I owe a special "thank you" to Dr. Dixie Bowman – my experience in your classroom re-affirmed my love for teaching the art and science of physical therapy.

There are current and past members of the Pittman lab that deserve special mention for their significant contributions to the success of my project. Dr. Bjorn Song: your surgical skills are invaluable – thank you for sharing them with me. Dr. Helena Carvalho: I enjoyed our trip to New Orleans together, cancelled flights and all. Thank

you for all of the good conversation, encouragement and support! Dr. Alex Golub: thank you for your frank, thoughtful and very helpful comments on my project through the years. Dr. Matt Barker: thank you for the support and helping me settle into the lab. Sirish Nama, Hiyab Yohannes, Jessica Webb and Heather Hammond: I hope I was able to offer some tidbits of "graduate student wisdom" to all of you. Best of luck in your future endeavors.

My dissertation committee, comprised of talented faculty from the Schools of Medicine and Allied Health, provided me with guidance, assistance and inspiration, without which I would not be where I am today. My heartfelt gratitude to Dr. Rakesh Kukreja and his entire lab, with special thanks to Dave Durrant and Dr. Anindita Das; Dr. Paul Ratz and his talented lab manager (and my friend) Amy S. Miner; Dr. Mary Shall: many, many thanks for allowing me to use your equipment and for the many hours you spent patiently instructing me in the techniques at which you are so adept; and Dr. Sheryl Finucane, to which I owe a huge debt of gratitude for your guidance and suggestions for sources of extramural funding and physical therapy faculty positions.

Finally, there are several members of the Department of Physiology & Biophysics, the School of Medicine and the Virginia Commonwealth University community at large that I would like to thank, including: Dr. George Ford, Dr. Clive Baumgarten, Dr. John Povlishock and lab (especially John Greer), Debbie Bohn, Dr. Linda Costanzo, Dr. Diomedes Logothetis, Christina Meliagros, Dr. Scott Henderson,

Natasha Purdie, Dr. Sid Ghosh and Sarah Reese. Finally, I would like to recognize Dr. Aleksander Popel at Johns Hopkins University for his thoughts on my project through the years.

Unfortunately, no matter how hard I try, I am certain I have neglected to include a few names in the above. Please accept my apologies as your contributions were just as valuable as those from the individuals mentioned above. And again: thank you to all!

Table of Contents

List of Tables

Page

List of Figures

Page

Abstract

SPATIAL DISTRIBUTION AND MODULATION OF NITRIC OXIDE SYNTHASE IN A HYPERTENSIVE RAT MODEL

By Andrew T. Yannaccone, P.T., Ph.D.

A dissertation submitted in partial fulfillment of the requirements for the degree of Doctor of Philosophy at Virginia Commonwealth University.

Virginia Commonwealth University, 2012

Major Director: Dr. Roland Pittman
Professor, Department of Physiology & Biophysics

There are gaps in the fundamental understanding of the expression of nitric oxide synthases (NOS) in the microvasculature. We examined co-localization of NOS1 (nNOS), NOS2 (iNOS) and NOS3 (eNOS) in the spinotrapezius muscle of young adult male Wistar-Kyoto (WKY) and Spontaneously Hypertensive (SHR) rats according to fiber type using immunohistochemistry and brightfield microscopy. Data regarding fiber distribution, population and morphology data were collected. Alkaline phosphatase staining was used to determine capillary density and average number of capillaries around

a fiber. Gel electrophoresis and Western blot techniques were used to compare myosin heavy chain (MHC) protein expression with fiber type population data and to determine NOS1-3 protein expression in whole muscle homogenate. This study should provide a more accurate understanding of differences in NOS expression between these two strains of rats.

INTRODUCTION

Overview: The relationship between nitric oxide (NO), the enzyme that produces it, nitric oxide synthase (NOS), and hypertension has been the subject of much recent research. There is a large volume of literature dealing with this very broad topic so this chapter will attempt to elucidate the current scientific understanding about the relationship between impaired NO production/bioavailability and hypertension, as well as the significance of co-localization of various NOS isoforms within specific skeletal muscle fiber types. This will be accomplished by giving an overview of nitric oxide synthase nomenclature, structure and regulation, followed by a review of the numerous physiological and patho-physiological roles that NO is implicated in playing in mammalian animal species. Special attention and discussion will be given to the so-called "NO and L-arginine paradoxes" as well as NOS uncoupling, as they may be implicated in the pathogenesis of hypertension. Next, the pathogenesis and clinical presentation of hypertension in humans will be discussed. The specific role of NO in hypertension, as it is currently understood in the literature, will then be discussed thoroughly, but concisely. The goal of this introduction is to impart to the reader a clearer understanding of the complex relationships among NOS, NO, skeletal muscle fiber type and hypertension.

Given the voluminous amount of scientific literature on NO, only the properties of NO most relevant to the pathogenesis and presentation of hypertension will discussed here, so as to establish a clear link between the two. Therefore, brief answers to each of the following questions regarding NO will be discussed in turn: "What is NO?", "Where does NO come from?", "What does NO do under normal physiological conditions?", "What are the "NO and L-arginine paradoxes", "What is the significance of NOS co-localization within certain skeletal muscle fiber types?"

Finally, capillarity and the phenomenon known as "rarefaction" will be discussed and a brief review of skeletal muscle fiber-typing methods will be presented.

Properties of Nitric Oxide: Nitric oxide, which was initially known as endothelium-derived relaxing factor (EDRF), is a gaseous, lipophilic, free radical, bio-messenger molecule found in mammalian cells. There are numerous NO species, including $NO^{\bullet}$ [this is the specific free radical species of nitric oxide (with an unpaired electron) that is designated by the notation "NO" in this dissertation], NO^{+} (nitrosonium), NO^{-} (nitroxyl), $ONOO^{-}$ (peroxynitrite, which is the byproduct of the reaction of NO with superoxide), NO_2 (nitrogen dioxide), N_2O_3 (dinitrogen trioxide), and NO_2^{+} (nitronium). Clearly, one must exercise caution when talking about "nitric oxide," as each NO species plays unique roles in normal and patho-physiology.

Nitric oxide is a free radical with eleven valence electrons. As such it participates in numerous, rapid reactions *in vivo*, including activation of soluble guanylate cyclase (sGC), scavenging by hemoglobin and oxidation by superoxide (Beckman and Koppenol

1996, Condorelli and George 2001). NO that has not been consumed by the aforementioned reactions can produce autocrine and paracrine effects (through enzymatic sources) and endocrine effects (through non-enzymatic sources) and NO has been implicated in the maintenance of vessel wall function and structural integrity (Lane and Gross 2002, Cattaruzza et al. 2005, Sonveaux et al. 2006, Chen et al. 2008). Indeed, Chen et al. suggest that paracrine NO is responsible for basic homeostasis under basal conditions while endocrine NO contributes to hypoxic vasorelaxation (Chen et al. 2008). Furthermore, NO is in equilibrium with more stable nitrogen oxide-derived species in living systems and the interconversion of these species is regulated by chemical constraints and enzymes (Sonveaux et al. 2006).

How then does this simple molecule exert the numerous effects attributed to it? Responses to NO, like those that will be discussed in more detail later in this chapter, are primarily mediated by *S*-nitrosylation of cysteine redox centers or by coordinated, covalent interactions with heme [such as is found in cytochrome *c* oxidase and soluble guanylate cyclase (sGC)] or non-heme iron and copper. Ion channels, receptors, enzymes, transcription factors and small G-proteins all possess *S*-nitrosylation motifs, suggesting that all of these structures can be acted upon by NO in some fashion (Stamler and Meissner 2001). The variety of targets mentioned above reinforces the need, whenever discussing or reading literature about NO, for one to keep in mind that NO has numerous targets and that the location of interaction between NO and its target, as well as local NO concentrations, duration of exposure and concentrations of reaction byproducts, are important to a clear understanding of NO's effects in a particular tissue.

Distribution and Sources of NO: As mentioned earlier, the distribution of NO is extremely important when investigating NO's role in a particular tissue or biological process. This is especially true when investigating how NO affects vascular relaxation. *In vivo* experimental measurements using electrochemical methods to detect NO generally report perivascular NO concentrations (C_{NO}) between 200 and 1,000 nM under control conditions (Chen et al. 2008). On the other hand, *in silico* models of endothelial cells, constructed by theoreticians using data collected from other investigators, have predicted NO concentrations of ~100 nM near an arteriole (Chen et al. 2008). The role of NO distribution, especially involving NO's interactions with other molecules, will be discussed in more detail later in this chapter.

Nitric oxide can be supplied to a biological system both endogenously and exogenously and endogenous NO comes from both enzymatic and non-enzymatic sources. The endogenous enzymes that produce NO are referred to as nitric oxide synthases (NOS). These enzymes, which possess an amino-terminal oxidase domain and a carboxy-terminal reductase domain, utilize L-arginine, in the presence of molecular oxygen, nicotinamide adenine dinucleotide phosphate (NADPH) and the coenzyme tetrahydrobiopterin (BH_4) to produce equimolar amounts of L-citrulline and NO through a series of redox reactions with N-hydroxyl-L-arginine produced as an intermediate product. Currently, three NOS isoforms have been definitively indentified. These isoforms are named after the tissues in which they were originally discovered and include neuronal NOS (NOS1 or nNOS), inducible NOS (NOS2 or iNOS) and endothelial NOS (NOS3 or eNOS). The numerical

designations – NOS 1, NOS2 and NOS3 – correspond to the order in which they were discovered.

It should be noted, however, that NOS1 is also expressed in cardiac muscle and endothelial cells (Lacza et al. 2006), in the sarcolemma, cytosol and in the costomeres interposed by unstained membrane segments of the muscle fibers of hamster, human, rat and mouse muscle tissue (Segal et al. 1999, Frandsen et al. 2000, Punkt et al. 2002, Rothe et al. 2005), as well as around arterioles (Huang et al. 2002, Kashivagi et al. 2002, Talukder et al. 2004). Frandsen et al. also demonstrated stronger NOS1 staining in Type I fibers versus Type II fibers (Frandsen et al. 2000). Furthermore, Rothe et al. suggested that some NOS1 was associated with the outer membrane of the mitochondria in rat skeletal muscle tissue (Rothe et al. 2005). An investigation by Punkt et al. demonstrated the presence of NOS2 in Type I, IIA and IIB fibers of rat skeletal muscle while NOS3 appears to be expressed only in vascular endothelial cells (Punkt et al. 2002). NOS3 also produces NO in response to shear stress, acetylcholine (ACh), bradykinin, histamine, purines, leukotrienes and endothelin (in smooth muscle and the endothelial cell layer) and is regulated by numerous factors such as sub-cellular location, protein-protein interactions, phosphorylation at Ser1179 in the reductase domain and de-phosphorylation at Thr495 in the calmodulin (CaM) binding domain (which increases the enzyme's activity) and availability of obligate cofactors (Förstermann et al. 1998, Kähler et al. 2000 and 2001, Mitchell et al. 2001, Shah and Singh 2006, Singh et al. 2007, Schulz et al. 2008).

The existence of a fourth, calcium-dependent NOS isoform, mitochondrial NOS or mtNOS, is still a matter of debate. For the sake of completeness, this debate will be reviewed very briefly later in this chapter.

Characteristics of NOS Isoforms: NOS1 and NOS3 are constitutively active, calcium/calmodulin (Ca^{2+}/CaM)- dependent and are considered low-output producers of NO under basal conditions. NOS3, in particular, is considered the major source of NO regulating vascular tone (Lacza et al. 2006, Chen et al. 2008) and has even been shown to react with nitrite under anoxic conditions (Gautier et al. 2006). Calmodulin is a ubiquitous, calcium-binding protein that binds to numerous protein targets and regulates several processes, including inflammation, metabolism and apoptosis, among others. Calmodulin reversibly binds with NOS1 and NOS3 through changes in intracellular Ca^{2+} concentration. In the case of NOS2, however, calmodulin is permanently and tightly bound to the enzyme. In all three NOS isoforms the role of calmodulin is to bind to the protein linker connecting the reductase and oxidase domains, thereby regulating the activity of the enzyme by activating flavin mononucleotide (FMN)-to-heme electron transfer (Daff 2003).

NOS2 is unique in several ways. Its expression in macrophages is controlled at the gene transcription level, its activity is Ca^{2+} -independent and it is considered a high-output enzymatic source of NO (Lane and Gross 2002). NOS2 is involved in the immune system's response to inflammatory and pro-inflammatory mediators such as cytokines, bacterial components, lipopolysaccharide, IFN-γ, IL-1β and TNF-α and may be expressed

after ischemia-reperfusion injury (Lacza et al. 2006). Interestingly, in 2006, Kleinbongard et al. reported the existence of a functional form of NOS3 in erythrocytes (Kleinbongard et al. 2006), but this finding has been repudiated by data from other groups (Hilarius et al. 2007). It should also be noted that without a protective mechanism, any NO produced from this enzymatic source would be rapidly scavenged by hemoglobin. Indeed, Joshi et al. demonstrated that this consumption of intraluminal NO does indeed take place (Joshi et al. 2002). Although it is unclear how physiologically relevant NO from this source is, it has been suggested that blood-borne NO bioactivity is a key mechanism for matching blood flow to the metabolic activity of local tissue (Chen et al. 2008). Finally, in an interesting 1996 study by Gath et al., the authors presented evidence suggesting the presence of a "constitutive" NOS2 isoform in guinea pig skeletal muscle, confirming earlier reports of NOS2 expression in normal tissues (Morrissey et al. 1994, Gath et al. 1996)

Two other enzymatic sources of NO are worth noting here. The enzyme xanthine oxidoreductase functions by reducing nitrite, also a non-enzymatic source of NO, via an acid-catalyzed mechanism. The other enzymatic source is cytochrome P450 reductase, which reduces nitrate to nitrite, which is then reduced to NO by cytochrome P450.

Numerous arguments against the existence of a mitochondrial NOS isoform have been offered, including the lack of a NOS-like sequence in the mitochondrial genome (meaning the enzyme must be imported into the mitochondrion), lack of a mitochondrial transport signal in the sequences of the known NOS isoforms, potential lack of obligate NOS cofactors in the mitochondrial matrix, lack of L-arginine as a substrate and the

presence of agmatine, which is the product of arginine decarboxylase and a known NOS inhibitor. Furthermore, results demonstrating the presence of a mitochondrial NOS isoform have not been confirmed by complementary methods and have been difficult to reproduce, possibly due to minute mtNOS concentrations and contamination of experimental samples.

At this point it is important to note that investigators have detected a number of NOS splice variants. Four NOS1 splice variants have been identified to date, designated nNOSβ, nNOSγ, nNOSμ and nNOS-2 (Note: NOS splice variant designations per Alderton et al. 2001). While the regulation and biological significance of these NOS splice variants is poorly understood, nNOSμ is the predominant isoform expressed in rat skeletal muscle and the most extensively characterized NOS1 splice variant (Silvagno et al. 1996, Alderton et al. 2001). nNOS-2 has been detected in mouse brain and human neuroblastoma cell lines and has been implicated as a dominant negative regulator of NOS1 activity (Ogura et al. 1993, Fujisawa et al. 1994, Brenman et al. al 1997, Alderton et al. 2001). Little is known about NOS2 splice variants, however, mRNA transcripts have been detected in human epithelial cells, alveolar macrophages and endothelial kidney 293 cells (Alderton et al. 2001). Finally, no evidence currently exists for NOS3 splice variants (Alderton et al. 2001).

Some novel solutions to the aforementioned problems were proposed by Lacza et al. in a 2006 review of the current scientific literature both supporting and challenging the existence of mtNOS (Lacza et al. 2006). The Lacza group hypothesized that perhaps a mtNOS-like oxygenase enzyme uses the electron transport chain as an electron source

instead of its own reductase domain. There is, however, absolutely no experimental evidence to support this hypothesis. Lacza et al. offered the hypothesis that NOS3 is actually attached to the outer mitochondrial membrane, which would negate concerns about transport and folding of NOS proteins as well as required cofactors for NOS function not being present in the mitochondrial matrix (Lacza et al. 2006). Data supporting this hypothesis have been provided by two separate groups (Henrich et al. 2002, Gao et al. 2004). Finally, mitochondrial nitrosothiols including nitrated tyrosine residues and S-NO-glutathione may be the source of the mitochondrial NO, although this hypothesis has limited plausibility since such a synthetic pathway would require exogenous sources of NO (Lacza et al. 2006). Despite the limitations of the three hypotheses discussed above, the Lacza group concludes their review by suggesting that mitochondria likely do not produce physiologically relevant levels of NO but rather contribute biologically active nitrates to the living system (Lacza et al. 2006).

Non-enzymatic Sources of NO: Decreases in tissue O_2 tension (PO_2) and pH, either together or separately, can induce production or release of NO from non-enzymatic sources (Zweier et al. 1999, Singel and Stamler 2004). It is thought that, when tissue PO_2 drops, hemoglobin and glutathione release NO from their storage pools (Singel and Stamler 2004). Likewise, decreased tissue pH is thought to cause a release of NO from the reduction of circulating nitrite by deoxygenated hemoglobin or myoglobin, with the blood proteins acting as nitrite reductases (Huang et al. 2005, Shiva et al. 2007). Even iron-nitrosyl-hemoglobin, the product of deoxyhemoglobin and NO, can rapidly release NO in

the presence of oxidants (Sibmooh et al. 2007). These non-enzymatic sources are currently thought to serve as endocrine sources of NO, however, it is unclear just how much NO is stored and released from these sources and under what condition(s). This uncertainty is due, in part, to the biochemical complexity and lack of direct *in vivo* measurements of these reactions (Chen et al. 2008).

Despite the lack of *in vivo* measurements of NO production from non-enzymatic sources, computational models of NO release from intraluminal, non-enzymatic sources predict that 0.25 to 6 pM or ~40 pM NO is delivered to vascular smooth muscle (VSM) by intraerythrocytic *S*-nitrosohemoglobin (SNOHb), assuming there is an as yet unknown protective mechanism to prevent reaction of the NO with scavenging molecules in the vessel lumen and that the concentration of NO from the luminal nitrite reservoir is about ~40 – 260 pM under physiologic conditions (Chen et al. 2008). Assuming such a protective mechanism is absent, the calculated concentration of NO in VSM is about 0.08 pM (Jeffers et al. 2005). A complete and thorough review of the production, concentration and distribution of NO from non-enzymatic sources is outside the scope of this Introduction. However, the reader is referred to an excellent review by Chen et al. (2008) for further details regarding this important and interesting topic. What is important to keep in mind, however, is that it is generally thought that NO derived from endothelial cells acts in an autocrine manner (Lancaster 1994), while NO derived from non-enzymatic, intraluminal sources acts in an endocrine manner (Chen et al. 2008).

Biological Roles of NO: Nitric oxide serves a great number of functions in biological systems and new roles for this interesting molecule are being discovered all the time. A complete review of all of these functions, however concise, is well beyond the scope of this Introduction. Instead, the critical role of NO as an activator of sGC in VSM, which induces vasorelaxation, will be discussed in detail since aberrations in vasomotor control can lead to a number of pathological conditions, including hypertension. In addition to NO's role as a potent and important vasorelaxant, several other important functions are worthy of mention, including NO's ability to decrease mitochondrial O_2 consumption via the inhibition of the cytochrome *c* oxidase enzyme. Additionally, NO kills air- and food-borne pathogens (in high concentrations), modulates cardiac contractility, directs blood flow to ischemic tissues, regulates gastric motility, modulates glomerular filtration rate, is vasoprotective and is anti-atherogenic.

Nitric oxide affects VSM relaxation via a two-step process. Upon initially binding to sGC, a 150-kDa heterodimer consisting of α1 and β1 subunits which contains the same heme protoporphyrin IX as hemoglobin, NO partially activates the ultra-sensitive enzyme through the formation of a six-coordinate nitrosyl intermediate (Condorelli and George 2001). Subsequently, this species is converted to a five-coordinate nitroxyl complex through NO-dependent or NO-independent pathways (Zhao et al. 1999, Condorelli and George 2001, Tsoukias et al. 2004, Chen et al. 2008). The concentration of sGC, its turnover rate and NO concentration work together to determine the rate of cGMP production (Condorelli and George 2001). Interestingly, the concentration of NO required for half-maximal activation of sGC (the EC_{50}) has not yet been fully established. Studies

investigating the interactions between sGC and NO have demonstrated EC_{50} values ranging anywhere from 2.9 to 1,600 nM (Stone and Marletta 1996, Russwurm 1998, Bellamy et al. 2000, Artz et al. 2001, Roy and Garthwaite 2006, Rodrigues-Juarez 2007, Chen et al. 2008). An *in silico* analysis of sGC kinetics revealed an EC_{50} of approximate 23 nM (Condorelli and George 2001, Chen et al. 2008). Once produced, NO has a half-life of approximately one second, allowing it to diffuse both into and out of numerous cells in some cases (Pacher et al 2007).

NO Concentration *in vivo* and the "NO Paradox": If one accepts that the generally reported perivascular NO concentration values are valid and then considers reported sGC/NO EC_{50} values, in experiments conducted in the cellular environment using endogenous NO, of <10 nM, an apparent paradox arises: if the EC_{50} is indeed several nanomolar and perivascular concentrations of NO derived only from the endothelium are in the several hundred nanomolar range, how, then, is the vasculature regulated, since these values suggest the smooth muscle tissue would be constantly and maximally relaxed. This question is, as yet, unanswered and, in fact, confounded by recent data suggesting that NO concentrations of less than one nanomolar can trigger maximal vascular relaxation (Kollau et al. 2005, Chen et al. 2008).

This "NO paradox" may be resolved, at least in part, by further investigation of the NO-mediated regulation of sGC in smooth muscle. This regulation, as it is currently understood, can be mediated by both amplitude- and frequency-dependent mechanisms. Continuous, low-level (tonic) production forms stable and low-activity sGC heme

complexes. Conversely, acute and transient NO production may provide a more efficient means of sGC activation and can increase cGMP formation sevenfold (Tsoukias et al. 2004, Silva et al. 2007, Chen et al. 2008). Taken together, these data suggest that it may be the frequency of NO bursts that limit cGMP formation and regulate vascular tone (Tsoukias et al. 2004, Chen et al. 2008).

Another intriguing solution to this paradox was suggested in a comprehensive review of NO and peroxynitrite physiology by Pacher et al. in 2007. The authors suggested that erythrocytes serve as a major sink for perivascular NO, requiring the endothelium to produce 10- to 40-fold more NO than is required to activate sGC within vascular smooth muscle cells (VSMCs). It appears likely that this elevated NO production is what perivascular microelectrodes are detecting. This measurement, however, is misleading because it is likely that most of the NO being produced is immediately being scavenged by circulating erythrocytes. The authors estimate that the endothelium needs to produce ~100 nM of NO to achieve a VSMC NO concentration of only 5-10 nM, concentrations which have been predicted by mathematical models (Pacher et al. 2007).

Although a detailed discussion of NO's regulation of O_2 delivery through its binding to cytochrome *c* oxidase is beyond the scope of this Introduction, it is important to note that NO's two primary targets, sGC and cytochrome *c* oxidase, vary in their sensitivities to NO by a factor of 50. This implies that the NO-to-cGMP pathway in smooth muscle tissue would be fully saturated before endothelium-derived NO has a chance to exert its regulatory effects on mitochondrial respiration in parenchymal cells. This observation further compounds the "NO paradox" and led Chen et al. to hypothesize

that there are multiple sources of NO in the perivascular space and that heterogeneity of NO distribution is an important factor in the regulation of microvascular oxygen delivery (Chen et al. 2008). Obviously, further research that accurately and quantitatively determines the contribution(s) of NO from its numerous sources in the vasculature is required to resolve this paradox.

The "L-arginine Paradox": The "L-arginine paradox" is a phenomenon observed in human subjects in which introduction of exogenous L-arginine results in a transient increase in NO production. This is paradoxical because L-arginine concentration in the cytoplasm of endothelial cells is ~800 μM, which largely saturates NOS3, whose K_m to utilize L-arginine is only 3 μM (Dioguardi 2011, Shin et al. 2011). This paradox is important clinically as long-term L-arginine supplementation is ineffective and can result in deleterious effects on the patient (i.e. persistent ureagenesis), especially those receiving supplementation to improve vasodilation after myocardial infarction (Chin-Dusting et al. 1996, Schulman et al. 2006, Van de Poll et al. 2007, Dioguardi 2011).

L-arginine regulation and metabolism in human physiology is complex and a detailed discussion of its role in various metabolic pathways is outside the scope of this Introduction. Therefore, the reader is referred to an excellent review on the topic by Dioguardi (2011). However, given its clinical significance and relationship to the production of NO in vivo, a brief discussion of possible explanations for this paradox is warranted.

One possible explanation for this paradox is discussed in a 2011 study by Shin and colleagues. The authors suggest the plasma concentration of L-arginine, ~50-100 μM, may

play a more crucial role in the explanation for this paradox than previously thought. The cationic amino acid transporter 1 (CAT-1) is constitutively active and co-localizes with NOS3 in caveoli of endothelial cells, suggesting direct delivery of extracellular L-arginine to NOS3 (Zharikov and Block, 1998, Bednarz et al. 2004). A 2005 study by Zani et al. suggests L-arginine transported by CAT-1 is not in rapid equilibrium with the bulk intracellular L-arginine and that this extracellular L-arginine concentration is crucial to the mediation of NO release from endothelial cells (Zani et al. 2005, Shin et al. 2011). Using an L-arginine ethyl ester that passively diffuses through the endothelial cell membrane, siRNA to partially silence the CAT-1 transporter and by assaying nitrite/nitrate concentrations produced by cultured HVECs, Shin et al. (2011) concluded that once L-arginine is transported into the endothelial cell it no longer has access to the membrane-bound NOS3 enzyme as noted by the absence of increased NOS3 activity (Shin et al. 2011). It should be noted that even if one accepts the authors' conclusions, plasma concentrations of L-arginine are still well above the reported 3 μM K_m for NOS3 to utilize L-arginine. Shin et al. suggest that this higher cellular K_m value reflects incorporation of additional rate-limiting steps, including cellular transport, that are not present when working with purified enzyme (Shin et al. 2011).

Another possible explanation for the "L-arginine paradox" is proposed by Dioguardi (2011). The authors suggest that endogenous arginases, which directly compete for L-arginine and whose activities exceed that of NOS under any conditions, have a K_m 100-fold higher and a maximal catalytic rate more than 1,000 times higher than NOS,

thereby significantly impairing NOS efficiency, especially in the presence of excess substrate (Wu and Morris 1998, Santhanam et al. 2008).

Study of this puzzling and intriguing paradox continues and results of future studies in both human and smaller mammalian models should prove interesting.

Hypertension Definition and Causes: According to the American Heart Association, about one-third of U.S. adults (approximately 73 million) have hypertension (http://www.americanheart.org/presenter.jhtml?identifier=2114). Left untreated, hypertension can lead to a plethora of diseases and conditions, including cerebral vascular accidents, myocardial infarction, cardiac damage and failure, nephropathy and end-stage renal disease (amongst others) and mortality (http://www.americanheart.org/presenter.jhtml?identifier=2114, Carretero and Oparil 2000). A thorough review of the current scientific and medical understanding of each of the possible causes of hypertension is clearly beyond the scope of this Introduction. However, a brief review of some of the proposed causes of hypertension will be presented. Hypertension is diagnosed when the average of two or more diastolic blood pressure (DBP= diastolic blood pressure; BP= blood pressure) measurements on at least two subsequent occurrences is ≥90 mmHg or when the average of multiple systolic BP (SBP) readings on two or more subsequent occurrences is consistently ≥140 mmHg and a BP of ≥140/90 mmHg is considered isolated systolic hypertension (Carretero and Oparil 2000). According to the Sixth Report of the Joint National Committee on Prevention, Detection, Evaluation, and Treatment of High Blood Pressure (JNC VI), "hypertension" in adults can be classified as borderline, Stage 1 (mild), Stage 2 (moderate) or Stage 3 (severe) while

"isolated hypertension" is classified as either borderline or frank isolated hypertension (JNC VI 1997, Carretero and Oparil 2000). United States demographic data indicate that hypertension is more prevalent in males, blacks, residents of the southeastern part of the country and is inversely correlated to socioeconomic status (Carretero and Oparil 2000).

A detailed definition of "essential," "primary," or "idiopathic" hypertension is necessary in order to facilitate a logical discussion of how NO production and bioavailability relate to hypertension. It may be useful to think of hypertension as a sequel to other pathological conditions or a result of lifestyle choices rather than as a disease completely unto itself. This mindset becomes especially useful when searching the literature for information about hypertension since the vast majority of articles discuss hypertension as it presents in or accompanies preeclampsia, reno-vascular disease, renal failure, aldosteronism and metabolic syndrome (which includes diabetes mellitus, obesity, glucose intolerance, insulin resistance and dyslipidemia) (Carretero and Oparil 2000, Hayashi 2001, Calhoun 2006, Yanai et al. 2008). Essential hypertension, then, is high BP in the absence of the secondary causes noted above and accounts for 95% of all cases (Carretero and Oparil 2000).

Much work remains to be done to elucidate the pathogenesis (and especially the genetic causes) of essential hypertension. This work is extremely important since modifiable lifestyle traits like excessive alcohol consumption, excessive salt intake, lack of exercise, stress and low potassium and calcium intake can exacerbate what may only be a mild, inherited, essential hypertension. Definitively identifying the genetic causes of hypertension is likely to be a long and painstaking process since both cardiac output and

total peripheral resistance (TPR) regulate BP. These factors are in turn regulated by other factors such as autonomic responses, vasoactive hormones, body fluid volumes, renal function and the structure of the cardiovascular system itself. Finally, a greater understanding of other non-modifiable risk factors, such as obesity, the aging process and the metabolic syndrome may provide non-pharmacological targets for anti-hypertensive therapies.

No fewer than ten genes have been demonstrated to increase or decrease BP by increasing or decreasing salt and water reabsorption by the kidney (Carretero and Oparil 2000). Several syndromes resulting from aberrations in this pathway have been identified and include glucocorticoid-remediable aldosteronism, Liddle's syndrome and apparent mineralcorticoid excess. Blood pressure is also sensitive to dietary salt intake and it is thought that this sensitivity results from the combined effects of hyperinsulinemia, hyperaldosteronism and increased sympathetic nervous system activity (Carrertero and Oparil 2000). Using Dahl salt-sensitive rats, Takenaka et al. demonstrated that salt-sensitive hypertension reduces afferent arteriolar resistance and impairs the arteriolar myogenic response, strongly suggesting that salt sensitivity determines renal microvascular reactivity to pressure, as well as tubular sodium handling (Takenaka et al. 1992, Hayashi 2001).

Of the syndromes mentioned above, aldosteronism has been of particular interest to hypertension researchers of late. Conventional medical wisdom has, until now, held that primary aldosteronism is an uncommon cause of hypertension. This wisdom has been challenged recently by data suggesting that perhaps as many as 15% of patients with

essential hypertension and approximately 20% of patients with resistant hypertension (defined as elevated BP despite the use of three anti-hypertensive agents) also meet the biochemical criteria for primary aldosteronism (Calhoun 2006). Furthermore, primary aldosteronism is present in approximately 20% of individuals with resistant hypertension (that is, hypertension that is refractory to standard anti-hypertensive therapies) (Calhoun 2006). Cross-sectional studies by El-Gharbawy et al. and Grim et al. studying black American and white French Canadian patients with hypertension demonstrated a significant correlation between plasma aldosterone and 24-hour ambulatory blood pressure levels. The BP levels in both groups were unrelated to plasma renin activity, suggesting that aldosterone has a greater contribution to worsening hypertension than renin-angiotensin II (El-Gharbawy et al. 2001, Grim et al. 2005). Aldosterone's role in the pathogensis of hypertension is further supported by work from Vasan et al. in which a prospective analysis demonstrated that serum plasma aldosterone levels amongst normotensive individuals participating in the Framingham Offspring Study were related to subsequent increases in BP and the development of sustained hypertension, which is defined as a BP measurement of >140/90 mmHg or the use of anti-hypertensive medications (Vasan et al. 2004). It should be noted, however, that renin activity was not measured in the Vasan study, thus preventing a comparison of the predictive value of aldosterone versus renin (Calhoun 2006). Finally, the effectiveness of antihypertensive mineralocorticoids such as spironolactone and eplerenone, which reduces BP even further after administration of renin-angiotensin blockades in patients without primary aldosteronism, suggests a broader role for aldosterone in hypertension (Calhoun 2006).

Hypertension and the Metabolic Syndrome: Obesity, glucose intolerance, dyslipidemia and hypertension are all hallmark characteristics of the metabolic syndrome and it has been estimated that as many as one third of hypertensive patients also have the metabolic syndrome (although not all patients with metabolic syndrome are hypertensive) (World Health Organization 1999, Expert Panel on Detection, Evaluation, and Treatment of High Blood Cholesterol in Adults 2001, Cuspidi et al. 2004, Schillaci et al. 2004, Guerro-Romero et al. 2005). More specifically, visceral obesity is thought to play a critical role in the development of hypertension via the deranged production and secretion of bioactive substances, or adipocytokines, including leptin, tumor necrosis factor-α (TNF-α), interleukin-6 (IL-6), angiotensinogen and non-esterified fatty acids (NEFA) (Yanai et al. 2008). These adipocytokines are also responsible for another key characteristic of the metabolic syndrome, insulin resistance.

Insulin resistance causes sodium retention and potentiates both the production and vasoconstrictive action of endothelin-1, which in turn leads to hypertension (Rocchini 2000, Sarafidis and Bakris 2007). More relevant to the topic of nitric oxide's relationship to hypertension is the fact that insulin stimulates NO production. In a state of insulin resistance, endothelial NO production is attenuated and vascular tone consequently increases. Additionally, sodium retention has been shown to decrease renal medullary NO production, which decreases the elevated renal blood flow typically associated with obesity (Fujiwara et al. 1999, Hayashi 2001). In 2005, Roberts et al. presented data collected from rats with metabolic syndrome, demonstrating significant NO inactivation down-regulation

of NOS (Roberts et al. 2005). These results suggest oxidative stress and endothelial dysfunction play a very strong role in the pathogenesis of hypertension in the metabolic syndrome. For the purposes of this chapter, "endothelial dysfunction" is a chronic inflammatory disease referring to an "imbalance between relaxing and contracting factors" in the vasculature, which can attenuate NO's ability to cause vasodilation, although other problems such as increased endothelial permeability and increased endothelial adhesion for leukocytes are often associated with endothelial dysfunction (DeMeyer and Herman 1997, Lum and Roebuck 2001, Cattaruzza et al. 2005, Buerk 2007).

In addition to the numerous factors already mentioned, the activated renin-angiotensin system, or RAS, also regulates blood pressure by modulating both renal function and vascular tone. In 2003, Engeli et al. determined that food intake plays a major role in regulating the RAS by increasing formation of angiotensin II in adipocytes (Engeli et al. 2003). Furthermore, angiotensin II inhibits the action of insulin through its interaction with the angiotensin 1 receptor (AT_1) and an increase in oxidative stress (amongst other mechanisms) via mitogen-activated (MAP) kinases and NAD(P)H oxidases (Fujita 2001). The increased concentration of reactive oxygen species (ROS), which are normally ubiquitous and short-lived, has numerous effects, including inhibition of PI3K/Akt signaling, which decreases endothelial NO production and increases vascular tone (Lum and Roebuck 2001, Sowers 2004).

ROS exert numerous other dose-dependent effects on their targets: in low concentrations, ROS stimulate cytokine secretion and cell proliferation, while at high concentrations they modify proteins by oxidation, peroxidize lipids and nick DNA strands.

Just what becomes the target of a ROS is dependent on several factors including lipid solubility, the cellular location of ROS generation and the half-life of the oxidant (Lum and Roebuck 2001). At this point it should be clear that ROS serve as important signaling molecules at numerous points in numerous pathways. The role of ROS as a signaling molecule in the pathogenesis of hypertension will be discussed later in this chapter.

In 2001, Fujita published a brief review presenting several lines of evidence linking an activated renin-angiotensin system to the pathogenesis of hypertension (Fujita 2001). In rats chronically infused with pressor and non-pressor doses of angiotensin II, both endothelial dysfunction and hypertension developed as a result of increased vascular superoxide anion production, which is thought to occur in the endothelium, media and adventitia (Mollnau et al. 2002, Schulz et al. 2008). Incubation of smooth muscle cells with low-density lipoproteins (LDL) increases AT_1 expression and mechanical stretch up-regulates angiotensinogen, renin and angiotensin converting enzyme genes (Fujita 2001). Perhaps most interestingly, the LDL receptor Cd36 has been implicated as a gene for hypertension in spontaneously hypertensive rats (SHR) (Fujita 2001). While Fujita's review elucidates some very important mechanisms related to the pathogenesis of hypertension, many other potential mechanisms exist.

NO, Lipid Rafts and Redox Signaling: One of these mechanisms is redox signaling by clusters of cholesterol- and sphingolipid-rich lipid rafts, or LRs, which are situated in the cell membranes of many mammalian cells (Simons and Ikonen 1997, Simons and Toomre 2000, Kabouridis 2006, Li et al. 2007). Lipid rafts are defined by Li

et al. as "dynamic assemblies of cholesterol and lipids with saturated acyl chains that include sphingolipids and glycosphingolipids in the exoplasmic leaf of the membrane bilayer" (Li et al. 2007). Phospholipids with saturated fatty acids and cholesterol in the inner leaflet are also important components (Li et al. 2007). It has been proposed that the long fatty acids of sphingolipids in the outer leaflet couple the inner and outer leaflets together through interdigitation to form very stable, detergent-resistant membrane structures which are able to either include or exclude proteins when cells respond to physiological or pathological stimuli (Simons and Toomre 2000, Magee and Parmryd 2003, Li et al. 2007b). While a complete and thorough review of LR formation and function is outside the scope of this chapter, the role of LRs in endothelial function/dysfunction and the pathogenesis of hypertension warrants further discussion.

Lipid rafts have recently been implicated as a signaling component of endothelial cells, regulating several important endothelial functions including the endothelium-dependent vasorelaxant or constrictor response (Patschan et al. 2006, Zhang et al. 2006, Li et al. 2007b). This signaling capability comes from LRs' temporal-spatial organization with caveolae, which allows LRs to use molecules such as vascular endothelial growth factor (VEGF), hydrogen peroxide (H_2O_2) and NO to regulate endothelial function through exertion of numerous effects, including the up- or down-regulation of NO production (Pritchard et al. 2002, Yang et al. 2006, Li et al. 2007b). It is thought that large redox signaling molecules aggregate in LR "clusters" which subsequently produce superoxide and other ROS and contribute to the regulation of the endothelium-related vasomotor response. Data supporting this hypothesis have been collected in intact coronary arteries

by Li et al. and the reader is referred to an excellent 2007 forum review by that group which discusses the current scientific understanding of the function of lipid raft redox signaling platforms in endothelial dysfunction (Li et al. 2007b). There is now much evidence to suggest that >95% of superoxide in the vasculature is produced by non-mitochondrial NADPH oxidases (NOXs), with the balance coming from xanthine/xanthine oxidase and uncoupled NOS (Mohazzab et al. 1994, Rajagopalan et al. 1996, Griendling et al. 2000, Cai 2005, Li et al. 2007b). Consequently, NOX is believed to play a critical role in the normal regulation of endothelial function and development of several diseases, including hypertension (Li et al. 2007b), and will be the focus of this chapter.

In order to discuss how NOS and NO are regulated by LRs, it is first necessary to elaborate on the connection between caveolae and NOX. Caveolae are small, flask-shaped invaginations that can occupy up to 30% of the plasma membrane and can contain LRs (Goligorsky et al. 2002). Studies indicate that there is a correlation between caveolae formation, NOS location/NO production and endocytosis in endothelial cells (Goligorsky et al. 2002, Stan 2002, Li et al. 2007b). This pairing of caveolae and NOS is important because it allows for interaction between NOS and other signaling proteins including caveolin-1, calmodulin and Akt, among others (Pritchard et al. 2002). Caveolin-1, the primary coat protein of caveolae in blood vessels, is associated with and inhibits NOS3 within caveolae under basal conditions by inhibiting the reductase domain function of the enzyme (Bernatchez et al 2005). It has been suggested that cortical F-actin also co-localizes with NOS3 in the caveolae of pulmonary artery endothelial cells and that the actin polymerization state and/or protein contents regulate NOS3 activity in a post-

translational manner (Su et al. 2003). However, NOS3 has also been detected in non-caveolae LRs, which cluster in response to agonists or other stimuli to induce signaling (Pritchard et al. 2002, Li et al. 2007a, Li et al. 2007b). Such distribution suggests NOS and other enzymes may mediate different pathways within the same cell, depending on the type of stimulus present (Li et al. 2007b). NOX has also been shown to be present in both caveolae-associated (with caveolin-1) and non-caveolae-associated LRs. Since angiotensin II stimulates caveolae-associated NOX to produce superoxide, this is one potential mechanism by which NO could be scavenged in and around the vasculature, leading to endothelial dysfunction as NO reacts faster with superoxide and is present in high enough concentrations so as to outcompete endogenous superoxide dismutase (Hilenski et al. 2004, Ushio-Fukai and Alexander 2004, Zuo et al. 2005, Li et al. 2007b, Pacher et al 2007).

It is particularly telling that in their 2007 review, Li et al. state "the functional significance of LR redox signaling platforms is still far from clear" (Li et al. 2007b). However, the authors hypothesize that the formation of redox signaling platforms contributes to endothelial dysfunction (associated with various death receptor agonists such as FasL and TNF-α) which may lead to hypertension (among other diseases) (Li et al. 2007b). Research has shown that endothelial cells have endogenous Fas ligand (FasL) on their surface, making them resistant to FasL-induced apoptosis under normal physiological conditions (Shakibaei et al. 2005, Li et al. 2007b). If this endogenous pathway is disrupted in some way, such as by the presence of an excess of FasL, endothelial dysfunction (versus frank apoptosis) may result. Unlike FasL, stimulation of endothelial cells with TNF-α produces both pro- and anti-apoptotic cellular signals (Madge and Pober 2001, Shakibaei

et al. 2005, Li et al. 2007b). If enough TNF-α receptors are activated, apoptosis results, although there is general agreement amongst experts in the field that there are certain mechanisms in endothelial cells that protect them against apoptosis. To this end, Lefer and Ma as well as Zhang et al. have shown that TNF-α attenuates endothelium-dependent vasorelaxation in a variety of vascular beds (Lefer and Ma 1993, Zhang et al. 2002, Li et al. 2007b). Finally, it has been suggested that endothelial dysfunction is actually a normal precursor to apoptosis (Li et al. 2007b).

However, the question still remains: "What is the mechanism by which death receptor activation causes endothelial dysfunction (as defined for the purpose of this chapter)?" Researchers have proposed several theories, including NOS3 inhibition (Zhang et al. 1997, Makino et al. 2005, Li et al. 2007b), which will be discussed shortly, and a decrease in the anti-oxidant enzyme superoxide dismutase (SOD), which catalyzes the reaction: $2O_2^- + 2H^+ \rightarrow H_2O_2$ (Whitsett et al. 1992, Lum and Roebuck 2001, Li et al. 2007b). But it is the decrease in NO bioavailability due to the aggregation and enhancement of NOX activity and superoxide production that is generally considered the primary cause of impairment of endothelium-dependent vasorelaxation (Li and Shah 2001, Lum and Roebuck 2001, Zhang et al. 2003, Li et al. 2007b). Results from experiments using coronary arteries suggest this NOX aggregation and up-regulation is a consequence of ceramide-related LR clustering induced by FasL binding (Li et al. 2007b). The excess NOX-derived superoxide, produced in the vascular adventitia (which itself acts as a functional barrier to NO), reacts with the endogenous NO at a rate three times faster than it reacts with SOD, making the NO unavailable to exert its intended vasorelaxant effects

(Thomson et al. 1995, Wang et al. 1998). It is precisely because this reaction between NO and superoxide is so fast that some experts hypothesize that superoxide is targeted by NO is some vascular tissues in order to control endothelium-dependent vasorelaxation (Griendling et al. 2000, Lassègue and Clempus 2003, Li et al. 2007b).

NOS "Uncoupling:" It was mentioned earlier that the interaction of NO and superoxide produces peroxynitrite, a highly reactive free radical that can traverse cell membranes through anion channels, which then breaks down to form two other potent ROS**:** hydroxyl radical (•OH) and nitrogen dioxide (NO_2•) (Beckman et al. 1990, Lum and Roebuck 2001, Pacher et al. 2007). Once formed, peroxynitrite oxidizes a critical cofactor for NOS function, tetrahydrobiopterin (BH_4), to dihydrobiopterin (BH_2) (Vásquez-Vivar et al. 1998, Zou et al. 2002, Li et al. 2007b). This causes "NOS uncoupling" where electrons normally flowing from the reductase domain of one subunit to the oxygenase domain of the other subunit are diverted to molecular oxygen instead of L-arginine, causing the flavin proteins present in the enzyme to directly reduce oxygen, thereby producing excess superoxide instead of NO (Xia and Zweier 1997, Vásquez-Vivar et al. 1998, Zou et al. 2002, Schulz et al. 2008).

A decrease in BH_4 bioavailability, thereby altering the stoichiometric relationship between BH_4 and NOS3, can also cause the enzyme to uncouple (Singh et al. 2007). Disruption of either the de novo synthetic pathway (in which GTP is a precursor) or salvage pathway, by which BH_4 is produced, can also diminish BH_4 bioavailability (Singh et al. 2007). In 2002, Zou and colleagues suggested that it was not the oxidation of BH_4 to

BH_2 that causes NOS uncoupling but rather oxidation/disruption of the zinc-thiolate (ZnS_4) center or "cluster" formed by a zinc ion coordinated with pairs of cysteine residues at the NOS dimer interface by peroxynitrite in a concentration-dependent manner, causing a release of zinc which effects a structural change that cleaves NOS dimers into monomers under reducing conditions and forms disulfide bonds between the monomers (Zou et al. 2002). The group bases their conclusions on numerous pieces of experimental evidence. They cite papers in which X-ray crystallography confirms the presence of the aforementioned zinc-thiolate "cluster." Other studies have also demonstrated that peroxynitrite reactions are greatly facilitated in the presence of metal-ion centers or heme-thiolate "clusters", such as those present in NOS enzymes. Next, the group determined that the zinc-thiolate center in the NOS3 enzyme is disrupted at peroxynitrite concentrations of 1 – 10 μM, which are 10- to 100-fold lower than concentrations required to oxidize BH_4 and that a 5,000-fold excess of BH_4 over NOS3 did not prevent NOS3 dimer dissociation. The interaction between peroxynitrite and the zinc-thiolate NOS center appears to be highly selective because the addition of physiological concentrations of glutathione (10 mM), physiological and high concentrations of L-arginine (0.5 mM and 1 mM, respectively) and BH_4 (0.1 mM and 100 μM, respectively) and high concentrations of exogenous reduced thiols did not prevent peroxynitrite-induced disruption of the centers. Furthermore, zinc has the highest charge-to-atomic radius ratio of any element and will attract anionic oxidants like peroxynitrite, which reacts with zinc-thiolate "clusters" 1000 times faster than with cysteine-thiols. The paper goes on to report that high glucose concentrations (30 mM) cause NOS3 dimers to dissociate into monomers by increasing the

cellular content of 3-nitrotyrosine, which inactivates prostacyclin synthase through tyrosine nitration, thereby attenuating vasorelaxation (Zou et al. 2002). Finally, the authors report that the zinc chelator NNNN-tetrakis (2-pyridylmethyl) ethylenediamine (TPEN) mimicked the effects of peroxynitrite, suggesting it is indeed peroxynitrite and not another molecule responsible for the experimental results they observed, and that H_2O_2 oxidizes free thiols without affecting NOS3 dimers or zinc content, suggesting that the NOS zinc-thiolate center (versus free thiols) truly are the target of peroxynitrite.

Regardless of the cause, the excess superoxide produced from NOS uncoupling contributes to oxidative stress within the cell and reduces the amount of NO available to produce endothelium-dependent vasorelaxation (Katusic 2001, Tiefenbacher 2001, Zou et al. 2002, Li et al. 2007b). Support for the interaction between BH_4 bioavailability, NO bioavailability and ROS production comes from several clinical studies in which administration of BH_4 reduced endothelial dysfunction in patients with hypercholesterolemia, coronary artery disease and a history of smoking (Stroes et al. 1997, Heitzer et al. 2000, Maier et al. 2000, Thöny et al. 2000, Singh et al. 2007). In 2007, Heeba et al. demonstrated that 3-hydroxy-3-methylglutarylcoenzymeA (HMG-CoA) reductase inhibitors (statins) can attenuate endothelial dysfunction in both normal and highly dysfunctional human umbilical vein endothelial cells (HUVECs) by shifting the NO/peroxynitritie balance in a favorable direction, suggesting that therapies currently used for other conditions may someday play a role in directly combating endothelial dysfunction (Heeba et al. 2007).

NOS Downregulation: Nitric oxide bioavailability can also be attenuated by down-regulation of the NOS enzyme itself. This phenomenon has been particularly well-studied in the NOS3 isoform, which is down-regulated by numerous factors including TNF-α, hypoxia, endothelial proliferation, mixtures of interferon-γ and interleukin 1β in the blood of individuals with microangiopathy, polymorphisms in the NOS3 haplotype, oxidized low density lipoproteins, C-reactive protein [which activates NOX, causing ROS generation and which blunts phosphorylation at Ser1179 in the reductase domain by agonists such as VEGF, high density lipoproteins and insulin], hypertension and from the endogenous NOS inhibitor asymmetric dimethyl-L-arginine (ADMA) in individuals with hyperglycemia (Mantovani et al. 1992, Rosenkranz-Weiss et al. 1994, McQuillan et al. 1994, Flowers et al. 1995, Chou et al. 1998, Fard et al. 2000, Lin et al. 2002, Makino et al. 2005, Heeba et al. 2007, Singh et al. 2007).

In 2005, Makino et al. conducted a study investigating whether the negative effects of TNF-α on NOS3 and apoptosis occur in the endothelial cells of patients with microvascular complications (Makino et al. 2005). Their methodology included examining NOS3 protein expression and the presence of apoptosis in human umbilical vein endothelial cells (HUVECs) after incubation with serum from Type 2 diabetic patients both with and without microvascular complications. The authors acknowledge that the mechanism(s) underlying endothelial dysfunction in diabetic patients is/are not well understood; however, they offered some possible explanations for their results. They discovered elevated levels of TNF-α and TNF-R1 (a TNF cell-surface receptor) in the serum of patients with microangiopathy, leading the group to propose that high serum

TNF-α level may partly contribute to endothelial dysfunction in diabetic patients via down-regulated NOS3. The authors also found elevated levels of ADMA in patients with microangiopathy, but stopped short of implying that elevated ADMA levels activate TNF-α.

The fascinating connection between NOS3 polymorphisms, NOS3 down-regulation and endothelial dysfunction warrants further discussion. In 2005, Cattaruzza et al. demonstrated that a CC genotype of the ^{786}C/T single-nucleotide polymorphism in the NOS3 promoter region causes impaired shear stress sensitivity in NOS3 expressed in patients with coronary disease and that this genotype is associated with a deficit in NOS3 expression in human endothelial cells upon exposure to laminar shear stress, with reduced NO-mediated vasomotor function in freshly isolated human blood vessels and with a significant increase in the presence of coronary heart disease in individuals under 65 years of age undergoing quantitative coronary angiography (Cattaruzza et al. 2005). These data are important clinically because they suggest that reduced shear stress-dependent NOS3 activation may contribute to coronary heart disease (Cattarruzza et al. 2005, Landmesser and Drexler 2005). Prior to the 2005 study by Cattaruzza's group, three NOS3 gene polymorphisms were known to exist: 1) a 27 bp tandem repeat in intron 4 which may affect basal NOS3 expression, 2) a G to T single nucleotide polymorphism at position 894 which results in an exchange of Glu 298 to Asp, which may alter protein stability, and 3) a T to C transition at position -786 in the NOS3 promoter which is thought to be unlikely to affect the function of the mature enzyme (Uwabo et al. 1998, Tesauro et al. 2000, Cattaruzza et al. 2005).

A study by Sandrim et al. in 2006 concluded that NOS3 haplotypes associated with hypertension were independent of ethnicity (Sandrim et al. 2006). That is to say, statistically significant differences in haplotype were only found when comparing hypertensive to normotensive subjects (Sandrim et al. 2006, Marson 2008). It should also be noted that the authors only studied individuals of black or white descent. In contrast to this finding, Srivastava et al. reported that Asian Indians carrying the Asp allele of the Glu298Asp NOS3 gene polymorphism may be at higher risk for essential hypertension (Marson 2008, Srivastava et al. 2008). Given this apparent discrepancy it is clear that much work remains to be done to determine what role NOS3 gene markers may have in predicting the susceptibility of different populations to hypertension (Marson 2008).

Specific Roles of sGC and cGMP: The roles that sGC and cGMP play in the complex NO/hypertension relationship warrant further discussion. In 1996, Rajagopalan and colleagues found that hypertensive rats demonstrated decreased responsiveness to the endothelium-independent nitro-vasodilators sodium nitroprusside and nitroglycerin as well as endothelium-dependent vasodilators (Rajagopalan et al. 1996, Schulz et al. 2008). In a 2008 review, Schulz et al. attributed this finding, in part, to decreases in 1) expression of one or both subunits (α_1 and β_1) of sGC and 2) NO-dependent sGC activity which has been observed in both genetic and drug-induced hypertensive animal models (Ruetten et al. 1999, Jacke et al. 2000, Klöss et al. 2000, López-Farré et al. 2002, Witte et al. 2002, Schulz et al. 2008). A decrease in blood pressure normalized or enhanced sGC expression, but had differing effects on vascular superoxide production, suggesting that the decrease in

sGC expression seen in hypertension is not exclusively linked to increased superoxide formation and/or increased levels of vasoconstrictor peptides (Schulz et al. 2008). Interestingly, Schulz et al. go on to report that angiotensin II and endothelin-1, both of which are up-regulated in hypertension, seem to cause an up-regulation of sGC in VSMCs. However, this up-regulation seems to be "overwhelmed" by as yet unknown mediators of hypertension, which then cause a decrease in sGC expression (and therefore NO/cGMP signaling), leading to endothelial and smooth muscle dysfunction (Schulz et al. 2008).

Finally, there is some *in vitro* evidence that increased cGMP metabolism may contribute to endothelial dysfunction. In 2001, Kim et al. found that angiotensin II increased both the expression and activity of the cGMP-specific phosphodiesterase 1A1 in cultured smooth muscle cells, suggesting that increased cGMP metabolism may promote endothelial dysfunction in angiotensin II-induced hypertension (Kim et al. 2001, Schulz et al. 2008).

Capillarity and Rarefaction in Skeletal Muscle Tissue: In an excellent 2006 review of hypertension as a disease of the microcirculation, Feihl et al. define capillaries as "vessels ranging from 4 to 12 μm in diameter in which the walls are composed exclusively of endothelial cells more or less fenestrated according to the organ and a basement membrane" (Feihl et al. 2006). The endothelial cells are rolled up into tubes that comprise one segment of the capillary. Their function is to ensure fluid-metabolite exchange between plasma and tissues which requires high wall permeability. However, a consequence of this high permeability is fragility of the vessel. While normal systemic

capillary pressure is a relatively low 10 – 30 mmHg, distal capillaries can be damaged by local hypertension. Myogenic tone, an intrinsic property of vascular smooth muscle which causes it to contract when stretched, protects these fragile capillaries by amplifying arteriolar resistance to flow (Feihl et al. 2006).

The pattern of the capillary network in skeletal muscle has been the subject of study for well over 100 years. In 1919, August Krogh presented the first model of capillary anatomy in skeletal muscle, consisting of a parallel arrangement of vessels embedded in a skeletal muscle fiber matrix (Krogh 1919, Skalak and Schmid-Schönbein 1986). However, the model was considered too simplistic to form the foundation for quantitative predictions of transport in skeletal muscle as it ignores capillary network arrangement and fails to describe how arterioles and venules connect with the capillary network (Skalak and Schmid-Schönbein 1986). Therefore, in 1986, Skalak and Schmid-Schönbein set out to propose a new network model for skeletal muscle capillaries. Interestingly, their work was carried out in the spinotrapezius muscle of 16-20 week old male WKY and SHR rats (Skalak and Schmid-Schönbein 1986). They discovered that capillaries are interconnected across a limited number of fibers, creating "capillary bundles" which are in turn connected by transverse arterioles or collecting venules which may interconnect with several bundles. The arterioles and venules branch out in an alternating sequence, creating a "capillary bundle element" which consists of the segment from a transverse arteriole to its neighboring collecting venule (Skalak and Schmid-Schönbein 1986). It is important to note that this arrangement allows for control of

capillary pressure in the presence of large flow fluctuations by the vasoactive transverse arterioles by purely anatomical means.

Another interesting finding of the Skalak and Schmid-Schönbein study was that in the SHR the capillary network exhibits relatively straight arteriovenous pathways with a reduced density of the meshwork. However, they failed to find any indication of a reduced number of parallel pathways per bundle element (Skalak and Schmid-Schönbein 1986). The importance of this finding will be discussed shortly, but first it is important to present what is known about capillary density and the arrangement of vessels in mammalian species.

In a comprehensive 1975 study, Plyley and Groom studied the geometrical distribution of capillaries in dog, cat, rabbit, rat and guinea pig striated muscle and set out to answer the question "how many vessels are needed around the circumference of a muscle fiber in order to satisfy its O_2 requirements?" (Plyley and Groom 1975). They counted capillaries in tissue sections from each species and calculated number of capillaries around a fiber, mean capillary:fiber ratio and the mean number of capillaries and fibers per square millimeter. Several conclusions regarding capillary number and density were drawn from these data. One conclusion is that although capillary density varied between species, the frequency distribution for capillaries around a fiber was nearly the same in all species studied, suggesting that any differences in capillary density are primarily a consequence of differences in mean fiber size. Another conclusion supports the notion that differences in mean fiber size indicate differences in metabolic rate and rate of O_2 supply. Thirdly, the authors suggest that nature prefers to increase O_2 supply by

decreasing the diameter of a muscle fiber rather than by increasing the number of capillaries around the perimeter of the fiber. When the arrangement of vessels and fibers in transverse sections of red (oxidative) and white (glycolytic) fibers were compared, the authors were surprised to see there were no significant differences in the mean number of vessels around a fiber and were unable to conclusively explain the reasons for the discrepancy, suggesting the literature, with reports both confirming the refuting the present findings, is far from clear regarding capillary density in red versus white muscle fibers (Plyley and Groom 1975). Sullivan and Pittman also failed to detect a significant difference in the number of capillaries surrounding oxidative and glycolytic fibers in hamster striated muscle tissue (Sullivan and Pittman 1983).

Although there are still unanswered questions about capillary density in different fiber types, a report in 1991 by Bennett et al. suggests that capillaries are preferentially located in the vertices of striated muscle tissue (Bennett et al. 1991). The authors offered two explanations for this finding. First, perhaps there may be more room for capillaries to grow in the vertex region than between muscle fibers. Second, this observation may be a result of efficient ordering of the capillaries and muscle fibers (Bennett et al. 1991). In line with the observations mentioned above, Bennett et al. also noted that the average shape of male golden skeletal hamster fibers is much closer to hexagonal than square (Bennett et al. 1991). These shape data are especially important when modeling transport and consumption of molecular oxygen and NO. Indeed, many investigators interested in such modeling normally collect "traditional" descriptors of capillarity, including capillary density, capillary:fiber ratio and number of capillaries around a fiber (Bennett et al. 1991).

However, a better assessment offered by Sullivan and Pittman (1987) is the percent of muscle fiber perimeter in contact with the capillary membrane (i.e. capillary-fiber contact) (Sullivan and Pittman 1983, Bennett et al. 1991). Interestingly, if this assessment is used, Sullivan and Pittman detected a significantly higher percent capillary-fiber contact in oxidative versus glycolytic fibers in hamster skeletal muscle tissue (Sullivan and Pittman 1983).

Another debate in the (primarily) hypertension literature is whether or not rarefaction of the microvasculature is a real phenomenon and, if so, to what degree does it occur. Rarefaction is defined as "a reduced spatial density of microvascular networks" (Feihl et al. 2006). However, rarefaction can be functional, structural or both. Feihl et al. define functional rarefaction as "an abnormal prevalence of anatomically existing but unperfused microvessels," whereas structural rarefaction "can be established either by quantitative histology or by the observation of microvascular beds in vivo under conditions maximal vasodilation and optimal perfusion pressure" (Feihl et al. 2006). Chen et al. (1981) reported structural rarefaction in 4-week old SHRs and a 1982 report by the same group in SHRs ranging in age from 6 to 18 weeks of age demonstrated similar results (Prewitt et al. 1982). Furthermore, Green et al. (1990) observed an approximately 14% reduction in capillary density in SHRs compared to age-matched controls. Although Skalak and Schmid-Schönbein (1986) did not observe evidence of rarefaction, they did note that there were fewer anastomotic connections in the capillary network of SHRs compared to the WKY subjects, suggesting a less tortuous path of flow in capillaries of the SHR than in those of the WKY (Skalak and Schmid-Schönbein 1986).

Although the cause(2) of rarefaction remain(2) elusive, a recent study using 12- to 14-week old SHR rats with established diminished functional capillary density in their skin and skeletal muscles compared to their age-matched controls, provided evidence that anti-hypertensive drugs have "distinct capacities for reducing or reversing functional and/or structural microvascular alterations in arterial hypertension…" (Sabino et al. 2008).

Given that NOS3 was first demonstrated in endothelial cells, the role of NO in rarefaction has been the subject of study as well. It has been suggested that NO plays a key role in appropriate vascular budding in wound healing and stimulates the expression of vascular growth factors, including vascular endothelial growth factor (VEGF) (Lee et al. 1999, Feihl et al. 2006). Furthermore, impaired angiogenesis has been directly demonstrated in experimental hypertension induced by chronic pharmacological inhibition of NO synthesis (Kiefer et al. 2002, Feihl et al. 2006). These findings further illustrate the ongoing need for an accurate technique to measure NO in vivo to further explore the crucial connection between NO and angiogenesis. Future studies in this area will hopefully shine some light on this puzzling phenomenon.

Fiber Type Nomenclature: Although a thorough review of the development of the immunohistochemical fiber typing techniques used in this project are beyond the scope of this Introduction, a few words about the fiber type nomenclature used in the study are warranted and the reader is referred to an excellent review of this topic by Pette and Staron (1990). Pioneering work by Barnard et al. (1971) and Peter et al. (1972) lead to the development of a fiber type nomenclature based on a combination of metabolic enzyme-

based and mATPase-based histochemical study. This combination technique lead to the isolation of three major fiber types in guinea pig and rabbit: slow-twitch oxidative (SO), fast-twitch oxidative glycolytic (FOG) and fast-twitch glycolytic (FG) (Barnard et al. 1971, Peter et al. 1972, Pette and Staron 1990). In the late 1960s it was discovered that fast and slow myosins have different alkaline and acid stabilities (Sréter et al. 1966, Seidel 1967, Pette and Staron 1990). These observations lead to more refined methods for mATPase-based fiber delineation as fast fibers display high mATPase activity under alkaline conditions and low activity under acid conditions whereas slow fibers exhibit the inverse (Pette and Staron 1990).

Further study indicated that distinction into only two fiber types was an oversimplification and led to delineation of fast fiber sub-types based on the intensity of staining after pre-incubation at varying pH: IIA, IIB and IIC. An additional myosin heavy chain protein, IId, was discovered by Pette and colleagues and the fibers containing this isoform were designated IID (Note: lower case letters designate the protein while upper case letters designate the fiber type in which the protein is expressed) (Bär and Pette 1988, Termin et al. 1989, Hämäläin and Pette 1993, Delp and Duan 1996). However, the Type IID fiber was found to be synonymous with the Type IIX fiber identified by Schiaffino and colleagues and is now, therefore, referred to as Type IID/X (Schiaffino et al. 1985 and 1988, LaFramboise et al. 1990, Delp and Duan 1996). Importantly, Pette and Staron (1990) also reported that muscle fibers are capable of transforming from one fiber type extreme to the other (see Discussion for further details) while Bortolotto et al. (1999) reports that these hybrid fibers, as they are referred to while in transition, cannot be

reliably detected by either enzyme-based histochemistry or immunohistochemistry (Bortolotto et al. 1999)

Details regarding the compatibility of different histochemical classification schemes are beyond the scope of this Introduction so the reader is once again referred to Pette and Staron's 1990 review and Delp and Duan's comprehensive 1996 study examining the fiber composition of rat skeletal muscle (Pette and Staron 1990). However, it is clear from a review of the literature that data gathered using the fiber-typing results outline above must be interpreted with great care, especially when attempting to generalize results from one species to another or even one muscle or muscle group to another within the same species.

Goals of the Project and Conclusion: At this point it should be clear to the reader that the relationship between NO production/bioavailability and hypertension is extremely complex. Obviously, much work remains to be done in the fields of nitric oxide and hypertension research. Hopefully this Introduction has elucidated some important aspects of NO's role in mammaliam physiology and in some of the proposed pathogenic mechanisms of hypertension. Many of the mechanisms and molecular/biochemical pathways discussed here could potentially become novel anti-hypertensive therapy targets in the future and the future research produced by the groups mentioned in this Introduction should prove to be most interesting. In any case, there is little doubt that as long as humans continue to suffer from this devastating condition, the search for a cure will continue.

The overall goal of this project is to determine if there is a significant difference in the expression of the three NOS isoforms in SHR and WKY postural skeletal muscle (spinotrapezius) tissue. There are four hypotheses driving the current study: 1) NOS1 will be co-localized with Type I skeletal muscle fibers in both WKY and SHR rats, 2) NOS2 will be co-localized with Type II skeletal muscle fibers, 3) NOS3 will be located primarily, if not exclusively, in endothelial tissue and 4) NOS concentrations in the spinotrapezius muscle of SHR will be greater than the concentrations of the NOS isoforms in the spinotrapezius muscle of WKY rats. In addition to exploring the hypotheses mentioned above, morpho- and geometric data will be collected about Type I, IIA and IIB muscle fibers in each strain, expression of Type I, IIa and IIb MHC protein will be determined by gel electrophoresis and capillarity data from both strains will be collected via alkaline phosphatase staining for capillary endothelium.

MATERIALS AND METHODS

Experimental Animal Preparation: Nine Wistar-Kyoto (WKY) rats and nine spontaneously hypertensive rats (SHR) aged approximately 16.5 weeks (young adult with hypertension fully manifested in SHR subjects) were used in this study (Harlan, Indianapolis, IN). The rats were initially anesthetized with a ketamine/acepromazine mixture, i.p. (75 mg/kg and 2.5 mg/kg, respectively) and the spinotrapezius muscle was prepared, with minor modifications, according to the procedure described by Gray (1973). Other steps in the preparation, including cannulations and blood sampling, were carried out following the standard procedures used in our laboratory for several years. The muscle was kept moist with warm physiological saline during dissection. Mean arterial blood pressure was monitored via a cannula in the carotid artery. Supplemental anesthetic (Alfaxan 10 mg/ml; 0.02 ml/kg/minute; Vetoquinol UK Limited, Vetoquinol House, Great Slade, Buckingham Industrial Park, Buckingham, UK) was continuously infused via a cannula in the jugular vein. Animal and muscle temperatures were maintained at 37 ^{o}C by separate heat exchangers within the Lexan animal platform. Following collection of spinotrapezius muscle tissue, animals were euthanized with Euthasol (0.4 mg/kg i.v.;

pentobarbital 390 mg/ml and phenytoin 50 mg/ml; Delmarva, Midlothian, VA). All procedures were approved by the Institutional Animal Care and Use Committee of Virginia Commonwealth University.

Immunohistochemical Protocol for Detection of Nitric Oxide Synthase in Skeletal Muscle Tissue: The spinotrapezius muscles were exteriorized bilaterally, using the methods and techniques outlined in the preceding section. Care was taken to keep the muscles moist with frequent application of phosphate-buffered saline (PBS) until they were fully dissected away from underlying tissues and removed. The two spinotrapezius muscles, each approximately 500 µm thick, were placed one on top of the other (for ease of sectioning) and folded along the long axis of the muscles. The muscle tissue was then be pinned to a small section of dental wax, placed in a small foil container and submerged in a gel tissue freezing medium (TBS™, Triangle Biomedical Sciences, Durham, NC) for cryoprotection during freezing in liquid nitrogen-chilled isopentane (Thermo Fisher Scientific Inc, Waltham, MA). The frozen tissue was then cut into 10 µm thick cross sections on a cryostat (Thermo Fisher Scientific Inc, Waltham, MA) and affixed to glass slides (75 x 25 mm; Thermo Fisher Scientific Inc, Waltham, MA). A brightfield microscopy staining protocol, based on a protocol provided by the laboratory of Dr. Mary Shall of the Department of Physical Therapy and modified from Segal et al. 1999, was utilized during the preparation of the sectioned specimens for immunohistochemical analysis. The sections were fixed for 15 minutes in 2% paraformaldehyde-phosphate buffer solution (PFA-PBS: PBS from Sigma-Aldrich, St. Louis, MO; PFA from Electron

Microscopy Sciences, Hatfiled, PA) chilled to 4 °C. After rinsing with room temperature (RT) 0.05 M Tris saline (TSS; Tris from BioRad Laboratories, Hercules, CA) six times quickly, the sections were permeabilized for 20 minutes at RT in 0.1% Triton X-100/0.05 M TSS (VWR International, Radnor, PA). After rinsing six times quickly with RT 0.05 M TSS, endogenous peroxidase activity was quenched by incubation in RT 3% hydrogen peroxide diluted in 40% 0.05 M TSS-60% methanol (Thermo Fisher Scientific Inc, Waltham, MA). After rinsing six times quickly with RT 0.05 M TSS, the sections were blocked for four (4) hours at RT in normal goat serum from the Vectastain Avidin: Biotinylated enzyme Complex (ABC) Peroxidase Elite Series kit (Vector Laboratories, Burlingame, CA). After pouring off the blocking solution, the sections were incubated at 4 °C overnight with the primary, rabbit, polyclonal antibody corresponding to the NOS isoform of interest. Primary NOS antibody dilutions were as follows: anti-NOS 1=1:2000 (Millipore, Temecula, CA), anti-NOS2=1:500 (Enzo Life Sciences, Plymouth Meeting, PA) and anti-NOS3=1:50 (Santa Cruz Biotechnology, Santa Cruz, CA). All primary antibody solutions contained 2% bovine serum albumin (BSA)-0.1 M TSS (BSA: Thermo Fisher Scientific Inc, Waltham, MA). After washing off the anti-NOS primary antibody three times for five minutes each with RT 0.05 M TSS, the sections were first incubated in anti-rabbit IgG biotinylated secondary antibodies (Vector Laboratories, Burlingame, CA) for 30 minutes at RT and then in Vector Laboratories' (Burlingame, CA) proprietary avidin-biotinylated enzyme complex reagent for 60 minutes at RT. Slides were then rinsed three times for five minutes each with 0.05 M TSS and then incubated in nickel-free 3,3-diaminobenzidine (DAB; Vector Laboratories, Burlingame, CA) for approximately 45-60

seconds and then rinsed in distilled water for five minutes. Slides were then carefully dried to remove excess moisture and CC/Mount Aqueous Mounting Medium™ (Sigma-Aldrich, St. Louis, MO) was applied. Sections were covered with a No. 1 coverslip (VWR International, Radnor, PA), slides sealed with clear nail polish and then stored at RT until ready for viewing.

Immunohistochemical Typing of Skeletal Muscle Fibers: Bilateral spinotrapezius muscles were exteriorized, frozen and sectioned as noted in the preceding section. A muscle fiber typing microscopy staining protocol, provided by the laboratory of Dr. Mary Shall of the Department of Physical Therapy, was utilized during the preparation of the sectioned specimens for immunohistochemical analysis. The sections were blocked in normal horse serum (for fast, slow and Type IIA fibers; Vector Laboratories, Burlingame, CA) or normal goat serum (for Type IIB fibers; Vector Laboratories, Burlingame, CA) for 20 minutes at room temperature. After pouring off the blocking solutions, the sections were incubated with the primary myosin heavy chain (MHC) antibody, corresponding to the fiber type of interest, for one hour at RT at the following dilutions: fast at 1:20 (Vector Laboratories, Burlingame, CA), slow at 1:50 (Vector Laboratories, Burlingame, CA), Type IIA at 1:50 (DSHB, Iowa City IA) and Type IIB at 1:50 (American Type Culture Collection, Manassas, VA). The MHC, fast, IIA antibody 2F7 developed by Christine Lucas (Department of Physiology, University of Sydney, Sydney, Australia) was obtained from the Developmental Studies Hybridoma Bank developed under the auspices of the NICHD and maintained by the University of Iowa, Department of Biology, Iowa City, IA

52242. After rinsing the primary MHC antibodies off the slides with phosphate-buffered saline (PBS) for 10 minutes, the sections were incubated with either Vectastain Anti-Mouse IgG (for fast and slow fibers), biotinylated anti-mouse rat-absorbed IgG (for Type IIA fibers) or biotinylated anti-mouse IgM (for Type IIB fibers) for 30 minutes at RT. All secondary antibodies were from Vector Laboratories, Burlingame, CA. Secondary antibodies were rinsed from sections with PBS for five minutes and sections then incubated in Vectastain Avidin: Biotinylated enzyme Complex (ABC; Vector Laboratories, Burlingame, CA) for 30 minutes at RT. Slides were then rinsed with PBS, incubated in 3,3-diaminobenzidine (DAB; Vector Laboratories, Burlingame, CA) for approximately 60-90 seconds and then rinsed in deionized water. Slides were then dehydrated through serial alcohols (10 dips in 95% ethanol 2 times; 60 seconds in absolute ethanol 2 times) and xylenes (alcohols and xylenes from Thermo Fisher Scientific, Waltham, MA), coverslipped with Permount Mounting Medium (Thermo Fisher Scientific, Waltham, MA), sealed with clear nail polish and stored at RT until ready for viewing.

Immunohistochemical Staining for Endothelial Cells in Skeletal Muscle Tissue using Alkaline Phosphatase Protocol: Bilateral spinotrapezius muscles were exteriorized, frozen and sectioned as described in the preceding sections. An alkaline phosphatase staining protocol for frozen sections was obtained from the website http://www.ihcworld.com/_protocols/special_stains/alkaline phosphatase.htm and modified for use in the laboratory to prepare sectioned specimens for immunohistochemical analysis of co-localization of endothelial cells and endothelial NOS

(NOS 3). Sections were fixed in ice-cold acetone (Thermo Fisher Scientific, Waltham, MA) for five minutes and then allowed to air dry for five minutes. Slides were then placed in the substrate working solution, consisting of a napthol AS-MX phosphate/N, N dimethylformamide (DMF) solution (napthol phosphate from Sigma-Aldrich, St. Louis, MO; DMF from Thermo Fisher Scientific, Waltham, MA), Tris-HCl buffer at pH 8.74 (Tris from BioRad Laboratories, Hercules, CA) and deionized water for approximately 60 minutes at 37 °C. Slides were then rinsed in deionized water (3 times, 2 min per rinse), carefully dried to remove excess moisture and CC/Mount Aqueous Mounting Medium™ (Sigma-Aldrich, St. Louis, MO) was applied. Sections were covered with a No. 1 coverslip (VWR International, Radnor, PA) and slides sealed with clear nail polish and stored at RT until ready for viewing.

Microscopic Analysis of Immunohistochemical Staining

General Procedures and Procedures for NOS 1/2 Image Acquisition: All NOS images, with the exception of the NOS1 practice images used to determine NOS1 / Slow MHC fiber co-localization, were acquired with an Olympus microscope (Model BH-2, Olympus Optical Company, Ltd., Tokyo, Japan) using the ImagePro v7.0.0.591 software package (Media Cybernetics, Inc., Bethesda, MD). The scale factor was determined by measuring a known distance on a stage micrometer slide. The specimen was brought into focus at 20X and Köhler illumination was established. An area of interest (AOI) was then selected based on the following inclusion criteria: 1) fibers were undamaged by any one of the three aforementioned staining protocols; 2) no mounting medium artifact or air bubbles

were present; 3) fibers were a sufficient distance (at least 50 μm) from the edge of the specimen; and 4) there was no chromogen (DAB) artifact. Automatic software algorithms were used to calculate an exposure time of ~100 ms (± 10 ms) and to white balance the image prior to acquisition. All images, regardless of final image format, were processed using the Sharpen and HiGauss filters included in the ImagePro software package.

Grading of NOS1 Images: Serial sectioning and staining were used to locate NOS1 fibers that co-localized with Type I fibers. After screening images for qualitative differences in degree of staining, a total of 17 images were selected for grading by seven independent observers to quantify the degree of NOS co-localization. To ensure as much objectivity of scoring as possible, all grading was performed on the same PC/monitor setup under identical lighting conditions. Before grading began, the observers were issued an instruction sheet (Appendix A). After giving the observers time to read the instructions and answering any procedural clarification questions, the observers graded three "practice" images, all from WKY control animals, using the 0 to 3 scale described in Appendix A. No feedback regarding scoring was provided before observers began grading experimental images, which were obtained from both control (WKY) and experimental (SHR) animals.

Examination of NOS2 Images: Serial sectioning and staining were used to locate NOS2 fibers that co-localized with Type IIA/B fibers in both control (WKY) and experimental (SHR) animals. However, screening images for qualitative differences in degree of staining failed to detect appreciable differences requiring independent observer grading.

MHC Skeletal Muscle Fiber-typing Acquisition Protocol: Whenever possible, fibers from two separate regions of each muscle section were used for data collection. Type I, Fast (Type IIA/B), Type IIA and Type IIB fibers ("positive" fibers), as well as unstained ("negative") fibers within the AOI, were counted and seven metrics collected by outlining the fiber using ImagePro's tracing function. These metrics included: cross-sectional area (A; in μm^2), perimeter (P; in μm), maximum diameter (in μm), minimum diameter (in μm), maximum radius (in μm) and minimum radius (in μm). Since, visually, the muscle fibers exhibited an approximately elliptical shape, area and perimeter data were used to determine the major and minor diameters of an equivalent ellipse with the same cross-sectional area and perimeter. The major diameter of the equivalent ellipse (D; in μm) was determined using the following formula:

$$D = [(P / \pi) \bullet \{1 + \sqrt{[1 - (4\pi A/P^2)]^2}\}]^{1/2}$$

Likewise, minor diameter of the equivalent ellipse (d; in μm) was determined using the formula:

$$d = 4A/\pi \bullet D$$

Finally, as an index of the eccentricity (ε) of the ellipse, the minor diameter/major diameter ratio was determined using the formula:

$$\varepsilon = d/D$$

Fibers intersecting the upper transverse and left longitudinal lines of the AOI, as well as fibers that could not be entirely visualized, were excluded from counting.

NOS 3 Image Acquisition Protocol: All NOS3 images were collected according to the NOS1/2 image acquisition protocol outlined above. However, after capture, the color image was converted to an 8-bit grayscale image (grayscale 8) for ease of storage and transfer to other image-viewing platforms. Images were then processed using the Sharpen and HiGauss filters included in the ImagePro software package.

Examination of NOS3 Images: Images from WKY and SHR strains were scrutinized for qualitative differences in degree of staining in several structures, including arterioles, capillaries and venules.

Image Acquisition Protocol for Endothelial Cells in Skeletal Muscle Tissue Capillaries via Alkaline Phosphatase staining: After acquiring a fiber-typing image using the general procedures above, the image was converted to grayscale 8 for ease of storage, manipulation and analysis between image software platforms.

Capillary Counting Protocol: Image analysis began with the establishment of an AOI that includes as much tissue as possible without inclusion of gaps that were created when the samples were "bulked up" before sectioning as outlined in "Immunohistochemical Protocol for detection of Nitric Oxide Synthase in Skeletal Muscle Tissue" section. Total cross-sectional area of the AOI was recorded and total number of capillaries within the AOI was determined by manual counting, with care taken not to "double count" capillaries

that were in close proximity to one another. Capillary density was then determined by the formula:

Capillary density = number of capillaries in AOI/Cross-sectional area of AOI

To determine the average number of capillaries around a fiber, several fibers within the AOI and with clearly associated capillaries were selected. The fibers had to be entirely visible in order to be counted. These associated capillaries were counted and used to determine the number of capillaries around a fiber (CAF).

Western Blot Analysis of NOS Isoforms in Skeletal Muscle Tissue:

Two Western blots were performed. In the first blot, exposure times were corrected so that valid comparisons could be made between the NOS isoforms being studied. In the second blot, all membranes were simultaneously probed for both the NOS isoform of interest, as well as α-tubulin.

Tissue Preparation: Bilateral spinotrapezius muscles were exteriorized, blotted (taking care to remove all blood and connective tissue), weighed, snap-frozen in liquid nitrogen-chilled isopentane (Thermo Fisher Scientific Inc, Waltham, MA) and stored at -80 °C until ready for processing. Samples were then ground using a mortar and pestle that had been chilled with liquid nitrogen. Fresh lysis buffer was then prepared and consisted of 50 mM Tris-HCl, 5 mM EDTA, 10 mM EGTA, 50 µg/mL protease inhibitor (Thermo Fisher Scientific Inc, Waltham, MA) and 0.3% 2-mercaptoethanol. Lysis buffer was added to

ground tissue samples and first homogenized at 30 rpm for 10 repetitions and then sonicated for 20 seconds, three times per sample. Homogenized samples were placed on ice for 30 minutes and then centrifuged at 12,000 g for 10 minutes a 4 °C.

Total Protein Concentration Determination via the Bradford Method: Two µL of sample were mixed with 798 µL of deionized water and 200 µL Bradford reagent (BioRad Laboratories, Hercules, CA), shaken to mix and then vortexed before being transferred into spectrophotometer cuvettes. The spectrophotometer dilution setting was set to 500, optical density readings were made at 598 nm and then the samples were discarded.

Gel Electrophoresis Protocol: The sample buffer containing 50 µL betamercaptoethanol and 950 µL Laemmli buffer was added to homogenized tissue samples and vortexed, boiled for five to seven minutes and briefly centrifuged. 4-20% Criterion TGX Precast Gel (BioRad Laboratories, Hercules CA) was then loaded and sample buffer containing Tris, glycine and SDS was added. Samples were loaded and run at 190 V until the samples progressed through the stacking gel. Voltage was then reduced to 165 V and run for an additional 90 minutes.

Nitrocellulose Transfer Protocol: Finished gel was placed between layers of fibrous padding, filter paper and nitrocellulose (BioRad Laboratories, Hercules, CA), gently rolled to remove bubbles, placed in chilled transfer buffer and run at 300 mA and 40-60 V for 90 minutes.

Probing of Membrane: After verifying success of transfer with Ponceau stain (Sigma-Aldrich, Sigma-Aldrich, St. Louis, MO), the membrane was washed with Tris-buffered saline/Tween-20 (TBST) [100 mL TBS (Sigma-Aldrich, Sigma-Aldrich, St. Louis, MO), 900 mL deionized water, 500 µL Tween-20 (Sigma-Aldrich, Sigma-Aldrich, St. Louis, MO)] then blocked with 5% milk in TBST (5 g milk in 100 mL TBST; Tween-20 (Sigma-Aldrich, Sigma-Aldrich, St. Louis, MO) for at least one hour. Separate primary antibody solutions for NOS1-3, phosphorylated NOS1 and NOS3 and α-tubulin were prepared by adding 10 µL of antibody to 5% milk/TBST. The membrane was incubated in a cold room overnight with a single primary antibody in the following order: NOS1, NOS2, NOS3, phosphorylated NOS1 (first blot only), phosphorylated NOS3 (first blot only) and α-tubulin (NOS 1 antibody: Millipore, Temecula, CA; NOS2 antibody: Enzo Life Sciences, Plymouth Meeting, PA; NOS3 antibody: Santa Cruz Biotechnology, Santa Cruz, CA; phosphorylated NOS1 antibody: Millipore, Temecula, CA ; phosphorylated NOS3 antibody and α-tubulin antibodies: Cell Signaling Technology, Danvers, MA). After incubation the membrane was washed 4 – 5 times with TBST. The membrane was then incubated for at least one hour (and not more than three hours) in secondary antibody solution consisting of 3.5 µL donkey anti-rabbit IgG HRP-linked whole secondary antibody (GE Healthcare, Waukesha, WI) in 5% milk/TBST. After incubation the membrane was washed 4 – 5 times with TBST. The membrane was then incubated in a proprietary chemiluminescent reagent (Western Lighting *Plus*, PerkinElmer Inc., Waltham, MA) and developed on film (Eastman Kodak Company, Rochester, NY). Films were then

scanned into the ImageJ imaging software package (National Institutes of Health, Bethesda, MD) for processing.

Electrophoresis Gel Analysis of MHC Isoforms in Skeletal Muscle Tissue:

Tissue Preparation: Bilateral spinotrapezius muscles were exteriorized, blotted, weighed, snap-frozen in liquid nitrogen-chilled isopentane and stored at -80 °C until ready for processing. Individual, frozen muscles were first dehydrated for 1-2 hours before being minced in microcentrifuge tubes using microscissors and microforceps. Five hundred microliters of MHC extract solution (0.3 M NaCL, 0.15 M Na_2HPO_4 and 10 mM EDTA) per 1 mg of muscle tissue were added to the minced tissue before the samples were homogenized in microcentrifuge tubes using a miniature pestle. Homogenized samples were then refrigerated at 4 °C for 60 minutes (stirred every 10 minutes) before being centrifuged at 12,000 rpm for 10 minutes, yielding a final total protein concentration of 0.25 – 0.5 mg/mL. The supernatant was transferred to microcentrifuge tubes and stored at -70 °C until ready for use and the pellet was discarded.

Electrophoresis Stock Solutions: The following stock solutions were prepared prior to any electrophoresis experiments and stored for no more than one month at 4 °C, unless otherwise noted:

68.16% Glycerol: 68.16 mL glycerol in 100 mL deionized water.

29% Acrylamide-BIS : 14.21 g acrylamide and 0.29 g bis (N, N'-methylene-bis-acrylamide) in 50 mL deionized water. Solution was gravity filtered through Whatman #1 filter paper into a dark glass container and used immediately.

1.5 M Tris-HCl Base (pH 8.8): 9.085 g Tris in 50 mL deionized water. Tris was initially dissolved in 40 mL deionized water and pH adjusted to 8.8 with 6 N HCl before being volumized to 50 ml with deionized water.

0.5 M Tris-HCl Base (pH 6.8): 3.94 g Tris in 50 mL deionized water. Tris was initially dissolved in 40 mL deionized water and pH adjusted to 6.8 with 6 N HCl before being volumized to 50 ml with deionized water.

100 mM EDTA: 1.86 g EDTA in 50 mL deionized water.

10% Ethanol: 5 mL of absolute ethyl alcohol in 45 mL deionized water.

10% Sodium Docecyl Sulfate (SDS): 10 g SDS in 90 mL deionized water. Solution stored at RT.

Sample Buffer (2x Laemmli Sample Buffer): 12.5 mL 0.5 M Tris-HCl Base, 20 mL 10% SDS, 10 mL glycerol, 2 mL 2-mercaptoethanol, 2.5 mL bromophenol blue dye (3.5 mg bromophenol blue in 2.5 mL deionized water). Solution was stored in a dark glass container until ready for use.

10% Ammonium Persulfate: 0.050 g ammonium persulfate per 0.5 mL deionized water. Solution was prepared immediately prior to electrophoresis experiment.

Gel Electrophoresis Running Buffers: The following running buffers were prepared immediately prior to electrophoresis experiments and stored at 4 °C until ready for same-day use:

Upper Running Buffer (~380 mL required for gel electrophoresis): 100 mM Tris base, 150 mM glycine, 0.1% SDS and deionized water.

Lower Running Buffer (~1240 mL required for gel electrophoresis): 50 mM Tris base, 75 mM glycine, 0.05% SDS and deionized water.

Total Muscle Protein Assay: Protein concentration standards from BioRad Laboratories (Hercules, CA) were prepared according to proprietary instructions before being placed in a microtiter plate for analysis. The total protein concentration of each sample was determined using the Gel-Pro Analyzer software (Media Cybernetics, Inc., Bethesda, MD). After total protein concentration of each sample was determined, samples were diluted as necessary to a final concentration of 0.25 mg/mL by the addition of MHC extract solution.

Gel Preparation and Casting: Stock solutions were removed from the refrigerator and brought to room temperature. The 8% separating gel was prepared by combining the following components: 8.803 mL 68.16% glycerol, 5.520 mL 29% acrylamide-BIS, 2.667 mL 1.5 M Tris base, 2 mL 1 M glycine, 0.8 mL 10% SDS and 0.2 mL 10% ammonium persulfate. The mixture was thoroughly mixed and then degassed for 15 minutes and 10 µL tetramethylethylenediamine (TEMED; BioRad Laboratories, Hercules, CA) was added. The solution was drawn into a disposable pipette, taking care not to introduce air bubbles,

then slowly injected into a casting stand. A layer of 10% ethanol was then carefully placed on top of the separating gel, which was allowed to set for at least 30 minutes while the 4% stacking gel was prepared (4.494 mL 68.16% glycerol, 1.380 mL 29% acrylamide-BIS, 1.4 mL 0.5 M Tris base, 0.4 mL 100 mM EDTA, 0.4 mL 10% SDS, 1.821 mL deionized water and 0.1 mL 10% ammonium persulfate, all from BioRad Laboratories, Hercules, CA). The mixture was swirled and degassed for 15 minutes. Meanwhile, the 10% ethanol was poured off and glass gel casting plates carefully dried with Whatman #1 filter paper (GE Healthcare, Waukesha, WI). The well comb was placed at an angle between the glass plates of the casting stand and 5 µL of TEMED was added to the degassed solution. The solution was then drawn into a disposable pipette, taking care not to introduce air bubbles, and slowly injected into the casting stand. The well comb was tapped gently to remove any trapped air bubbles and the stacking gel was allowed to set for at least one hour.

Muscle Sample Preparation: Muscle samples and the pre-stained standard were removed from the freezer and allowed to thaw during preparation of the stacking gel. After thoroughly mixing the thawed samples, 30 µL of muscle sample was combined with 25 µL of sample buffer to yield a final sample concentration of 0.225 mg/mL. Samples were then boiled for 5 minutes and allowed to cool to RT.

Assembly of Electrophoresis Apparatus: After being allowed to set, gels were removed from the casting stand, clamped to a central cooling core and placed in the lower buffer chamber. A small amount (~10 mL) of upper running buffer was placed into the upper

buffer chamber and the well comb was slowly removed. Wells were gently cleaned with upper running buffer using a 5 mL syringe with a blunted 23 gauge needle. Gel loading pipette tips were used to load 20-40 µL of muscle sample (depending on concentration) into each well, excluding the first and last well for quality control purposes. The pre-stained standard was loaded into two wells.

Running Conditions: After the assembly was placed in the refrigerator, the upper and lower buffer chambers were filled with their respective buffers. After bubbles were gently removed from the bottom of the glass plates, 400 µL of 2-mercaptoethanol was added to the upper buffer chamber. Electrodes were secured to the apparatus and a constant voltage of 275 V and maximum current of 25 mA was applied for 90 minutes. The maximum current was then reduced to 15 mA/gel and the gel was allowed to run for 29 hours.

Processing: Gels were carefully scanned into a computer using the GelPro imaging software package (Media Cybernetics, Inc., Bethesda, MD) for later image processing.

Statistics:

Rat subject morphological data, fiber geometric data, MHC gel optical density data, mean capillary density scores, mean scores for degree of NOS1 staining and Western blot protein content comparisons between strains were all analyzed by the unequal variance *t*-test. Fiber geometric data, MHC gel optical density data and Western blot protein content

comparisons within one strain of rat were carried out with the Welch ANOVA and the Tukey-Kramer HSD post-hoc test was used to determine differences between means. For all analyses, differences were considered significant at $p < 0.05$. Values presented in the text, tables and graphs are means ± standard error (SE).

RESULTS

Rat Subjects

Summary statistics for the rat subjects used in the immunohistochemical (IHC), Western blot (WB) and myosin heavy chain (MHC) gel electrophoresis experiments are presented in Tables 1 and 2. SHR subjects used in IHC experiments were slightly, but significantly, older than their WKY controls. No statistically significant difference was found between the ages WKY and SHR rat subjects used in WB and gel electrophoresis experiments. As expected, mean invasive mean arterial blood pressures (MAP) of SHR subjects used in IHC experiments were found to be significantly higher than those of their age-matched WKY controls. Interestingly, mean invasive MAPs for WKY and SHR WB subjects were not significantly different. As mentioned in the Materials and Methods section, non-invasive hemodynamic data were also collected. However, these data were meant as a semi-quantitative measure to monitor and confirm the degree of hypertension in SHR subjects prior to tissue harvesting and are therefore not being presented, in deference to the more accurate invasive measurements. No statistically significant difference was found between the heart rates of age-matched WKY and SHR rat subjects used in IHC, WB and gel electrophoresis experiments. Unexpectedly, SHR subjects used in IHC, WB and MHC gel electrophoresis experiments weighed significantly more than their age-matched WKY

controls. There were no significant differences in the weights of either the left or right spinotrapezius muscles of the WKY and SHR subjects used in WB and gel electrophoresis experiments.

Table 1 SUMMARY STATISTICS FOR RAT SUBJECTS USED IN IHC EXPERIMENTS

Strain	*n*	Age (Weeks)	Body Weight (g)	Invasive MAP (mmHg)	Heart Rate (Beats/ Min)
WKY	5	16.0 ± 0.074	274.1 ± 2.43	102.0 ± 2.30	384.6 ± 8.05
SHR	5	16.4 ± 0.0*	344.9 ± 1.36*	155.9 ± 4.47*	376.4 ± 7.56

Values are mean ± SE. * = Significantly different from age-matched WKY, $p < 0.05$

Table 2 SUMMARY STATISTICS FOR RAT SUBJECTS USED IN WB AND MHC GEL ELECTROPHORESIS EXPERIMENTS

Strain	*n*	Age (Weeks)	Body Weight (g)	Invasive MAP (mmHg)	Heart Rate (Beats/Min)	Left Spinotrapezius Muscle Weight (g)	Right Spinotrapezius Muscle Weight (g)
WKY	4	17.0 ± 0.0	268.8 ± 0.4	114.4 ± 4.5	402.0 ± 19.5	0.087 ± 0.011	0.087 ± 0.011
SHR	4	17.0 ± 0.0	363.0 ± 0.7*	134.8 ± 10.8	403.0 ± 13.7	0.091 ± 0.015	0.103 ± 0.011

Values are means ± SE. * = Significantly different from age-matched WKY, $p < 0.05$

Myosin Heavy Chain (MHC) Determinations

MHC Fiber Type Distributions:

Examples of Images Collected: Figures 1 and 2 below are representative images of Type I fiber staining in WKY and SHR subjects, respectively. Note the lines designating the area of interest (AOI) within the image (scale bar = 50 µm). Figures 3 and 4 are examples of Type IIA fiber staining in WKY and SHR subjects, respectively. Note the lines designating the AOI within the image (scale bar = 50 µm). Figures 5 and 6 are examples of IIB fiber staining in WKY and SHR subjects, respectively. Note the lines designating the AOI within the image (scale bar = 50 µm). Negative control images were too dim to be adequately imaged.

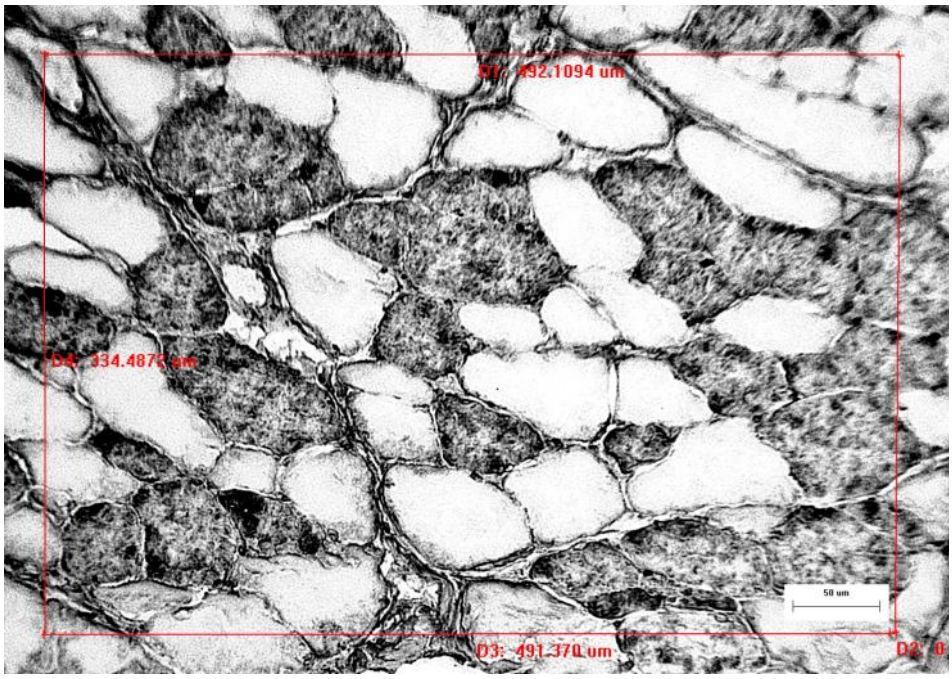

Figure 1. Representative image of Type I fiber staining in WKY rat. Scale bar = 50 µm

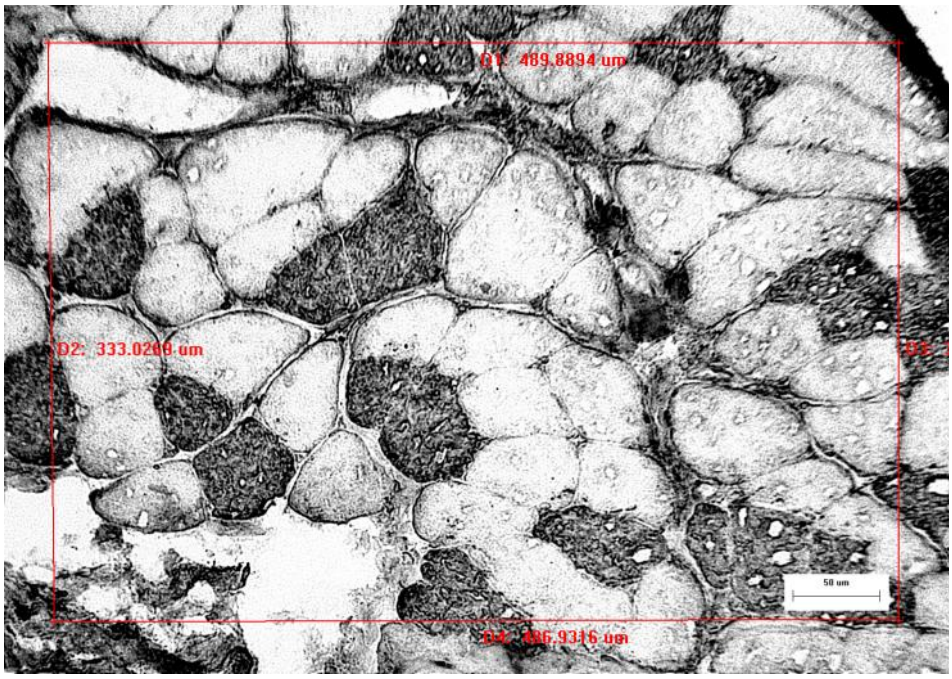

Figure 2. Representative image of Type I fiber staining in SHR. Scale bar = 50 µm

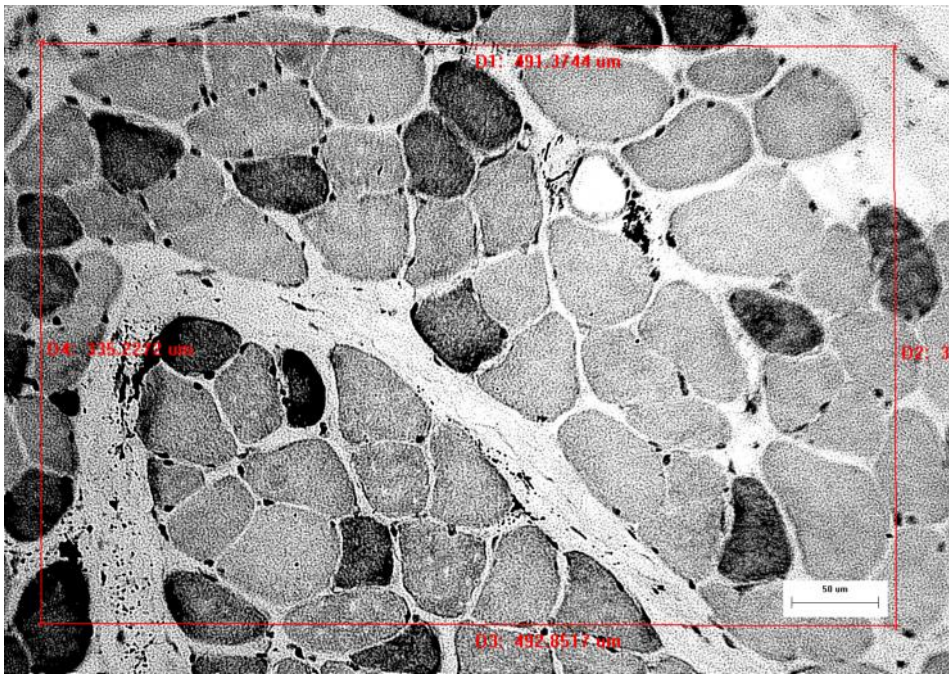

Figure 3. Representative image of Type IIA fiber staining in WKY rat. Scale bar = 50 µm

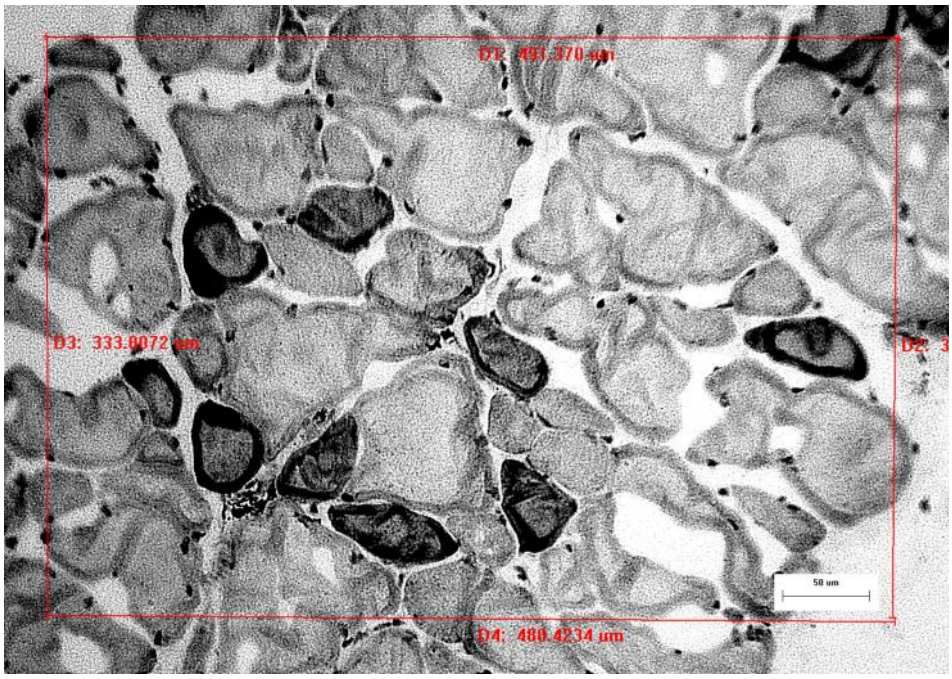

Figure 4. Representative image of Type IIA fiber staining in SHR. Scale bar = 50 µm

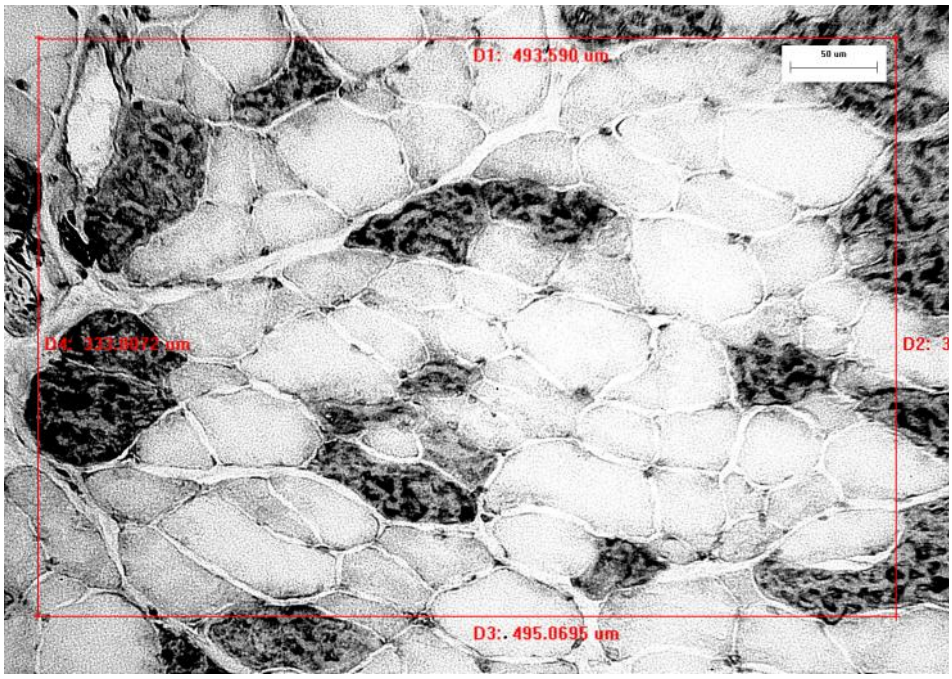

Figure 5. Representative image of Type IIB fiber staining in WKY rat. Scale bar = 50 µm

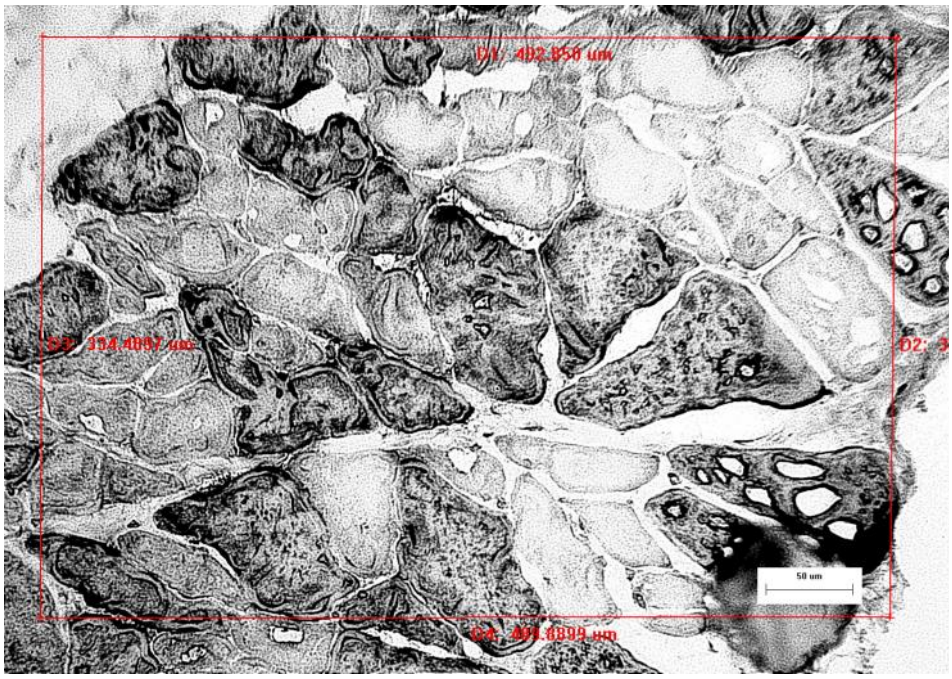

Figure 6. Representative image of Type IIB fiber staining in SHR. Scale bar = 50 µm

Fiber Type Distribution Statistics: Table 3 describes the distribution of positive-staining fibers as the number of positive fibers of each fiber type divided by total number of positive and negative (i.e., non-stained) fibers for that fiber type in WKY and SHR subjects. Table 4 describes the total cross-sectional area of positive fibers of each type divided by the total cross-sectional area of all positive and negative fibers of that type in WKY and SHR subjects.

Table 3 SUMMARY STATISTICS FOR PERCENT FIBER POPULATION (FIBER COUNT BASIS)

Fiber Type	WKY 2	WKY 3	WKY 4	WKY 5	Mean for WKY ± SE	SHR 4	SHR 5	Mean for SHR ± SE
Type I	40.9	47.8	32.5	42.1	40.8 ± 3.2	55.3	*	55.3
Type IIA	42.9	25.4	25.5	27.1	30.2 ± 4.2	19.4	19.8	19.6 ± 0.1
Type IIB	22.5	12.1	31.8	17.0	20.9 ± 4.2	23.2	*	23.2

Values are percentages. *Insufficient Type I and IIB fiber count data for SHR 5 to complete calculation of fiber population.

Table 4 SUMMARY STATISTICS FOR PERCENT FIBER POPULATION (TOTAL CROSS-SECTIONAL AREA BASIS)

Fiber Type	WKY 2	WKY 3	WKY 4	WKY 5	Mean for WKY ± SE	SHR 4	Mean for SHR ± SE
Type I	53.6	51.9	30.1	39.7	43.8 ± 5.5	43.6	43.6*
Type IIA	34.8	21.2	15.3	20.5	23.0 ± 4.2	9.9	9.9*
Type IIB	46.5	20.0	42.2	22.9	32.9 ± 6.7	48.0	48.0*

Values are percentages. *Insufficient data exist to calculate mean ± SE.

Analysis of MHC Isoform Expression by Gel Electrophoresis:

Figures 7 and 8 below are representative images of the MHC protein band images obtained from the electrophoretic gel. Note that there was some degradation in quality when the images were enlarged for insertion into this document. No statistically significant difference in the amount of Type I, IIa or IIb MHC protein, determined by gel electrophoresis and expressed as the intensity of the protein band, was detected between WKY and SHR subjects, as noted in Table 5. However, when levels of Type I, IIa and IIb MHC protein were compared within the WKY subjects, there was significantly less IIa MHC protein than Type I and IIb MHC protein (Table 6 and Fig. 9). There was no statistically significant difference between the intensities of Type I, IIa and IIb MHC isoforms in SHR subjects (Fig. 10). Type IId/x MHC protein was not detected in the gel electrophoresis experiment in either strain. Migration sequence of MHC isoforms was determined based on observations by Talmadge and Roy (1993).

Table 5 SUMMARY STATISTICS FOR INTENSITY OF MHC ISOFORM BANDS IN WKY VS. SHR SUBJECTS

Strain	*n*	Type I	Type IIA	Type IIB
WKY	4	37.0 ± 3.8	18.7 ± 1.2	44.3 ± 3.8
SHR	4	37.5 ± 2.1	25.9 ± 3.1	36.6 ± 5.0

Values are means ± SE (arbitrary units). No statistically significant difference detected between strains ($\alpha = 0.05$).

Table 6 SUMMARY STATISTICS FOR INTENSITY OF MHC ISOFORM BANDS WITHIN STRAINS

Strain	MHC Isoform	Mean ± SE
WKY ($n = 4$)	Type I	37.0 ± 3.8%*
	Type IIa	18.7 ± 1.2%†
	Type IIb	44.3 ± 3.8%*
SHR ($n = 4$)	Type I	37.5 ± 2.1%
	Type IIa	25.9 ± 3.1%
	Type IIb	36.6 ± 5.0%

Isoforms not connected by the same symbol are significantly different, $p < 0.05$

Figure 7. Representative image of MHC protein bands in WKY rat.

Figure 8. Representative image of MHC protein bands in SHR.

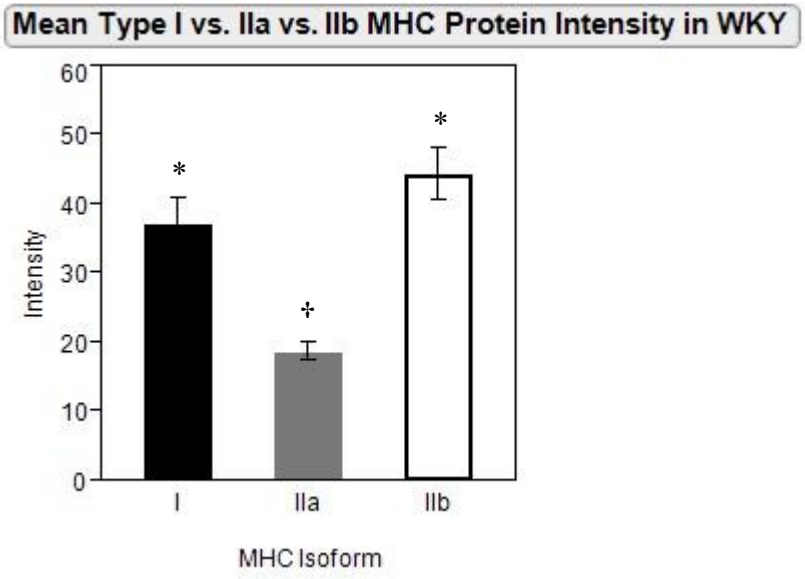

Figure 9. MHC Intensity for Type I vs. IIa vs. IIb in WKY (Mean ± SE, α = 0.05).
The three MHC isoform intensity means were compared using the unequal variance *F*-test and found to be significantly different.
[(F(2,9) = 17.3), *p*-value = 0.0008].
Isoforms not connected by the same symbol are significantly different.

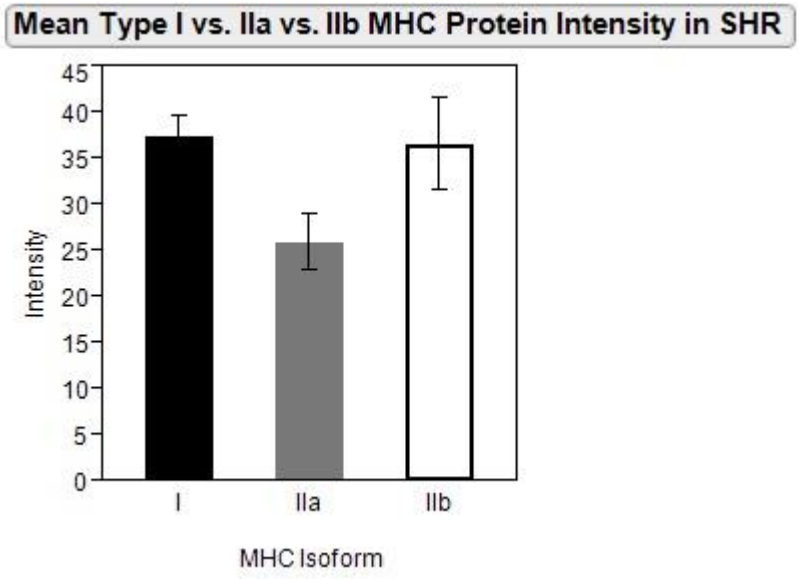

Figure 10. MHC Intensity for Type I vs. IIA vs. IIB in SHR (Mean ± SE, $\alpha = 0.05$). The three MHC isoform intensity means were compared using the unequal variance *F*-test and not found to be significantly different.
[$(F(2,9) = 3.23)$, *p*-value = 0.0878].

MHC Fiber Geometric Data

Fiber Cross-sectional Area: Mean cross-sectional areas of Type I fibers from each strain were compared and WKY fibers were demonstrated to be significantly larger than SHR fibers (Table 7). Mean cross-sectional areas of Type IIA fibers were compared between strains and not found to be significantly different. Mean cross-sectional areas of Type IIB fibers were compared and SHR fibers were demonstrated to be significantly larger than WKY fibers (Table 7).

Fiber Perimeter: Mean perimeters of WKY Type I fibers were found to be significantly greater than those of SHR subjects (Table 7). There were no significant differences between the mean perimeters of WKY and SHR Type IIA fibers (Table 7). However, mean perimeters of SHR Type IIB fibers were found to be significantly greater than those of age-matched WKY control subjects (Table 7).

Minimum Fiber Diameter: The mean minimum diameters of WKY Type I fibers was found to be significantly greater than that of SHR subjects. The mean minimum diameters of WKY and SHR Type IIA fibers were not found to be significantly different (Table 7). The mean minimum diameter of SHR Type IIB fibers was found to be significantly greater than that of age-matched WKY control subjects (Table 7).

Maximum Fiber Diameter: The mean maximum diameter of WKY Type I fibers was found to be significantly greater than that of SHR subjects (Table 7). The mean maximum diameters of WKY and SHR Type IIA and IIB fibers were not found to be significantly different (Table 7).

Min/Max Fiber Diameter Ratio: No statistically significant differences were detected in the minimum/maximum fiber diameter ratios for Type I, IIA and IIB fibers between the WKY and SHR strains (Table 7).

Minor Elliptical Fiber Diameter: The mean minor elliptical diameter of WKY Type I fibers was found to be significantly greater than that of SHR subjects (Table 8). There was no significant difference between the mean minor elliptical diameters of WKY and SHR Type IIA fibers (Table 8). The mean minor elliptical diameters of SHR Type IIB fibers were found to be significantly greater than those of age-matched WKY control subjects (Table 8).

Major Elliptical Fiber Diameter: The mean major elliptical diameter of WKY Type I fibers was found to be significantly greater than that of SHR subjects (Table 8). The mean major elliptical diameters of WKY and SHR Type IIA fibers were not found to be significantly different (Table 8). The mean major elliptical diameter of SHR Type IIB fibers was found to be significantly greater than that of age-matched WKY control subjects (Table 8).

Minor/Major Elliptical Diameter Ratio: No statistically significant differences were detected in the minor/major fiber elliptical diameter ratios for Type I, IIA and IIB fibers between the WKY and SHR strains (Table 8).

Table 7 SUMMARY STATISTICS FOR BASIC MHC FIBER GEOMETRIC DATA

Strain	MHC Fiber Type	*n*	Minimum Fiber Diameter	Maximum Fiber Diameter	Min/Max Diameter Ratio	Fiber Perimeter	Fiber Cross-sectional Area
WKY	Type I	331	36.3 ± 0.6	66.7 ± 1.2	0.57 ± 0.01	177.9 ± 3.0	2079.3 ± 61.0
	Type IIA	203	27.3 ± 0.5	50.9 ± 1.1	0.56 ±0.01	134.4 ± 2.5	1204.2 ± 39.5
	Type IIB	181	42.1 ± 0.8	83.4 ± 2.0	0.53 ± 0.01	226.4 ± 5.1	3006.7 ± 115.7
SHR	Type I	227	32.3 ± 0.7*	61.3 ± 1.5*	0.55± 0.01	162.5 ± 4.0*	1767.2 ± 74.8*
	Type IIA	129	28.6 ± 0.9	51.7 ± 1.3	0.56 ± 0.01	136.4 ± 3.3	1283.8 ± 58.2
	Type IIB	101	47.8 ± 1.6*	90.1 ± 3.2	0.55 ± 0.01	251.7 ± 8.8*	3865.7 ± 249.2*

Values are means ± SE in μm [except for cross-sectional area (in μm^2) and ratio (unitless)]. *n* = number of fibers measured. * = Significantly different from age-matched WKY, $p < 0.05$.

Table 8 SUMMARY STATISTICS FOR MHC FIBER ELLIPTICAL DATA

Strain	MHC Isoform	*n*	Minor Fiber Elliptical Diameter	Major Elliptical Diameter	Minor/Major Elliptical Diameter Ratio
WKY	Type I	327	34.9 ± 0.5	71.7 ± 1.4	0.51 ± 0.01
	Type IIA	202	27.1 ± 0.5	53.9 ± 1.1	0.52 ± 0.01
	Type IIB	180	39.1 ± 0.7	93.7 ± 2.3	0.44 ± 0.01
SHR	Type I	223	32.3 ± 0.6*	65.6 ± 1.8*	0.52 ± 0.01
	Type IIA	129	28.4 ± 0.8	54.2 ± 1.4	0.53 ± 0.01
	Type IIB	101	43.9 ± 1.3*	104.1 ± 3.8*	0.44 ± 0.01

Values are means ± SE in µm [except ratio (unitless)]. *n* = number of fibers measured.
* = Significantly different from age-matched WKY, $p < 0.05$.

Alkaline Phosphatase Staining to Reveal Capillary Endothelium

Capillary density and the number of capillaries around a fiber (CAF) were calculated for both strains of rats using the procedures outlined in the Materials and Methods section. There was no significant difference in either capillary density or mean CAF between the two strains (Table 9). Figures 11 and 12 below are examples of alkaline phosphatase staining to reveal capillary endothelium in WKY and SHR subjects, respectively. Scale bars = 50 μm.

Table 9 SUMMARY STATISTICS FOR CAPILLARITY

Metric	Strain	Observations	Mean ± SE
Capillary Density (capillaries/mm^2)	WKY	12	224.3 ± 23.0
	SHR	11	200.1 ± 16.1
Capillaries Around a Fiber (CAF)	WKY	41	2.51 ± 0.224
	SHR	30	2.87 ± 0.208

Observations for: 1) Capillary Density = regions of interest examined, 2) CAF = number of fibers examined.
No statistically significant difference detected between strains for either metric ($\alpha = 0.05$).

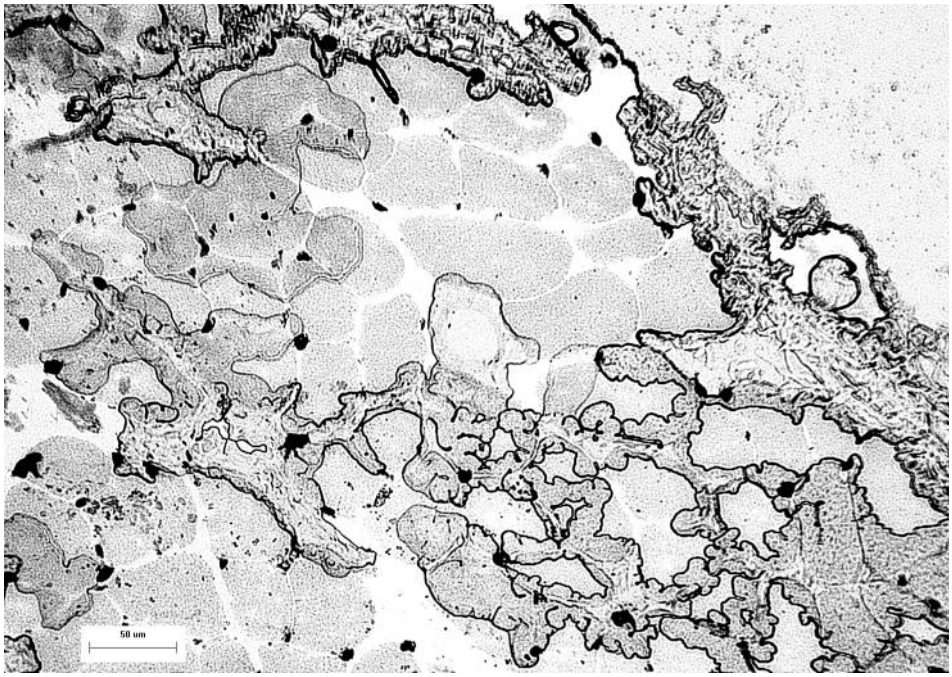

Figure 11. Representative image of alkaline phosphatase staining for capillary endothelium in WKY rat.
Scale bar = 50 μm

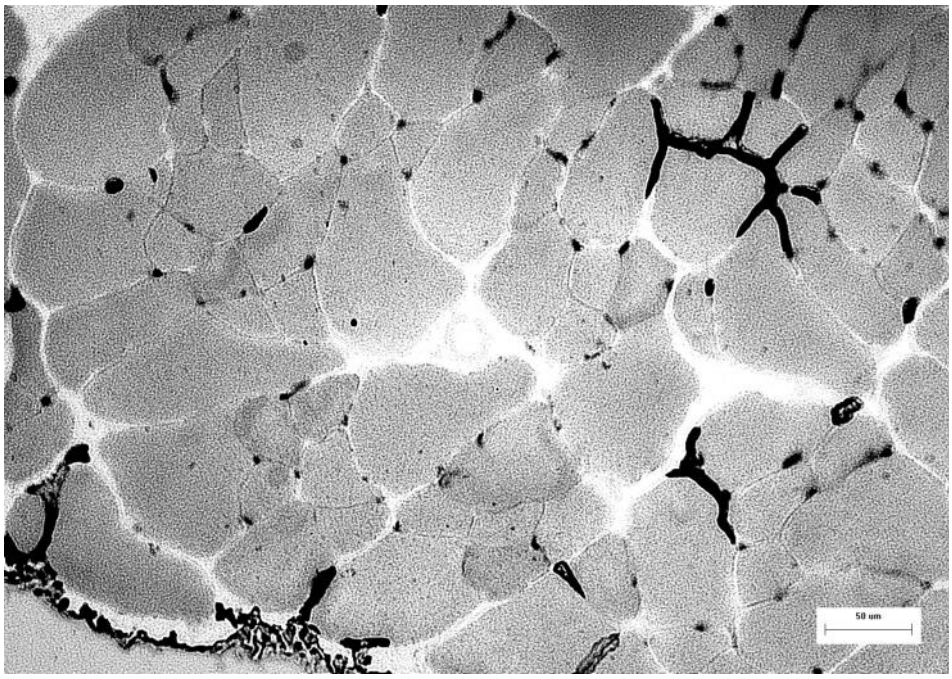

Figure 12. Representative image of alkaline phosphatase staining for capillary endothelium in SHR.
Scale bar = 50 µm

Co-localization Studies of Nitric Oxide Synthase Isoforms

Nitric Oxide Synthase 1 (NOS1): Figures 13 and 14 below are representative images of NOS1 staining in WKY and SHR subjects, respectively. Scale bar = 50 µm. The numerically labeled fibers were determined also to contain the Type I MHC isoform by serial tissue sample sectioning and staining. The degree of NOS1 / Type I MHC staining / co-localization was determined using the following numerical scale:

0 = absent 1 = light staining 2 = intermediate staining 3 = dark staining

The image grading instruction sheet given to all seven observers can be found in Appendix A. There was no significant difference in the practice mean numeric grading scores among observers (Appendix B). Summary statistics for the practice grading session are presented in Appendix C. As noted, observers #4, #6 and #7 detected statistically significant differences in the degree of NOS1 staining between experimental WKY and SHR subjects (Table 10). Visual inspection revealed sarcolemmal and sub-sarcolemmal NOS1 staining in nearly all of Type I examined. However, some fibers demonstrated a diffuse and somewhat granular staining pattern, which often varied in intensity between fibers in the same image.

Table 10 SUMMARY STATISTICS FOR EXPERIMENTAL NUMERIC STAINING GRADES

Observer	Strain	Mean Numeric Score ± SE
1	WKY (n = 3)	1.59 ± 0.07
	SHR (n = 4)	1.64 ± 0.08
2	WKY (n = 3)	1.32 ± 0.08
	SHR (n = 4)	1.51 ± 0.07
3	WKY (n = 3)	1.48 ± 0.06
	SHR (n = 4)	1.64 ± 0.06
4	WKY (n = 3)	1.17 ± 0.08
	SHR (n = 4)	1.58 ± 0.08*
5	WKY (n = 3)	1.83 ± 0.09
	SHR (n = 4)	1.81 ± 0.10
6	WKY (n = 3)	1.23 ± 0.09
	SHR (n = 4)	1.58 ± 0.09*
7	WKY (n = 3)	0.85 ± 0.06
	SHR (n = 4)	1.18 ± 0.06*

All observers graded a total of 81 WKY fibers and 72 SHR fibers. n = number of animals.
* = Significantly different from age-matched WKY, $p < 0.05$.

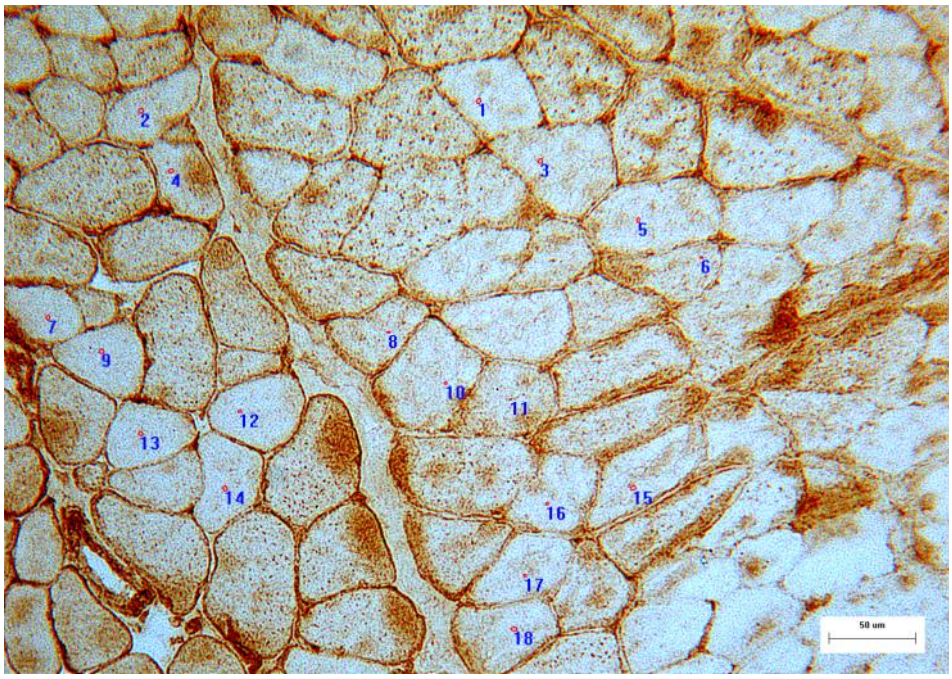

Figure 13. Representative image of NOS1 staining in WKY rat. Scale bar = 50 µm

Figure 14. Representative image of NOS1 staining in SHR.
Scale bar = 50 µm

Nitric Oxide Synthase 2 (NOS2): Figures 15 and 16 are representative images of NOS2 staining in WKY and SHR subjects, respectively. Scale bar = 50 µm. The numerically labeled fibers were determined also to contain the Type IIA and IIB MHC isoforms (as determined by staining with a proprietary primary antibody that recognizes both Type IIA and IIB MHC isoforms) by serial tissue sample sectioning and staining. Inspection of the entire image series revealed evenly distributed staining that appeared somewhat punctate with little variation in the degree of staining between individual fibers and with no discernable difference between rat subject strains. It was therefore determined that, unlike the NOS1 staining, NOS2 staining analysis would not benefit significantly from further semi-quantitative analysis by a group of individual observers.

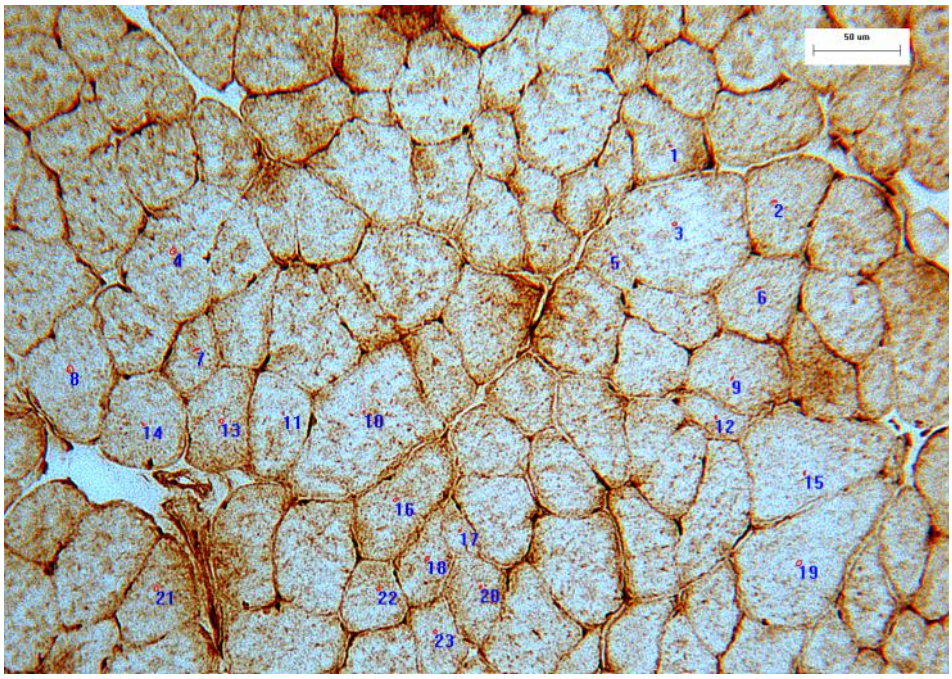

Figure 15. Representative image of NOS2 staining in WKY rat. Scale bar = 50 µm

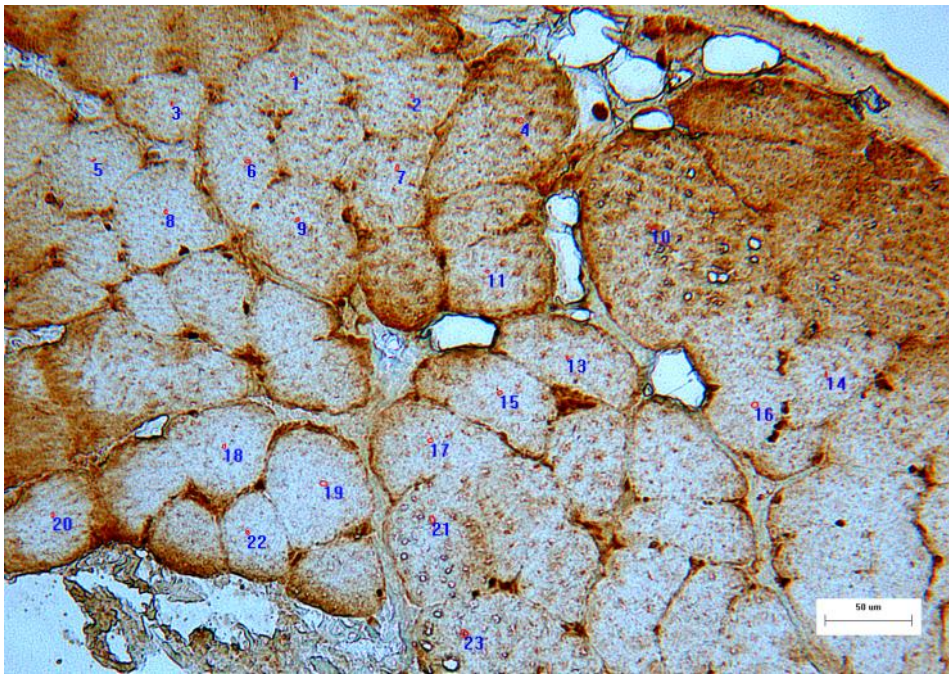

Figure 16. Representative image of NOS2 staining in SHR. Scale bar = 50 µm

Nitric Oxide Synthase 3 (NOS3): Figures 17 and 18 below are representative images of NOS3 staining in WKY and SHR subjects, respectively. Scale bar = 50 µm. Inspection of the entire image sequence revealed uniform, punctate-like NOS3 staining within muscle fibers, regardless of rat subject strain being examined. Most striking was the intense staining of the arteriolar endothelium and, to a lesser extent, the venular endothelium. This intense level of staining raises several questions which will be addressed in the Discussion section.

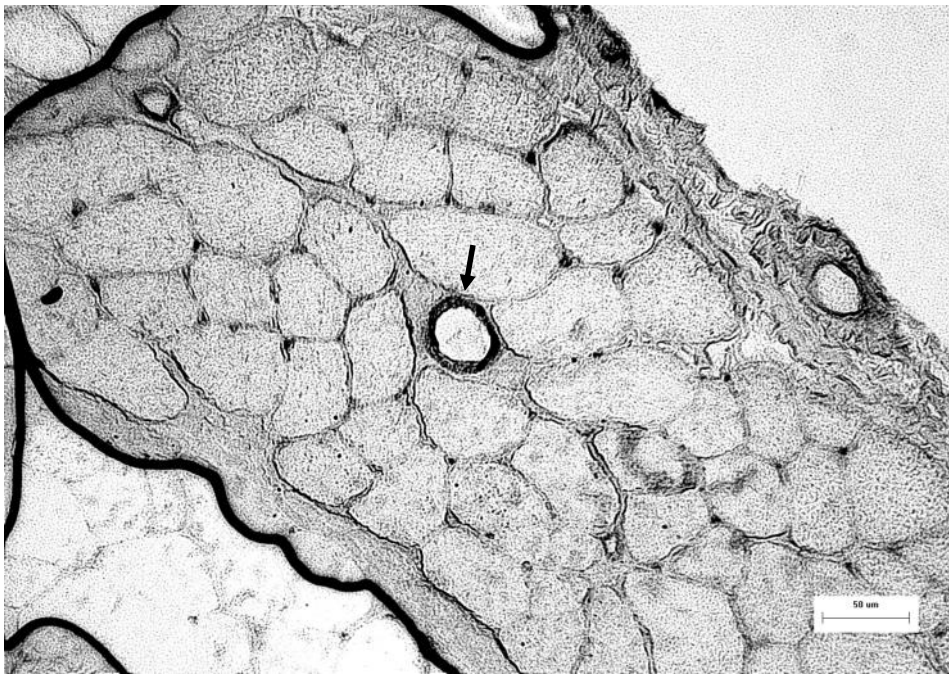

Figure 17. Representative image of NOS3 staining in WKY rat.
Scale bar = 50 µm

Intense arteriolar staining is denoted by arrow in center of image.

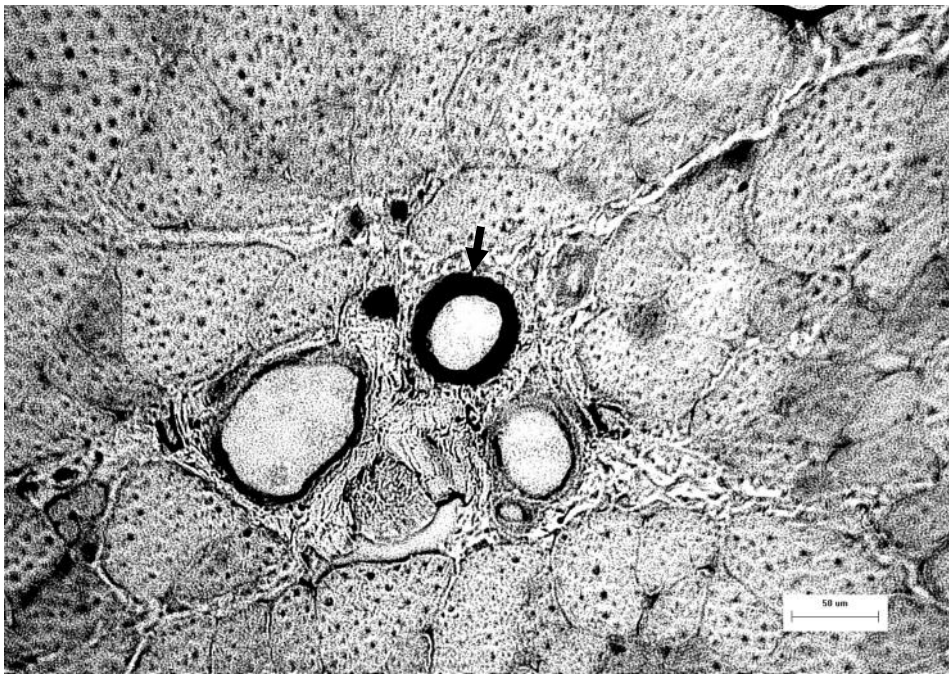

Figure 18. Representative image of NOS3 staining in SHR.
Scale bar = 50 µm

Intense arteriolar staining is denoted by arrow in center of image.

Co-localization of NOS3 and Alkaline Phosphatase (AP) Staining for Capillary Endothelium:

Data from the twenty three pairs of images collected from both WKY and SHR subjects revealed that 46.6% of the NOS3 "spots" detected co-localized with a corresponding AP "spot" in the next serial WKY rat spinotrapezius muscle section. In the SHR subjects, 32.3% of the NOS3 "spots" detected co-localized with a corresponding AP "spot" in the next serial tissue section. Of the NOS3 "spots" that lacked a corresponding AP "spot," 98% of those NOS3 "spots" were located between fibers in WKY subjects, as opposed to within a fiber, while only 55% of those NOS3 "spots" were located between fibers in the SHR subjects (Table 11).

Table 11 SUMMARY STATISTICS FOR CO-LOCALIZATION OF NOS3 AND ALKALINE PHOSPHATASE STAINING FOR CAPILLARY ENDOTHELIUM

Strain	Number of AP spots detected	Number of Corresponding NOS3 spots detected	% co-localization of AP and NOS3 spots	Number of spots on NOS3 image without corresponding AP spot	Number of NOS3 spots between fibers	% of NOS3 spots between fibers	% of NOS3 spots within fiber
WKY	163	76	46.6	97	95	98	2
SHR	158	51	32.3	80	44	55	45

Western Blot Analysis of NOS Isoforms:

Figure 19 below contains representative images of α-tubulin, NOS1, NOS2 and NOS3 protein bands from Western blots conducted to determine NOS expression in spinotrapezius muscle tissue samples. WKY protein samples occupy lanes 1 – 4, while SHR protein samples occupy lanes 5-7. In the first blot, no significant differences were found in the amount of NOS1, NOS2 or NOS3 between strains (Table 12 above). "Intensity" values are the ratios of the NOS Western blot intensity value divided by the corresponding α-tubulin value. There was significantly more NOS1 than either NOS2 or NOS3 in both WKY and SHR subjects used in the first blot (Fig. 20). Although the phosphorylated forms of both NOS1 and NOS3 were probed for, their corresponding protein bands were too faint to be sufficiently imaged in the first blot (data not shown) and were therefore not probed for in the second blot.

The second blot revealed significantly less NOS3 in SHR subjects versus their WKY controls (Table 13). Although there is relatively more NOS1 than both NOS2 and NOS3 in both strains, unequal variance statistical analysis failed to detect statistically significant differences in NOS1, NOS2 and NOS3 within subjects from either strain in the second blot (Fig. 21).

Table 12 SUMMARY STATISTICS FOR NOS1-3 EXPRESSION IN WKY AND SHR STRAINS AS DETERMINED BY WESTERN BLOT #1

Strain	NOS Isoform	*n*	NOS/α-tubulin Intensity Ratio
WKY	NOS1	4	2.14 ± 0.20
	NOS2	4	0.960 ± 0.06
	NOS3	4	0.936 ± 0.02
SHR	NOS1	3	2.18 ± 0.05
	NOS2	3	0.915 ± 0.01
	NOS3	3	0.940 ± 0.10

Values are means ± SE (unitless). *n* = number of animals.
No statistically significant differences in NOS1-3 expression detected between strains (α = 0.05).

Table 13 SUMMARY STATISTICS FOR NOS1-3 EXPRESSION IN WKY AND SHR STRAINS AS DETERMINED BY WESTERN BLOT #2

Strain	NOS Isoform	*n*	NOS/α-tubulin Intensity Ratio
WKY	NOS1	3	8.48 ± 2.13
	NOS2	3	2.32 ± 0.77
	NOS3	3	0.43 ± 0.02
SHR	NOS1	3	17.7 ± 9.0
	NOS2	3	3.58 ± 1.57
	NOS3	3	0.11 ± 0.05*

Values are means ± SE (unitless). *n* = number of animals.
* = Significantly different from age-matched WKY, $p < 0.05$.

Figure 19. Representative protein band images of A) α-tubulin (52 kDa), B) NOS1 (165 kDa), C) NOS2 (130 kDa) and D) NOS3 (140 kDa) in Western blots

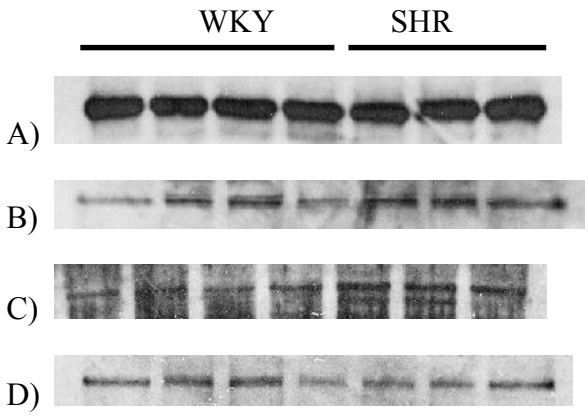

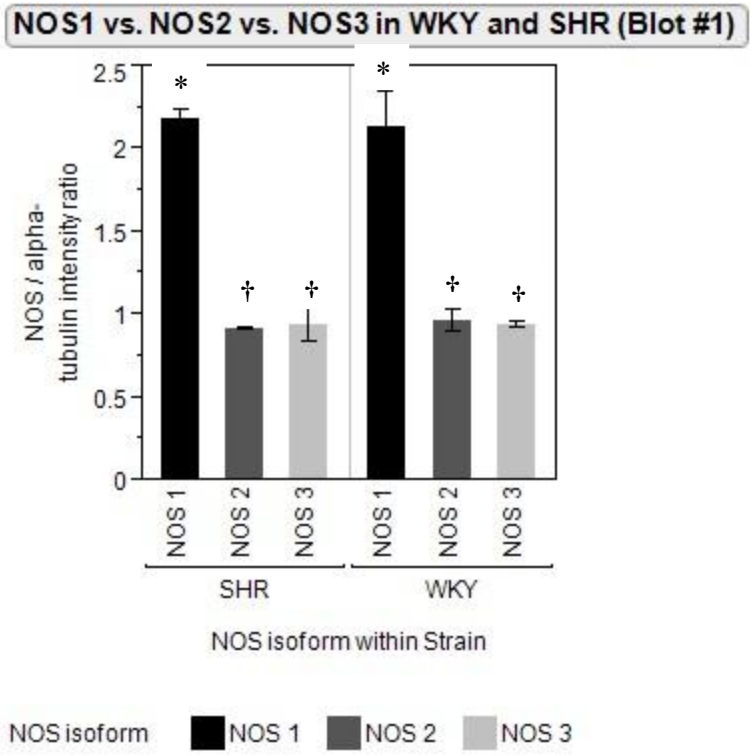

Isoforms not connected by the same symbol are significantly different, $p > 0.05$

Figure 20. NOS1 vs. NOS2 vs. NOS3 in WKY and SHR in Blot #1 ($\alpha = 0.05$).
The means were compared using an unequal variance *F*-test and found to be significantly different in both strains.
WKY = [($F(2, 4.26) = 15.6$), *p*-value = 0.0110]; SHR = [($F(2, 2.71) = 218.5$), *p*-value = 0.0010]

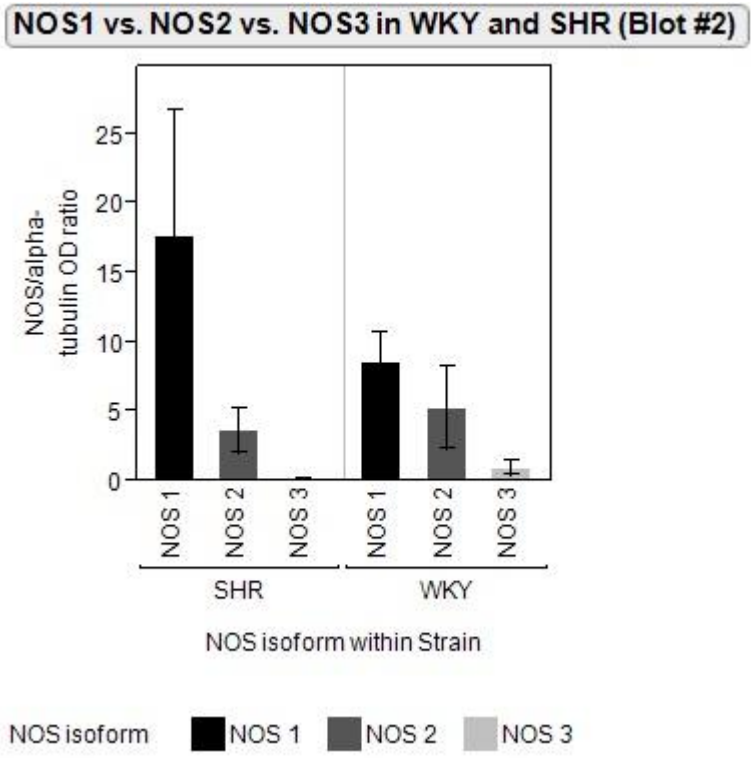

Figure 21. NOS1 vs. NOS2 vs. NOS3 in WKY and SHR in Blot #2 ($\alpha = 0.05$). The means were compared using an unequal variance *F*-test and found not to be significantly different in either strain.
WKY = [($F(2, 2.67) = 8.13$), *p*-value = 0.0732]; SHR = [($F(2, 2.67) = 3.49$), *p*-value = 0.1799]

DISCUSSION

Summary of Results:

Overview: As best as can be determined, this is the first study to characterize the fiber type population, geometric morphology, capillarity and nitric oxide synthase (NOS) expression of the spinotrapezius muscle of the spontaneously hypertensive rat (SHR) and make direct comparisons to its normotensive control, the Wistar-Kyoto rat (WKY) rat.

Fiber Type Populations: Percent fiber type population by fiber count from this study indicates the spinotrapezius muscle of the WKY is comprised of 40.8% Type I fibers, 30.2% Type IIA fibers and 20.9% Type IIB fibers. Using the same methodology, it was determined that the SHR is comprised of 55.3% Type I fibers, 19.4% Type IIA fibers and 23.2% Type IIB fibers. Percent fiber population by cross-sectional area (CSA) from this study indicates the spinotrapezius muscle of the WKY is comprised of 43.8% Type I fibers, 23.0% Type IIA fibers and 32.9% Type IIB fibers. Using the same methodology, it was determined the SHR is comprised of 43.6% Type I fibers, 9.9% Type IIA fiber and 48.0% Type IIB fibers. The fiber population percentages by CSA for the SHR add up to more than 100% (101.5%), but because of the variability of the individual fiber type percentages, the total is not significantly different from 100%. Considering the drawbacks

of using CSA to determine fiber populations, there is a reasonable explanation for this discrepancy which will be discussed later in this chapter.

Morphometry of Fibers:

Basic Fiber Geometry: Results from this study indicate that minimum and maximum fiber diameters, fiber perimeter and CSA of Type I fibers are all significantly smaller in the SHR compared to the WKY control. Conversely, minimum fiber diameter, fiber perimeter and CSA of Type IIB fibers are significantly larger in the SHR compared to the WKY. There were no statistically significant differences in any basic fiber geometry metric detected in Type IIA fibers between strains. Furthermore, no significant differences in the minimum/maximum fiber diameter ratio were detected between strains.

Elliptical Fiber Geometry: Results from this study indicate that minor and major elliptical diameters of Type I fibers in the SHR were significantly smaller than those of their age-matched WKY normotensive controls. Conversely, the minor and major elliptical diameters of Type IIB fibers in the SHR were significantly larger than those of their WKY normotensive controls. Finally, no significant differences in the minor/major elliptical fiber diameter ratio were detected between strains.

Capillarity: No statistically significant differences in either capillary density or average number of capillaries around a fiber (CAF) were detected between SHR and WKY strains.

NOS Expression:

Immunohistochemistry (IHC): Three of seven blinded observers detected significantly more NOS1 in Type I fibers of SHR subjects compared to their noromotensive controls. NOS2 appeared to be evenly distributed within Fast (Type IIA and IIB) muscle fibers in a punctate manner, with little variation in the degree of staining between individual fibers and with no discernable difference between rat subject strains. NOS3 appeared to be distributed in a uniform, punctate-like manner within muscle fibers, regardless of rat subject strain being examined, with strikingly intense staining of the arteriolar endothelium and to a lesser extent, the venular endothelium.

Western blot: The first of two blots detected no significant differences in the amount of NOS1, NOS2 or NOS3 between strains. However, there was significantly more NOS1 than either NOS2 or NOS3 in both WKY and SHR subjects used in the first blot. The second blot revealed significantly less NOS3 in SHR subjects versus their WKY controls while unequal variance statistical analysis failed to detect statistically significant differences in NOS1, NOS2 and NOS3 within subjects from either strain.

Animal Subjects:

Age: The mean age of the SHR rat subjects used in the IHC experiments was found to be significantly older than that of the WKY subjects (Table 1). Although the difference was minimal, it may explain why those SHR subjects weighed significantly more than their WKY controls. Previous authors have reported three stages in the development of

hypertension in the SHR: rising of blood pressures at 4-8 weeks, arrival of peak pressure at 14-18 weeks and the stabilization of blood pressure at ≥ 24 weeks (Prickar et al. 1994, Bortolotto et al. 1999). Therefore, since all components of this study required experimental animals (SHRs) with fully manifested hypertension, young adult animals aged approximately 16-17 weeks were selected. It is important to note that Harlan Laboratories, Inc., the supplier of the animals used in this study, cautions customers that normal blood pressure values for its animals may vary between colonies and differ from published literature. Harlan also suggests that further variation may be introduced by the customer's own pressure monitoring techniques. These suggestions should be kept in mind during the interpretation of blood pressure data presented here.

Mean Arterial Pressure (MAP): Since MAP is approximately equal to cardiac output (CO) multiplied by total peripheral resistance (TPR), an elevated MAP would suggest an increase in either CO, TPR or both. Furthermore, TPR may be increased due to vasoconstriction of the proximal arterioles and/or a decrease in available vascular pathways – especially in the microvessels, a phenomenon known as rarefaction. The capillarity component of this study allowed for direct investigation of possible rarefaction in the skeletal muscle microvascular bed of the SHR and those results will be discussed later in this chapter. However, in order to ensure the SHR subjects used in this study demonstrated fully manifested hypertension, both invasive and non-invasive MAP data were collected. The invasive MAPs of the SHR subjects used in IHC experiments were indeed significantly elevated above those of their WKY controls. No significant difference

in the invasive MAPs of WKY and SHR subjects used in the WB and MHC gel experiments was detected (Table 2). This result is best explained by the difference in MAP observations between the two strains (WKY = 9 and SHR = 18) and the resultant SE for the statistical analysis (Table 2). The difference in number of observations is due to the shorter duration of the surgical procedures to remove the spinotrapezius muscles from WKY versus SHR subjects. As mentioned previously in the Results section, non-invasive hemodynamic data were collected as a semi-quantitative measure to monitor and confirm the degree of hypertension in SHR subjects prior to tissue harvesting and therefore will not be discussed further.

Classification of Fibers:

Fiber Type Population Distributions By:

Fiber count vs. CSA: Before discussing the fiber type population distribution results, it is important to note that insufficient data were collected from SHR subjects to allow for statistical comparison of fiber populations. There are several reasons for this deficiency. The quality of SHR tissue sections was variable. Because serial sectioning was required to carry certain comparisons in this study (e.g., NOS1 / Type I fiber co-localization), if one tissue section was of poor quality, the entire sequence needed to be re-sectioned and the quantity of tissue available for sectioning became a concern. However, even if tissue specimen quality appeared sufficient at the time of sectioning, preparation artifact often appeared during or after processing of the tissue. The primary reason for the insuffici

ent amount of data from three of four SHR subjects was that, upon visual inspection under brightfield microscopy, the fiber-typing tissue specimens either did not allow for sufficient discrimination of positive and negative fibers (required for determination of percent population by fiber count) and/or fiber boundaries were not clearly discernable (required for determination of percent population by CSA) and image acquisition from these slides was not pursued. Therefore, the data collected in this phase of the study must be interpreted with caution.

Considering percent fiber populations as determined by CSA, the determination that Type IIA fibers comprise 9.9% of the spinotrapezius (ST) muscle in the SHR is in good agreement with Delp and Duan's (1996) determination that Type IIA fibers comprise 7% of the ST in adult male Sprague-Dawley rats. Likewise, this study's findings that Type I fibers constitute 43.8% of the fiber population (and 40.8% by fiber count) in the WKY and 43.6% in the SHR, and thatType IIB fibers comprise 32.9% of the ST in WKY subjects by CSA are also in good agreement with Delp and Duan's findings (1996). Delp and Duan's 1996 study of the composition and size of the spinotrapezius muscle from adult male Sprague-Dawley rats demonstrated that type IIB fibers make up 35 ± 5% of the total muscle mass, type IID/X fibers 17 ± 3%, type IIA fibers 7 ± 3%, and type I fibers 41 ± 2%. The CSA across all muscles was 4,248 ± 263μm^2 for type IIB fibers, 2,895 ± 468 μm^2 for type IID/X fibers, 1,448 ± 133 μm^2 for type IIA fibers, and 1,265 ± 73 μm^2 for type I fibers (Delp and Duan 1996).

According to the CSA data collected for this study, 48% of the SHR ST is comprised of Type IIB fibers. This is in agreement with the widely and long-held notion

that skeletal muscle tissue from hypertensive subjects contains a higher percentage of fast-twitch fibers than normotensive controls (Juhlin-Dannfelt et al. 1979, Frisk-Holmberg et al. 1988, Bortolotto et al. 1999, Benbachir-Lamrini et al. 1990 and 1993, Lewis et al. 1994). However, this phenomenon has been primarily observed in humans and other groups have found contradictory results in rodents (Gray 1988, Atrakchi et al. 1994). In fact, if percent population by fiber count is considered, this study found that 55% of the ST in the SHR is comprised of Type I fibers and 23.2% are Type IIB, results that are in contrast to the results rendered by CSA analysis. Given that tissue from only one SHR was studied, the SHR fiber population results presented here need to be interpreted with great care. This point is further illustrated by the fact that the fiber population percentages by CSA for the SHR add up to more than 100% (101.5%), but this result is tempered by the observed variability of fiber type composition. This result can likely be explained by the fact that a trackball mouse was used to collect data from images under the ImagePro software package as it was the only type of mouse compatible with the PC being used for this portion of the project. The trackball may have introduced error in the fiber outlines and, in aggregate, caused the discrepancy in total fiber population by CSA in the SHR.

By both fiber count and CSA methodologies, there were a greater percentage of Type IIA fibers in both SHR and WKY rats than predicted by Delp and Duan (1996). This result must be interpreted with great care for the following two reasons. First, muscle fibers are capable of transforming from one fiber type extreme to another in response to numerous stimuli including altered functional demands, changes in neural input and hormonal signals (Pette and Staron 1990, Delp and Duan 1996). Second, Delp and Duan

warn that because skeletal muscle fibers are capable of such extreme transformations, grouping of fibers into distinct types may be artifactual and that the muscle sizes, composition and oxidative potentials reported in their paper may only be applicable for rats of the same strain, age and gender, thereby rendering any comparisons herein between WKY and SHR problematic (Delp and Duan 1996). If any or all of these stimuli were present in the SHR and/or WKY rats used in this study, it is possible the Type IIA fibers counts obtained here are merely temporary and not generalizable to the lifespan of the animal.

Totaling the WKY and SHR ST fiber population percentages presented in Tables 3 and 4 (except SHR fiber population by CSA analysis as noted above) produce totals that are less than 100%. This "shortfall" likely represents the contribution of IID/X fibers in the ST muscle that were not specifically probed for in this project. The decision not to pursue these fibers is primarily because it was never a goal of this study to exhaustively characterize the fiber type composition of the ST muscle in the WKY and SHR strains. At the inception of the project the goal of the IHC experiments was merely to determine the general distribution of NOS in the ST in both WKY and SHR animals. As the literature was reviewed it became clear that knowledge of the slow- vs. fast-twitch fiber composition of subjects' ST muscles was important. It was decided that since tissue sections were being probed with antibodies against the various NOS isoforms, a similar approach would be used to detect Type I ("Slow") and Type IIA *and* Type IIB ("Fast") fibers using established antibodies. As the project progressed the aims of the study changed and an additional minor aim was to determine the populations of Type I, IIA and IIB fibers in the

ST muscle since antibodies against Type IIA and IIB MHC isoforms were readily available and their proper working dilutions for this application were known. Since Type I, IIA, IIB and IID/X fiber types comprise the fiber type population of the ST, the IID/X percent population can be determined by exclusion if the Type I, IIA and IIB fiber populations are known.

MHC Isoform Content via Gel Electrophoresis: IId/x MHC protein was undetectable via gel electrophoresis in either strain. This is in agreement with the determination that IID/X fibers would constitute only 0.3 – 8.1% of the fiber population in the WKY (by CSA and fiber count, respectively) and 2.1% of the population in the SHR (by fiber count). It is also in agreement with a portion of Bortolotto et al.'s (1999) findings where the group failed to detect any MHC IId/x protein in the soleus muscle of 16-week old WKYs. However, that group found significantly more MHC IId/x protein in soleus muscles of 16- and 24-week old SHRs compared to age-matched WKY controls (Bortolotto et al. 1999). This study's finding that there was significantly less Type IIa MHC protein than either Type I or IIb protein in the ST of WKY rats is in agreement with Delp and Duan's finding that Type IIA fibers comprised only 7% of the ST fiber population of adult male Sprague-Dawley rats and Bortolotto et al.'s finding that the MHC IIa isoform comprised only 9.2% of the MHC content in 16-week old WKYs (Delp and Duan 1996, Bortolotto et al. 1999). It bears repeating, however, that these results must be interpreted with caution since the ST is a postural muscle while the soleus is a muscle of locomotion with different metabolic demands.

Fiber Morphometry:

Indices of Fiber Shape: Previous work has determined that skeletal muscle fibers are not circular, as was often assumed, but rather more elliptical or hexagonal in shape and that a fiber's shape is relatively independent of its size (Barnard et al. 1971, Peter et al. 1972, Romanul 1974, Aquin et al. 1973, Sjøgaard 1982, Sullivan and Pittman 1984, Bennett et al. 1991). These findings are important for accurate modeling of O_2 transport and consumption, nitric oxide (NO) formation and transport and for drawing conclusions from capillarity data. Results from this study are in agreement with these prior findings as noted by the fact that the two indices of fiber shape, minimum/maximum diameter ratio and minor/major elliptical diameter ratio, were in the range of 0.53 – 0.57 and 0.44 – 0.53, respectively, indicating the fibers studied were not circular in shape, since the diameter ratio would be 1.00 for a circular cross-section.

Minimum Fiber Diameter: This study's finding that SHR Type I fibers had smaller minimum diameter and Type IIB fibers had larger minimum diameters than their age-matched WKY controls suggests a preference for the glycolytic metabolic pathway in the animals' ST muscle profile and is in agreement with the notion that skeletal muscle tissue from hypertensive subjects contains a higher percentage of fast-twitch fibers than normotensive controls, as discussed above (Juhlin-Dannfelt et al. 1979, Frisk-Holmberg et al. 1988, Bortolotto et al. 1999, Benbachir-Lamrini et al. 1990 and 1993, Lewis et al. 1994).

Maximum Fiber Diameter: As with minimum fiber diameter, this study's finding that SHR Type I fibers had significantly smaller maximum diameters than their age-matched WKY controls again suggests a preference for the glycolytic metabolic pathway in the animals' ST muscle profile. However, caution is warranted with this interpretation as SHR Type IIB fiber maximum diameter was not found to be significantly larger than that of the WKY controls.

Cross-sectional Area (CSA): Type I fibers in the SHR had smaller cross-sectional area and Type IIB fibers had larger cross-sectional area than their age-matched WKY controls. This finding is in agreement with Sullivan and Pittman's (1984) finding that fast-glycolytic (FG) fibers had larger CSA than both slow oxidative (SO) and fast oxidative-glycolytic (FOG) fibers from the same muscle (Sullivan and Pittman 1984).

Perimeter: Type I fibers in the SHR had smaller perimeters and Type IIB fibers had larger perimeters than their age-matched WKY controls. These results are consistent with the other morphometric data presented above and again suggest that the glycolytic metabolic pathway may be favored in the ST of SHR animals compared to their age-matched, normotensive controls.

Capillarity:

Two measures of capillarity were obtained in this study. The first was capillary density, expressed as the number of capillaries per square millimeter of tissue cross-section. The second was the number of capillaries around a fiber (CAF). These measures are important since capillaries are the primary "exchange" vessels in the circulation and their frequency

of occurrence is related to oxygen (O_2) and nutrient supply, as well as metabolic waste removal. Type I and IIA fibers have the greatest metabolic (O_2) requirements, while Type IIB fibers, the largest of the three fiber types studied here, have a lower O_2 demand but a greater need for removal of glycolytic metabolites.

Despite the significant differences in minimum fiber diameter, maximum fiber diameter, fiber perimeter and cross-sectional area detected in SHR subjects compared to their age-matched WKY controls, there were no significant differences in either mean capillary density or CAF between strains. These results are similar to those obtained by Plyley and Groom (1975) from rat gastrocnemius and soleus muscles (Plyley and Groom 1975). For reasons discussed earlier in this chapter, these data must be interpreted with caution since the ST is a postural muscle while the gastrocnemius and soleus are muscles of locomotion and whose fiber type distributions, and therefore capillarity profiles, likely vary between strain and by age. Additionally, Plyley and Groom (1975) did not identify the age or strain of rat they used in their study (other than to say they were adult animals). Despite these caveats, Plyley and Groom (1975) reasonably suggest that the higher O_2 demands of oxidative skeletal muscle tissue are met by a reduction in fiber size rather than an increase in microvessel (capillary) density and this study's finding that Type I fibers in the SHR are significantly smaller (by CSA and minimum/maximum diameter) than their WKY controls lends support to this notion (Plyley and Groom 1975).

The present findings are also in conflict with numerous reports of microvascular rarefacation in SHRs aged 4-18 weeks of age (Prewitt et al. 1982, Smith et al. 2004, Sabino et al 2008). For example, Greene et al. (1990) found an approximate 14%

reduction in the capillary density in the ST muscle of 12-week old SHRs compared to age-matched WKY controls (Greene et al. 1990). It is possible that these results represent a lack of anatomical or structural rarefaction of the capillary bed, a phenomenon discussed by Prewitt et al. (1982) in which there

is no discernable reduction in the number of microvessels in a particular vascular bed, but rather a reduction in the number of microvessels open to flow of red blood cells (RBCs) (Prewitt et al. 1982). The methodology used in this study, however, did not allow for determination of microvessel patency (i.e., the microvascular bed was not perfused under pressure to ensure patency of the vessels). The results of a future study that employs such methodology in subjects of the same strains and ages as those used in this study would likely yield interesting and useful information.

Another possibility is that there is indeed rarefaction of the microvascular bed present in the SHR ST muscle samples studied here, except it has manifested itself in reduced arteriolar density vs. capillary density. Prewitt et al. (1982) observed this phenomenon in the gracilis muscles of SHRs aged 16-18 weeks, suggesting it is reasonable to believe that a similar process is occurring in the SHRs used in the present study.

Tissue shrinkage is a known problem with many histological procedures and it is unknown if or to what degree tissue used in this study may have shrunk during processing. Future studies could better control for this by placing reference marks a known distance apart on the harvested tissue before freezing and then remeasuring after freezing. Furthermore, only one observer conducted the capillary counts presented in this study.

Future studies may benefit from having several independent observers conduct vessel counts in order to reduce the possibility of error or bias in the final results.

NOS Expression via IHC:

Three NOS isoforms were probed for in WKY and SHR ST muscle sections via IHC, including neuronal NOS (nNOS or NOS1), inducible NOS (iNOS or NOS2) and endothelial NOS (eNOS or NOS3). Although both nomenclatures can be found in the current literature, this discussion will use the NOS1/2/3 nomenclature to minimize possible confusion about location of the particular isoform being discussed.

Isoform Location by Fiber Type: The body of NO and NOS literature is immense and conflicting reports regarding the occurrence of NOS in skeletal muscles abound (to say nothing of visceral muscle and other tissues). It is also important to note that this study is, as best as can be determined, the first of its kind to investigate NOS distribution in the ST muscle of adult WKY and SHR subjects. Therefore, generalization of the results presented here to other rat strains, muscle groups, muscle types and other mammalian species must be made with caution. With these caveats in mind, the results obtained here are in agreement with several reports in the literature.

NOS1 in Type I skeletal muscle fibers in the ST: A goal of the present study was to determine, in a semiquantitative manner, to what degree NOS1 co-localizes with Type I skeletal muscle fibers in WKY and SHR ST tissue (using several independent observers as outlined in Materials and Methods and Appendix A) and to describe the staining distribution of the enzyme in the muscle fiber. In their 1996 and 2000 studies, Frandsen et

al. found NOS1 near the sarcolemma and in the cytoplasm of human vastus lateralis muscle from healthy subjects (Frandsen et al. 1996 and 2000). It should be noted that in the 2000 Frandsen study the group graded the degree of NOS staining in their samples in a manner similar to what was done in the present study, although details about who graded the staining and how this was done is not discussed in the article. In 1996, Capanni et al. described NOS1 staining in the gracilis muscle of 6- and 24-month old Wistar rats as "granular," and in 2001, Punkt et al. detected NOS1 in Type I skeletal muscle fibers of 6-month old male Wistar rats and described the staining as granular, diffused throughout the cytoplasm and near the sarcolemma, descriptions that nicely compliment the results of the present study (see Fig. 14;Capanni et al. 1996, Punkt et al. 2001). The Punkt group also determined the degree of NOS staining in a manner similar to that of Frandsen et al. (2005) and the present study. However, like the Frandsen group, Punkt et al. did not provide a detailed description of their semi-quantification methods in their article. A subsarcolemmal NOS1 staining pattern similar to that described by Punkt et al. (2001) was also detected by Gath et al. (1996) in guinea pig muscle and Buchwalow et al. (2005) in adult male Wistar rat quadriceps tissue (Gath et al. 1996, Buchwalow et al. 2005).

As best as can be determined, this is the first study to attempt to semi-quantify the degree to which NOS1 co-localizes with Type I MHC fibers in WKY and SHR rat strains. Therefore, comparisons between the current findings with those in established literature must be made with caution. Furthermore, given that fewer than half of the observers detected significantly more NOS1 in SHR vs. WKY subjects, the present results must also be interpreted with caution. However, it is conceivable that the apparent increase in NOS1

expression in the ST of SHR subjects is a compensatory mechanism for a deficiency in NOS3 in the same tissue, as detected by the second Western blot conducted in this study. This notion is supported by Biecker et al.'s (2004) finding that NOS1 mRNA levels are partially maintained in aortae of NOS3 deficient mice (Biecker et al. 2004).

NOS2 in Type IIA/B fibers: Another goal of the present study was to determine to what degree NOS2 co-localizes with Type IIA/B skeletal muscle fibers in WKY and SHR ST tissue and to describe the staining distribution of the enzyme in the muscle fiber. Examination of the NOS2 images collected from Type IIA/B fibers known to co-localize with NOS2 revealed a spotty, punctate staining pattern throughout the cytoplasm. These observations are in close agreement with Gath et al. (1996), who observed markedly similar staining patterns in guinea pig skeletal muscle tissue (the authors did not specify which muscle(s) they used in their study) (Gath et al. 1996). Interestingly, Gath et al. (1996) detected NOS2 in intracellular structures in "specific pathogen-free" animals, raising the intriguing possibility that NOS2 may, in fact, be constitutively active in some species (Gath et al. 1996). Punkt et al. (2002) also demonstrated NOS2 staining in rat hindlimb muscles in a manner similar to what is described here (Punkt et al. 2002). However, the immunoreactivity was stronger in tissue from young (embryonic and 21-day old) subjects than from older (21 and 75-day old) subjects and was primarily co-localized with Type IIA muscle fibers (Punkt et al. 2002). As mentioned in the Results section, inspection of the entire NOS2 image series revealed little variation in the degree of staining between individual fibers and with no discernable difference between rat subject strains. It

was therefore determined that, unlike the NOS1 staining, NOS2 staining analysis would not benefit significantly from further semi-quantitative analysis using individual observers.

This study's finding agrees with the notion proposed by Gath et al. (1996) that NOS2 demonstrates either a higher level of activity or is constitutively active in skeletal muscle tissue from more than one species, as Gath's study used guinea pigs (Gath et al. 1996). Like Gath et al., the staining pattern seen here is consistent with the sarcoplasmic reticulum and/or transverse tubule system, and future studies could probe more specifically for the co-localization of NOS2 with these structures in WKY and SHR ST tissue (Gath et al. 1996). Further interpretation of this particular result is difficult because the presence of the NOS2 enzyme does not necessarily equate to NO production in direct proportion to the concentration of enzyme present. This quandary highlights the need for more accurate methods of determining in vivo NO concentrations than currently exist.

NOS3 Association with Capillary Endothelium: As with NOS1 and NOS2, another goal of this study was to determine if NOS3 was localized solely in the endothelium of WKY and SHR capillaries by staining for NOS3 and capillary endothelium in serial sections. No attempt to investigate co-localization with a particular fiber type was made in this study since prior reports suggest NOS3 expresses a heterogeneous pattern within muscle fibers that does not differ systematically between fiber types (Reid 1998).

Frandsen et al. (1996) reported NOS3 immunoreactivity in the endothelium of larger vessels as well as microvessels of healthy human vastus lateralis tissue (Frandsen et al. 1996). This is in agreement with this study's findings that arterioles and venules, in addition to capillaries, also stained intensely for NOS3. Gath et al. (1996) made a similar

observation of their NOS3 staining patterns in guinea pig skeletal muscle tissue. Again, however, the authors did not specify which muscle(s) they used in their study (Gath et al. 1996). Interestingly, Punkt et al. (2001) found diffuse or granular staining throughout the cytoplasm of 6-month old Wistar rat skeletal muscle tissue, which they semi-quantified (using a scale similar to the one used in this study) as ranging from "very weak" to "strong" (Punkt et al. 2001). Although semi-quantification of NOS3 was not conducted in this study, a strikingly similar granular staining pattern in the ST muscle of SHR subjects was observed in the present results (see Figure 18).

Given the intensity of the NOS3 staining in arteriolar and venular endothelium described here, the question arises: "What might these patterns imply about potential sources of NO in these vessels?" One significant implication is that NOS3 is expressed in other structures in addition to the endothelial cells in these vessels. There is evidence for this notion in the literature. Villanueva and Giulivi (2010) reviewed literature investigating the cellular and sub-cellular locations of NOS isoforms and reported a number of studies in the literature that suggest NOS3 is located in a variety of tissues across species, including eosinophils, epithelial cells of human nasal mucosa, fibroblasts, gastrointestinal mucosae, hepatocytes, lymphocytes, neutrophils, skeletal muscle, syncytiotrophoblasts of human planceta and type II alveolar cells (Villanueva and Giulivi 2010). However, the most likely explanation comes from Buchwalow et al.'s 2008 study in which they found evidence for all three NOS isoforms, and strong staining for NOS3 in particular, in both intimal and medial cells of thoracic aorta, mesenteric artery and pulmonary artery sections from adult male Wistar rats that had been completely denudated

of endothelial tissue (Buchwalow et al. 2008). These finding correlate nicely with this study's results and offer some of the strongest evidence for NOS3 outside the endothelium of the vessels studied here.

This finding is particularly exciting because there is still considerable debate in the literature regarding many aspects of the physiology of NO in vivo. Numerous unanswered questions remain, including "How far does NO spread in biologically relevant concentrations," "What is the profile of NO release over time from different sources," and "How is it captured to elicit biological responses?" (Hall and Garthwaite 2009). While the goal of this study was not to provide definitive answers to these questions, the fact that a previous finding has been confirmed is important. In particular, this finding suggests another potential source of NO that lies a distance from the vessel lumen where red blood cells (RBCs), and in particular, hemoglobin, are known as substantial sinks for NO in vivo (Pacher et al. 2007). It is estimated that even with hemoglobin sequestered in erythrocytes, they scavenge so much NO that the endothelium must produce an estimated 100 nM NO to achieve the 5-10 nM NO concentrations required by smooth muscle tissue containing soluble guanylyl cyclase (sGC), the primary target of NO in vivo (Pacher et al. 2007). Clearly, the notion that smooth muscle is incapable of expressing NOS must be re-examined. Future studies further exploring the extent to which NOS may truly be expressed in smooth muscle tissue are clearly indicated.

Co-localization of NOS3 staining with alkaline phosphatase (AP) staining for capillary endothelium: As best as can be determined, this is the first time this particular comparison of NOS3 IHC and AP staining has been made in the ST of WKY and SHRs. Therefore,

conclusions from the data must be drawn with caution. The discrepancy between the percent co-localization results for WKY and SHR strains likely has more to do with limitations of the staining techniques employed. The NOS3 and AP staining protocols did not require dehydration of the tissues specimens. Therefore, these slides were mounted in an aqueous medium (see Materials and Methods) which is prone to air bubble artifact. Furthermore, it is possible that the seal between glass slide and coverslip was breached at some point between slide processing and viewing on the microscope, allowing air bubbles to contaminate the tissue and/or allowing the tissue to desiccate and shrink. While care was taken not to use slides with obvious artifact, the possibility of artifact cannot be discounted.

If the cautious assumption that the NOS3 "spots" detected in this portion of the study do indeed correspond to capillary endothelium, the finding that 98% of the of NOS3 "spots" without a corresponding AP "spot" lie between muscle fibers is in agreement with previously published results from striated hamster tissue (Bennett et al. 1991). However, as mentioned before, care must be taken when making such comparisons between strains. Interestingly, the finding for SHR that 55% of the NOS3 "spots" lacking an AP corollary were located within fibers coincides with the earlier finding that NOS3 appears in a granular pattern within skeletal muscle fibers of SHR subjects.

Limitations of IHC Technique: Although IHC techniques have been steadily advancing in recent years, limitations to the approach still exist. Since the spinotrapezius muscle of the rat is only ~500 µm thick, both muscles from each subject had to be extracted and then folded one upon the other in order to provide the bulk necessary for cryostat sectioning.

This caused unavoidable gaps in and distortions to the tissue as it was submerged in cryoprotectant medium and frozen. The use of serial sectioning required that each section in a particular series needed to be of comparable quality. Therefore, if one section was damaged during sectioning, the entire sequence needed to be re-sectioned. Although care was taken to prevent artifact (i.e., always ensuring the blade was sharp and temperature settings were correct), it is not possible to completely rule out some degree of chatter or tissue compression.

Biochemical supply vendors make it clear that final working concentrations of antibody purchased for a particular application must be determined by the end user. Although literature was reviewed to determine ideal initial concentrations to expedite antibody dilution experiments, it soon became clear that many protocols had been highly tailored and customized by the group performing the research and that these groups often used antibodies that were unavailable for the current project. Antibody concentrations used in the NOS IHC portion of this study ranged from 1:50 (NOS3) to 1:2000 (NOS1), suggesting the NOS3 antibody may be of lower quality due to the need for a higher concentration to achieve demonstrable results. Finally, all of the NOS antibodies used in this project were polyclonal, so some degree of non-specific binding may have occurred. In light of these drawbacks, all experiments were performed consistently under as identical working conditions as possible, using fresh reagents to minimize introduction of artifact.

NOS Expression via Western blot:

Expression of NOS isoforms: Greater-than-expected NOS2 protein expression levels in Sprague-Dawley rat ST muscle tissue have been detected before by Western blot in this lab (unpublished data). Therefore, data from both blots performed for this study indicating that all three isoforms are constitutively active at the protein level in WKY and SHR ST muscle tissues, and that NOS1 is the predominant isoform, were not unexpected and in accord with previous reports from several mammalian species (Gath et al. 1995, Grozdanovic et al. 1995, Stamler and Meissner 2001, Buchwalow et al. 2005, Punkt et al. 2006 and 2008).

The finding that there was less NOS3 expressed in SHR subjects compared to their age-matched controls in the second blot was expected insofar as there is much literature to support the notion that there may be less NOS3 expressed and/or diminished levels of bioavailable NO to effect vasodilation in SHRs with manifested hypertension (Malinsky et al. 1993, Cuevas et al. 1996, Dubois 1996, Crabos et al. 1997, Sunano et al. 1996). However, one hypothesis driving this study was that NOS3 expression would be increased in the SHR vs. WKY. This hypothesis was based on intriguing previous reports of increased plasma nitrate levels (an index of the formation of NO in the rat) in adult male Wistar rats and induction of NOS3 expression in canine coronary vascular tissue and on reports that SHRs demonstrate generalized vasoconstriction and blood hyperviscosity (De Clerck et al. 1980, Prewitt et al. 1992, Sessa et al. 1994, Nava et al. 1996). It is possible that the SHRs used in this study were still too young for the resultant vasculopathy of long-standing hypertension to have been fully manifested, including the hypothesized

upregulation of NOS3. It is also possible that this NOS3 upregulation has already occurred in other tissues (e.g., neural and renal) that were not studied in the current project.

Use of α-tubulin as loading control: Alpha-tubulin was selected as the loading control for the Western blots in this study over the more commonly used β-actin based on a 1983 report from Farmer et al. which reported that changes in cell growth conditions and interactions with extracellular matrix components may alter actin protein synthesis (Farmer et al. 1983). Furthermore, certain physiological conditions including, but possibly not limited to, hypoxia and diabetes can alter GADPH expression levels, also making it an unsuitable loading control for this study (Said et al. 2007). Therefore, α-tubulin, another commonly used loading control, was selected for use in this study as its expression has, thus far, only been found to vary according to resistance to antimicrobial and antimitotic drugs, neither of which the rat subjects used in this study were exposed to (Sangrajrang et al. 1998, Prasad et al. 2000).

Consistency of Results between Blots: In the first blot, significantly more NOS1 than NOS2 and NOS3 were detected within each strain, but no significant differences in NOS1-3 expression were noted between strains. The converse was true in the second blot; there was significantly less NOS3 in SHR compared to age-matched WKY subjects; however, no significant differences in NOS1-3 expression were detected within each strain. Furthermore, comparison between Figures 20 and 21 demonstrates differences in NOS / α-tubulin intensity ratio scales. This is because the signal-to-noise ratio was much lower in the second blot, possibly obscuring existing differences between isoform expression within strains. Given this lack of consistency of results between blots, any interpretation of the

data they yield should be made with great care and repetition of the blots is likely warranted in the future.

Overall Conclusions:

Purpose of Study: This study sought to fill in gaps in the literature regarding the distribution and modulation of NOS in postural skeletal muscle tissue of hypertensive rat subjects. A long-term goal of this project is to use the distribution data gathered here in computational models that describe NO distribution in postural skeletal muscle. These models take into account the numerous and detailed reactions that produce NO to predict in vivo NO concentrations in skeletal muscle tissue. Accurate and complete data of this type are crucial as input for these models, since the model results may presently be the best representatives of in vivo NO concentrations, perhaps even better than direct in vivo measurements with microelectrodes and indirect measurements via fluorescent indictors. This is because the accuracy and validity of such measurements were called into question in a comprehensive review by Hall and Garthwaite (2009). The review noted inconsistencies in the literature regarding physiological in vivo NO concentrations, which range from femtomolar to hundreds of micromolar, and a glaring lack of consensus between groups making these measurements (Hall and Garthwaite 2009). Despite the drawbacks of current in vivo measurement tools currently available, the need for in vivo measurements to confirm or refute the predictions made by computational models remains. Therefore, it is hoped that the data presented here will aid in the development of more accurate in vivo measurement techniques for NO.

Important Connections: Given the volume of literature on the topic, there is little doubt that NO is clearly an important signaling molecule in vivo and that it exerts numerous biological effects in a number of systems and tissues, including the microvasculature. Much is already known about the regulation of the NOS enzymes that create NO in a tightly controlled manner (see reviews by Alderton et al. 2001, Kone et al. 2003). However, the most relevant interactions that can be addressed by this study are those between NO and the tissues responsible for oxygen (O_2) supply and delivery, since every cell in an organism requires O_2 to survive.

To review briefly, this study has demonstrated the presence of significantly larger (by CSA) Type I MHC fibers in SHR subjects (Table 7). Given the highly oxidative nature of these fibers, it may be inferred that the presence of increased amounts of hemoglobin and myoglobin may act as NO sinks, potentially reducing the concentrations of bioavailable NO in the SHR to effect vasodilation, which in turn would reduce bioavailable O_2 for consumption by the mitochondria. Furthermore, since it is known that NO inhibits mitochondrial respiration, and results presented here demonstrated significantly more NOS1 in Type I fibers of the SHR (Table 10), it is possible the oxidative capacity of these fibers is abrogated somewhat by the (presumably) increased NO concentration (Stamler and Meissner 2001). It bears repeating that assumptions about NO activity based solely on NOS enzyme concentration must be made with great care. Finally, there are numerous reports that contractile function of mammalian skeletal muscle tissue is modulated by NO (for review see Stamler and Meissner 2001). However, there appears to be a lack of consensus about the exact nature of these effects as they depend on

the muscle preparation being studied, the experimental protocol, NO concentration and the NO source (Stamler and Meissner 2001). Although there are reports to the contrary, Kobzik et al. (1994) reported an inverse correlation between force generation in rat soleus, diaphragm and extensor digitorum longus muscles and NOS activity and suggested that NOS activity contributes to the intrinsic differences in force generation by Type I and Type II fibers (Kobzik et al. 1994, Stamler and Meissner 2001). Although measurements of force production by the ST muscle were not made for the current study, results from a future study in light of the NOS distribution results collected here could further elucidate the exact nature of the relationship between NOS expression and skeletal muscle type in hypertension.

Another conclusion that may be drawn from the current results is that NOS expression appears to be altered in hypertension as noted by significantly more NOS1expression in SHR Type I skeletal muscle fibers (Table 10), significantly less NOS3 expression in the ST muscle compared to WKY controls (Table 13) and an apparently constitutively active NOS2 isoform that is expressed to the same relative degree in both strains (Figs. 15 and 16, Tables 12 and 13). The exact consequences remain to be elucidated by the future studies both already discussed and outlined below, as well as by computational models of in vivo NO concentrations for which the data presented here can be used.

Recommendations for Future Studies:

In addition to the suggestions for future work already mentioned in this chapter, studies exploring the potential co-localization of Type IIA/B/D/X MHC fibers with NOS1 could be carried out using confocal microscopy. These would allow for fluorescent labeling of more than one antigen of interest in a single tissue section and eliminate the need for serial sections, which are somewhat problematic for the reasons discussed above. Further delineation of the role of NO in O_2 supply and demand (VO_2) could be determined with in vivo experiments on WKY and SHR spinotrapezius muscles, similar to those conducted by Smith et al. (2004) in the presence of NOS inhibitors and/or NO donors. Such studies may also benefit from determination of NOS activity in the subjects used via plasma nitrite, nitrate and L-citrulline concentrations to allow for more accurate correlations of NOS enzyme expression and actual NO production in vivo. Finally, given the variability between the Western blots performed for this project, it may be beneficial to conduct the blots again under identical circumstances to further confirm or refute the conclusion that NOS3 expression is indeed diminished in the ST of the SHR.

Literature Cited

Literature Cited

Alderton, W.K., C.E. Cooper, R.G. Knowles (2001). "Nitric oxide synthases: structure, function and inhibition." *Biochem J* **357**(Pt 3):593-615.

Aquin, L., A.J. Lechner, A.H. Sillau and N. Banchero (1980). "Analysis of the shape changes of muscle fiber cross sections in guinea pigs raised at 22 degrees C and 5 degrees C." *Pflugers Arch* **385**(3):223-8.

Artz J.D., V. Toader, S.I. Zavorin, B.M. Bennett and G.R. Thatcher (2001). "In vitro activation of soluble guanylyl-cyclase and nitric oxide release: a comparison of NO donors and NO mimetics." *Biochemistry* **40**(31):9256-64.

Atrakchi A., S.D. Gray and R.C. Carlsen (1994). "Development of soleus muscles in SHR: relationship of muscle deficits to rise in blood pressure." Am J Physiol **267**(3 Pt 1):C827-35.

Bär, A., and D. Pette (1988). "Three fast myosin heavy chains in adult rat skeletal muscle." *FEBS Lett* **235**(1-2):153-5.

Barnard, R.J., V.R. Edgerton, T. Forukawa and J.B. Peter (1971). "Histochemical, biochemical, and contractile properties of red, white, and intermediate fibers." *Am J Physiol* **220**(2):410-4.

Beckman, J.S., T.W. Beckman, J. Chen, P.A. Marshall and B.A. Freeman (1990). "Apparent hydroxyl radical production by peroxynitrite: implications for endothelial injury from nitric oxide and superoxide." *Proc Natl Acad Sci USA* **87**(4):1620-4.

Beckman, J.S. and W.H. Koppenol (1996). "Nitric oxide, superoxide, and peroxynitrite: the good, the bad, and ugly." *Am J Physiol* **271**(5 Pt 1):1424-37.

Bellamy, T.C., J. Wood, D.A. Goodwin and J. Garthwaite (2000). "Rapid desensitization of the nitric oxide receptor, soluble guanylyl cyclase, underlies diversity of cellular cGMP responses." Proc Natl Acad Sci USA **97**(6):2928-33.

Benbachir-Lamrini, L., B. Sempore, M.H. Mayet and R.J. Favier (1990). "Evidence of a slow-to-fast fiber type transition in skeletal muscle from spontaneously hypertensive rats." *Am J Physiol (Regulatory Integrative Comp Physiol* **258**:R352-57.

Benbachir-Lamrini, L., H. Koubi, B. Sempore, M.H. Mayet, J. Frutoso, J.M. Cottet-Emard and R.J. Favier (1993). "Soleus muscle alterations in spontaneously hypertensive rats are not dependent on activation of beta 2-adrenergic receptors." *J Auton Nerv Syst* **44**(2-3):161-70.

Bennett, R.A.O., R.N. Pittman and S.M Sullivan (1991). "Capillary spatial pattern and muscle fiber geometry in three hamster striated muscles." *Am J Physiol Heart Circ Physiol* **260**(2 Pt 2):H579-85.

Bernatchez, P.N., P.M. Bauer, J. Yu, J.S. Prendergast, P. He and W.C. Sessa (2005). "Dissecting the molecular control of endothelial NO synthase by caveolin-1 using cell-permeable peptides." *Proc Natl Acad Sci USA* **102**(3):761-6.

Biecker, E., M. Neef, H. Sägesser, S. Shaw, A. Koshy and J. Reichen (2004). "Nitric oxide synthase 1 is partly compensating for nitric oxide synthase 3 deficiency in nitric oxide synthase 3 knock-out mice and is elevated in murine and human cirrhosis" *Liver Int* **24**(4):345-53.

Bortolotto, S.K., D.G. Stephenson and G.M.M. Stephenson (1999). "Fiber type populations and Ca^{2+} -activation properties of single fibers in soleus muscles from SHR and WKY rats." *Am J Physiol* **276**(3 Pt 1):C628-37.

Brenman, J.E., H. Xia, D.S. Chao, S.M. Black and D.S. Bredt (1997). "Regulation of neuronal nitric oxide synthase through alternative transcripts." *Dev Neurosci* **19**(3):224-31.

Buchwalow, I.B., E.A. Minin, V.E. Samoilova, W. Boecker, M. Wellner, W. Schmitz, J. Neumann and K. Punkt (2005). "Compartmentalization of NO signaling cascade in skeletal muscles." *Biochem Biophys Res Commun* **330**(2):615-21.

Buchwalow, I.B., S. Cacanyiova, J. Neumann, V.E. Samoilova, W. Boecker and F. Kristek (2008). "The role of arterial smooth muscle in vasorelaxation." *Biochem Biophys Res Commun* **377**(2):504-7.

Buerk, D.G. (2007). "Nitric oxide regulation of microvascular oxygen." *Antioxid Redox Signal* **9**(7):829-43.

Cai, H. (2005). "NAD(P)H oxidase-dependent self-propagation of hydrogen peroxide and vascular disease." *Circ Res* **96**(8):818-22.

Calhoun, D.A. (2006). "Aldosteronism and hypertension." *Clin J Am Soc Nephrol* **1**(5):1039-45.

Capanni, C., S. Squarzoni, S. Petrini, M. Villanova, C. Muscari, N.M. Maraldi, C. Guarnieri and C.M. Caldarera (1998). "Increase of neuronal nitric oxide synthase in rat skeletal muscle during ageing." *Biochem Biophys Res Commun* **245**(1):216-9.

Carretero, O.A. and S. Oparil (2000). "Essential hypertension. Part I: definition and etiology." *Circulation* **101**(3):329-35.

Cattaruzza M., T.J. Guzik, W. Słodowski, A. Pelvan, J. Becker, M. Halle, A.B. Buchwald, K.M. Channon and M. Hecker (2005). "Shear stress insensitivity of endothelial nitric oxide synthase expression as a genetic risk factor for coronary heart disease." *Circ Res* **95**(8):841-7.

Chen, I.I., R.L. Prewitt and R.F. Dowell (1981). "Microvascular rarefaction in spontaneously hypertensive rat cremaster muscle." *Am J Physiol* **241**(3):H306-10.

Chen, K., R.N. Pittman and A.S. Popel (2008). "Nitric oxide in the vasculature: where does it come from and where does it go? A quantitative perspective." *Antioxid Redox Signal* **10**(7):1-14.

Chin-Dusting, J.P.F., C.T. Alexander, P. Arnold, W.C. Hodgson, A.S. Lux and G.L.R. Jennings (1996). "Effects of in vivo and in vitro L-arginine supplementation on healthy human vessels." *J Cardiovasc Pharmacol* **28**(1):158-66.

Chou, T.C., M.H. Yen, C.Y. Li and Y.A. Ding (1998). "Alterations of nitric oxide synthase expression with aging and hypertension in rats." *Hypertension* **31**(2):643-8.

Condorelli, P. and S.C. George (2001). "In vivo control of soluble guanylate cyclase activation by nitric oxide: a kinetic analysis." *Biophys J* **80**(5):2110-9.

Crabos, M., P. Coste, M. Paccalin, L. Tariosse, D. Daret, P. Besse and S. Bonoron-Adele (1997). "Reduced basal NO-mediated dilation and decreased endothelial NO-synthase expression in coronary vessels of spontaneously hypertensive rats." *J Mol Cell Cardiol* **29**(1):55-65.

Cuevas, P., M. Garcia-Calvo, F. Carceller, D. Reimers, M. Dazo, B. Cuevas, I. Munoz-Willery, F. Martinez-Coso, S. Lamas and G. Gimenez-Gallego (1996). Correction

of hypertension by normalization of endothelial levels of fibroblast growth factor and nitric oxide synthase in spontaneously hypertensive rats." *Proc Natl Acad Sci USA* **93**(21):11996-2001.

Cuspidi, C., S. Meani, V. Fusi, B. Severgnini, C. Valerio, E. Catini, G. Leonetti, F. Magrini and A. Zanchetti (2004). "Metabolic syndrome and target organ damage in untreated essential hypertensives." *J Hypertens* **22**(10):1991-8.

Daff, S. (2003). "Calmodulin-dependent regulation of mammalian nitric oxide synthase." *Biochem Soc Trans* **31**(Pt 3):502-5.

De Clerck, F., M. Beerens, L. Van Gorp and R. Xhonneux (1980). "Blood hyperviscosity in spontaneously hypertensive rats." *Thromb Res* **18**(1-2):291-5.

Delp, M.D. and C. Duan (1996). "Composition and size of type I, IIA, IID/X, and IIB fibers and citrate synthase activity of rat muscle." *J Appl Physiol* **80**(1):261-70.

DeMeyer, G.R.Y. and A.G. Herman (1997). "Vascular endothelial dysfunction." *Progress in Cardiovascular Disease* **39**:325-42.

Dioguardi, F.S. (2011). "To give or not to give? Lessons from the arginine paradox." *J Nutrigenet Nutrigenomics* **4**(2):90-8.

Dubois, G. "Decreased L-arginine-nitric oxide pathway in cultured myoblasts from spontaneously hypertensive versus normotensive Wistar-Kyoto rats." *FEBS Lett* **392**(3):242-4.

El-Garbawy, A.H., V.S. Nadig, J.M. Kotchen, C.E. Grim, K.B. Sagar, M. Kladunski, P. Hamet, Z. Pausova, D. Gaudet, F. Gossard and T.A. Kotchen (2001). "Arterial pressure, left ventricular mass, and aldosterone in essential hypertension." *Hypertension* **37**(3):845-50.

Engeli, S., P. Schling, K. Gorzelniak, M. Boschmann, J. Janke and G. Ailhaud (2003). "The adipose-tissue renin-angiotensin system: role in the metabolic syndrome?" *Int J Biochem Cell Biol* **35**(6):807-25.

Expert Panel on Detection, Evaluation, and Treatment of High Blood Cholesterol in Adults (2001). "Executive summary of the third report of the national cholesterol education program (NCEP) expert panel on detection, evaluation and, treatment of high blood cholesterol in adults (Adult Treatment Panel III)." *JAMA* **285**(19):2486-97.

Fard, A., C.H. Tuck, J.A. Donis, R. Sciacca, M.R.D. Tullio, H.D. Wu, T.A. Bryant, N.T. Chen, M.T. Tamayo, R. Ramasamy, L. Berglund, H.N. Ginsberg, S. Homma and P.J. Cannon (2000). "Acute elevations of plasma asymmetric dimethylarginine and impaired endothelial function in response to high-fat meal in patients with type 2 diabetes." *Arterioscler Thromb Vasc Biol* **20**(9):2039-44.

Farmer, S.R., K.M. Wan, A. Ben-Ze'ev and S. Penman (1983). "Regulation of actin mRNA levels and translation responds to changes in cell configuration." *Mol Cell Biol* **3**(2):182-9.

Flowers, M.A., Y. Wang, R.J. Stewart, B. Patel and P.A. Marsden (1995). "Reciprocal regulation of endothelin-1 and endothelial constitutive NOS in proliferating endothelial cells." *Am J Physiol* **269**(6 Pt 2):H1988-97.

Förstermann, U., J.P. Boissel and H. Kleinert (1998). "Expressional control of the 'constitutive' isoforms of nitric oxide synthase (NOS I and NOS III)." *FASEB J* **12**(10):773-90.

Frandsen, U., M. Lopez-Figueroa and Y. Hellsten (1996). "Localization of nitric oxide synthase in human skeletal muscle." *Biochem Biophys Res Commun* **227**(1):88-93

Frandsen, U., L. Höffner, A. Betak, B. Saltin, J. Bangsbo and Y. Hellsten (2000). "Endurance training does not alter the level of neuronal nitric oxide synthase in human skeletal muscle." *J Appl Physiol* **89**(3):1033-8.

Frisk-Holmberg, M., B Essén, M. Fredrikson, G. Ström and L. Wibell (1988). "Muscle fibre composition in relation to blood pressure response to isometric exercise in normotensive and hypertensive subjects." *Acta Med Scand* **213**(1):21-6.

Fujita, T. (2001). "Symposium on the etiology of hypertension--summarizing studies in 20th century. 5. Renin-angiotensin system and hypertension." *Intern Med* **40**(2):156-8.

Fujisawa, H., T. Ogura, Y. Kurashima, T. Yokoyama, J. Yamashita and H. Esumi (1994). "Expression of two types of nitric oxide synthase mRNA in human neuroblastoma cell lines." *J Neurochem* **63**(1):140-5.

Fujiwara, K., K. Hayashi, H. Matsuda, E. Kubota, M. Honda, Y. Ozawa and T. Saruta (1999). "Altered pressure-natriuresis in obese Zucker rats." *Hypertension* **33**(6):1470-5.

Gao, S., J. Chen, S.V. Brodsky, H. Huang, S. Adler, J.H. Lee, N. Dhadawal, L. Cohen-Gould, S.S. Gross and M.S. Goligorsky (2004). "Docking of endothelial nitric

oxide synthase (eNOS) to the mitochondrial outer membrane: a pentabasic amino acid sequence in the autoinhibitory domain of eNOS targets a proteinase K-cleavable peptide on the cytoplasmic face of mitochondria." *J Biol Chem* **279**(16):15968-74.

Gath, I., E.I. Closs, U. Gödtel-Armbrust, S. Schmitt, M. Nakane, I. Wessler and U. Förstermann (1996). "Inducible NO synthase II and neuronal NO synthase I are constitutively expressed in different structures of guinea pig skeletal muscle: implications for contractile function." *FASEB J* **10**(14):1614-20.

Gautier, C., E. van Faassen, I. Mikula, P. Martasek and A. Slama-Schwok (2006). "Endothelial nitric oxide synthase reduces nitrite anions to NO under anoxia." *Biochem Biophys Res Commun* **341**(3):816-21.

Goligorsky, M.S., H. Li, S. Brodsky and J. Chen (2002). "Relationships between caveolae and eNOS: everything in the proximity and proximity of everything." *Am J Physiol Renal Physiol* **283**(1):F1-10.

Gray, S.D. (1988). "Histochemical analysis of capillary and fiber-type distributions in skeletal muscles of spontaneously hypertensive rats." *Microvasc Res* **36**(3):228-38.

Greene, A.S., J.H. Lombard, A.W. Cowley Jr., and F.M. Hansen-Smith (1990). "Microvessle changes in hypertension measured by Griffonia simplicifolia I lectin." *Hypertension* **15**(6 Pt 2):H508-14.

Griendling, K.K., D. Sorescu and M. Ushio-Fukai (2000). "NAD(P)H oxidase: role in cardiovascular biology and disease." *Circ Res* **86**(5):494-501.

Grim, C.E., A.W. Cowley, P. Hamet, D. Gaudet, M.L. Kaldunski, J.M. Kotchen, S. Krishnaswami, Z. Pausova, R. Roman, J. Tremblay and T.A. Kotchen (2005). "Hyperaldosteronism and hypertension: ethnic differences." *Hypertension* **45**(4):766-72.

Grozdanovic, Z., G. Nakos, G. Dahrmann, B. Mayer and R. Gossrau (1995). "Species-independent expression of nitric oxide synthase in the sarcolemma region of visceral and somatic striated muscle fibers." *Cell Tissue Res* **281**(3):493-99.

Guerro-Romero, F. and M. Rodriguez-Moran (2005). "Concordance between the 2005 international diabetes federation for diagnosing metabolic syndrome with the national cholesterol education program adult treatment panel III and the world health organization." *Diabetes Care* **28**(10):2588-9.

Hall, C.N. and J. Garthwaite (2009). "What is the real physiological NO concentration in vivo?" *Nitric Oxide* **21**(2):92-103.

Hämäläinen, N. and D. Pette (1993). "The histochemical profiles of fast fiber types IIB, IID, and IIA in skeletal muscles of mouse, rat, and rabbit." *J Histochem Cytochem* **41**(5):733-43.

Hayashi, K. (2001). "Symposium on the etiology of hypertension--summarizing studies in 20th century. 4. Pathogenesis of hypertension--kidney as a pathogenetic organ of hypertension." *Intern Med* **40**(2):153-6.

Heeba, G., M.K.A. Hassan, M. Khalifa and T. Malinski (2007). "Adverse balance of nitric oxide/peroxynitrite in the dysfunctional endothelium can be reversed by statins." *J Cardiovasc Pharmacol* **50**(4):391-8.

Heitzer, T., C. Brockhoff, B. Mayer, A. Warnholtz, H. Mollnau, S. Henne, T. Meinertz and T. Münzel (2000). "Tetrahydrobiopterin improves endothelium dependent vasodilation in chronic smokers: evidence for a dysfunctional nitric oxide synthase." *Circ Res* **86**(2):e36-41.

Henrich, M., K. Hoffman, P. Konig, M. Gruss, T. Frischbach, A. Godecke, G. Hempelmann and W. Kummer (2002). "Sensory neurons respond to hypoxia with NO production associated with mitochondria." *Mol Cell Neurosci* **20**(2):307-22.

Hilarius P.M., P.T. Goedhart, C. Ince and A.J. Verhoeven (2007). "Human erythrocytes contain negligible amounts of endothelial type NO synthase (eNOS): Abstracts of the Second International Meeting of the Role of Nitrite in Physiology." *Pathophysiol Therapeut* 90-9.

Hilenski, L.L., R.E. Clempus, M.T. Quinn, J.D. Lambeth and K.K. Griendling (2004). "Distinct subcellular localization of Nox1 and Nox4 in vascular smooth muscle cells." *Arterioscler Thromb Vasc Biol* **24**(4):677-83.

Huang, A., D. Sun, E.G. Shesely, E.M. Levee, A. Koller and G. Kaley (2002). "Neuronal NOS-dependent dilation to flow in coronary arteries of male eNOS-KO mice." *Am J Physiol Heart Circ Physiol* **282**(2):H429-36.

Huang, Z., S. Shiva, D.B. Kim-Shapiro, R.P. Patel, L.A. Ringwood, C.E. Irby, K.T. Huang, C. Ho, N. Hogg, A.N. Schechter and M.T. Gladwing (2005). "Enzymatic function of hemoglobin as a nitrite reductase that produces NO under allosteric control." *J Clin Invest* **115**(8):2099-107.

Jacke, K., K. Witte, L. Huser, S. Behrends and B. Lemmer (2000). "Contribution of the renin-angiotensin system to subsensitivity of soluble guanylyl cyclase in TGR(mREN2)27 rats." *Eur J Pharmacol* **403**(1-2):27-35.

Jeffers, A., X. Xu, K.T. Huang, M. Cho, N. Hogg, R.P. Patel and D.B. Kim-Shapiro (2005). "Hemoglobin mediated nitrite activation of soluble guanylyl cyclase." *Comp Biochem Physiol A Mol Integr Physiol* **142**(2):130-5.

Johsi, M.S., T.B. Ferguson Jr., T.H. Han, D.R. Hyduke, J.C. Liao, T. Rassaf, N. Bryan, M. Feelisch and J.R. Lancaster (2002). "Nitric oxide is consumed, rather than conserved, by reaction with oxyhemoglobin under physiological conditions." *Proc Natl Acad Sci USA* **99**(16):10341-6.

Joint National Committee on Prevention, Detection, Evaluation, and Treatment of High Blood Pressure (1997). "The Sixth Report of the Joint National Committee on Prevention, Detection, Evaluation, and Treatment of High Blood Pressure (JNC VI)." *Arch Intern Med* **157**(21):2413-46.

Juhlin-Dannfelt, A.M., M Frisk-Holmberg, J. Karlsson and P. Tesch (1979). "Central and peripheral circulation in relation to muscle-fibre composition in normo- and hyper-tensive man." *Clin Sci (Lond)* **56**(4):335-40.

Kabouridis, P.S. (2006). "Lipid rafts in T cell receptor signaling." *Mol Membr Biol* **23**(1):49-57.

Kähler , J., S. Mendel, J. Weckmuller, H.D. Orzechowski, C. Mittmann, R. Koster, M. Paul, T. Meinertz and T. Münzel (2000). "Oxidative stress increases synthesis of big endothelin-1 by activation of the endothelin-1 promoter." *J Mol Cell Cardiol* **32**(8):1429-37.

Kähler, J., A. Ewert, J. Weckmuller, S. Stobbe, C. Mittmann, R. Koster, M. Paul, T. Meinertz and T. Münzel (2001). "Oxidative stress increases endothelin-1 synthesis in human coronary artery smooth muscle cells." *J Cardiovasc Pharmacol* **38**(1):49-57.

Kashiwagi, S., M. Kajimura, Y. Yoshimura and M. Suematsu (2002). "Nonendothelial source of nitric oxide in arterioles but not in venules: alternative source revealed in vivo by diaminofluorescein microfluorography." *Circ Res* **91**(12):e55-e64.

Katusic, Z.S. (2001). "Vascular endothelial dysfunction: does tetrahydrobiopterin play a role?" *Am J Physiol Heart Circ Physiol* **281**(3)H981-6.Kiefer, F.N., H. Misteli, N. Kalak, K. Tschudin, J. Fingerle, M. Van der Kooij, M. Stumm, L.T. Sumanovski,

C.C. Sieber and E.J. Battegay (2002). "Inhibition of NO biosynthesis, but not elevated blood pressure, reduces angiogenesis in rat models of secondary hypertension." *Blood Press* **11**(2):116-24.

Kim, D., S.D. Rybalkin, X. Pi, Y. Wang, C. Zhang, T. Münzel, J.A. Beavo, B.C. Berk and C. Yan (2001). "Upregulation of phosphodiesterase 1A1 expression is associated with the development of nitrate intolerance." *Circulation* **104**(19):2338-43.

Kleinbongard, P., R. Schulz, T. Rassaf, T. Lauer, A. Dejam, T. Jax, I. Kumara, P. Gharini, S. Kabanova, B. Ozuyaman, H.G. Schnurch, A. Godecke, A.A. Weber, M. Robeneck, H. Robeneck, W. Bloch, P. Rosen and M. Kelm (2006). "Red blood cells express a functional endothelial nitric oxide synthase." *Blood* **107**(7):2943-51.

Klöss, S., A. Bouloumié and A. Mülsch (2000). "Aging and chronic hypertension decrease expression of rat soluble guanylyl cyclase." *Hypertension* **35**(1 Pt 1):43-7.

Kobzik, L., M.B. Reid, D.S. Bredt and J.S. Stamler (1994). "Nitric oxide in skeletal muscle." *Nature* **372**(6506):546-8.

Kollau, A., A. Hofer, M. Russwurm, D. Koesling, W.M. Kueng, K. Schmidt, F. Brunner and B. Mayer (2005). "Contribution of aldehyde dehydrogenase to mitochondrial bioactivation of nitroglycerin: evidence for the activation of purified soluble guanylate cyclase through direct formation of nitric oxide." *Biochem J* **385**(Pt 3): 769-77.

Kone, B.C., T. Kuncewicz, W. Zhang, and Z.Y. Yu (2003). "Protein interactions with nitric oxide synthases: controlling the right time, the right place, and the right amount of nitric oxide." *Am J Physiol Renal Physiol* **285**(2):F178-90.

Krogh, A. (1919). "The supply of oxygen to the tissues and the regulation of the capillary circulation." *J Physiol* **52**(6):457-74.

Lacza, Z., E. Pankotai, A. Csordás, D. Geroö, L. Kiss, E.M. Horváth, M. Kollai, D.W. Busija and C. Szabó (2006). "Mitochondrial NO and reactive nitrogen species production: does mtNOS exist?" *Nitric Oxide* **14**(2):162-8.

LaFramboise, W.A., M.J. Daood, R.D. Guthrie, P. Moretti, S. Schiaffino and M. Ontell (1990). "Electrophoretic separation and immunological identification of type 2X myosin heavy chain in rat skeletal muscle." *Biochim Biophys Acta* **1035**(1):109-12.

Lancaster, J.R. Jr. (1994). "Simulation of the diffusion and reaction of endogenously produced nitric oxide." *Proc Natl Acad Sci USA* **91**(17):8137-41.

Landmesser, U. and H. Drexler (2005). "The clinical significance of endothelial dysfunction." *Curr Opin Cardiol* **20**(6):547-51.

Lane, P. and S.S. Gross (2002). "Nitric oxide: promiscuous and duplicitous." Science and Medicine

Lassègue, B. and R.E. Clempus (2003). "Vascular NAD(P)H oxidases: specific features, expression, and regulation." *Am J Physiol Regul Integr Comp Physiol* **285**(2):R277-97.

Lee, P.C., A.N. Salyapongse, G.A. Bragdon, L.L. Shears 2nd, S.C. Watkins, H.D. Edington and T. R. Billiar (1999). "Impaired wound healing and angiogenesis in eNOS-deficient mice." *Am J Physiol* **277**(4 Pt 2):H1600-8.

Lefer, A.M. and X.L. Ma (1993). "Cytokines and growth factors in endothelial dysfunction." *Crit Care Med* **21**(2 Suppl):S9-14.

Lewis, D.M.A., A.J. Levi, P. Brooksby and J.V. Jones (1994). "A faster twitch contraction of soleus in the spontaneously hypertensive rat is partly due to changed fibre type composition." *Exp Physiol* **79**(3):377-86.

Li, J.M. and A.M. Shah (2001). "Differential NADPH- versus NADH-dependent superoxide production by phagocyte-type endothelial cell NADPH oxidase." *Cardiovasc Res* **52**(3):477-86.

Li, P.L. and E. Gulbins (2007a). "Lipid rafts and redox signaling." *Antioxid Redox Signal* 9(9):1411-15.

Li, P.L., Y. Zhang and F. Yi (2007b). "Lipid raft redox signaling platforms in endothelial dysfunction." *Antioxid Redox Signal* 9(9):1457-70.

López-Farré, A., J.A. Rodriguez-Feo, E. García-Colis, J. Gomez, A. López-Blaya, J. Fortes, R. de Andrés, L. Rico and S. Casado (2002). "Reduction of the soluble cyclic GMP vasorelaxing system in the vascular wall of stroke-prone spontaneously hypertensive rats: effect of the alpha1 – receptor blocker doxazosin." *J Hypertens* **20**(3):463-70.

Lum, H. and K.A. Roebuck (2001). "Oxidant stress and endothelial cell dysfunction." *Am J Physiol Cell Physiol* **280**(4):C719-41.

Madge, L.A. and J.S. Pober (2001). "TNF signaling in vascular endothelial cells." *Exp Mol Pathol* **70**(3):317-25.

Magee, A.I. and I. Parmryd (2003). "Detergent-resistant membranes and the protein composition of lipid rafts." *Genome Biol* **4**(11):234.

Maier, W., F. Cosentino, R. Lutolf, M. Fleisch, C. Seiler, O.M. Hess, B. Meier and T.F. Lüscher (2000). "Tetrahydrobiopterin improves endothelial function in patients with coronary artery disease." *J Cardiovasc Pharmacol* **35**(2):173-8.

Makino, N., T. Maeda, M. Sugano, S. Satoh, R. Watanabe and N. Abe (2005). "High serum TNF-alpha level in Type 2 diabetic patients with microangiopathy is associated with eNOS down-regulation and apoptosis in endothelial cells." *J Diabetes Complications* **19**(6):347-55.

Malinsky, T., M. Kapturczak, J. Dayharsh and D. Bohr (1993). "Nitric oxide synthase activity in genetic hypertension." *Biochem Biophys Res Commun* **194**:654-8.

Mantovani, A., F. Bussolino and E. Dejana (1992). "Cytokine regulation of endothelial cell function." *FASEB Journal* **6**(8):2591-9.

Marson, B. (2008). "eNOS polymorphisms in hypertension." *Clin Chim Acta* **390**(1-2):161.

McDonald, K.K., S. Zharikov, E.R. Block and M.S. Kilberg (1997). "A caveolar complex between the cationic amino acid transporter 1 and endothelial nitric-oxide synthase may explain the "arginine paradox." *J Biol Chem* **272**(50):31213-6.

McQuillan, L.P., G.K. Leung, P.A. Marsden, S.K. Kostyk and S. Kourembanas (1994). "Hypoxia inhibits expression of eNOS via transcriptional and posttranscriptional mechanisms." *Am J Physiol* **267**(5 Pt 2):H1921-7.

Mitchell, B.J., Z.P. Chen, T. Tiganis, D. Stapleton, F. Katsis, D.A. Power, A.T. Sim and B.E. Kemp (2001). "Coordinated control of endothelial nitric-oxide synthase phosphorylation by protein kinase C and the cAMP-dependent protein kinases." *J Biol Chem* **276**(21):17625-8.

Mohazzab, K.M., P.M. Kaminski and M.S. Wolin (1994). "NADH oxidoreductase is a major source of superoxide anion in bovine coronary artery endothelium." *Am J Physiol* **266**(6 Pt 2):H2568-72.

Mollnau, H., M. Wendt, K. Szocs, B. Lassègue, E. Schulz, M. Oelze, H. Li, M. Bodenschatz, M. August, A.L. Kleschyov, N. Tsilimingas, U. Walter, U. Forstermann, T. Meinertz, K. Griendling and T. Münzel (2002). "Effects of angiontensin II infusion on the expression and function of NAD(P)H oxidase and components of nitric oxide/cGMP signaling." *Circ Res* **90**(4):E58-65.

Morrissey, J.J., R. McCracken, H. Kaneto, M. Vehaskari, D. Montani and S. Klahr (1994). "Location of an inducible nitric oxide synthase mRNA in the normal kidney." *Kidney Int* **45**(4):998-1005.

Nava, E., N.P. Wiklund and F.J. Salazar (1996). "Changes in nitric oxide release in vivo in response to vasoactive substances." *Br J Pharmacol* **119**(6):1211-6.

Nava, E., A.L. Farré, C. Moreno, S. Casado, P. Moreau, F. Cosentino and T.F. Lüscher (1998). "Alterations to the nitric oxide pathway in the spontaneously hypertensive rat." *J Hypertens* **16**(5):609-15.

Ogura, T., Y. Yokoyama, H. Fujisawa, Y. Kurashima and H. Esumi (1993). "Structural diversity of neuronal nitric oxide synthase mRNA in the nervous system." *Biochem Biophys Res Commun* **193**(3):1014-22.

Pacher, P., J.S. Beckman and L. Liaudet (2007). "Nitric oxide and peroxynitrite in health and disease." *Physiol Rev* **87**(1):315-424.

Patschan, S., H. Li, S. Brodsky, D. Sullivan, D.A. Angelis, D. Patschan and M.S. Goligorsky (2006). "Probing lipid rafts with proximity imaging: actions of proatherogenic stimuli." *Am J Physiol Heart Circ Physiol* **290**(6):H2210-9.

Peter, J.B., R.J. Barnard, V.R. Edgerton, C.A. Gillespie and K.E. Stempel (1972). "Metabolic profiles of three fiber types of skeletal muscle in guinea pigs and rabbits." *Biochemistry* **11**(14):2627-33.

Pette, D. and R.S. Staron (1990). "Cellular and molecular diversities of mammalian skeletal muscle fibers." *Rev Physiol Biochem Pharmacol* **116**:1-76.

Plyley, M.J. and A.C. Groom (1975). "Geometrical distribution of capillaries in mammalian striated muscles." *Am J Physiol* **228**(5):1376-83.

Prasad V., R. Scotch, A.R. Chaudhuri, C. Walss, D.B. Fathy, C. Miller and R.F. Ludueña (2000). "Interactions of bovine brain tubulin with pyridostigmine bromide and N,N'-diethyl-m-toluamide." *Neurochem Res* **25**(1):19-25.

Prewitt, R.L., I.I.H. Chen and R. Dowell (1982). "Development of microvascular rarefaction in the spontaneously hypertensive rat." *Am J Physiol* **243**(2):H243-51.

Prickar, J.G., R.C. Carlsen, A. Atrakchi and S.D. Gray (1994). "Increased Na(+)-K+ pump number and decreased pump activity in soleus muscles in SHR." *Am J Physiol* **267**(3 Pt 1):C836-44.

Pritchard, K.A., A.W. Ackerman, J. Ou, M. Curtis, D.M. Smalley, J.T. Fontana, M.B. Stemerman and W.C. Sess (2002). "Native low-density lipoprotein induces endothelial nitric oxide synthase dysfunction: role of heat-shock protein 90 and caveolin-1." *Free Radic Biol Med* **33**(1):52-62.

Punkt, K., S. Zaitsev, J.K. Park, M. Wellner, I.B. Buchwalow (2001). "Nitric oxide synthase isoforms I, III and protein kinase-C theta in skeletal muscle fibres of normal and streptozotocin-induced diabetic rats with and without Ginkgo biloba extract treatment." *Histochem J* **33**(4):213-9.

Punkt, K., A. Naupert, M. Wellner, G. Asmussen, C. Schmidt and I.B. Buchwalow (2002). "Nitric oxide synthase II in rat skeletal muscles." *Histochem Cell Biol* **118**(5):371-9.

Punkt, K., M. Fritzsche, C. Stockmar, P. Hepp, C. Josten, M. Wellner, S. Schering and I.B. Buchwalow (2002). "Nitric oxide synthase in human skeletal muscles related to defined fibre types." *Histochem Cell Biol* **125**(5):567-73.

Rajagopalan, S., S. Kurz, T. Münzel, M. Tarpey, B.A. Freeman, K.K. Griendling and D.G. Harrison (1996). "Angiontension II-mediated hypertension in the rat increases vascular superoxide production via membrane NADH/NADPH oxidase activation. Contribution to alterations of vasomotor tone." *J Clin Invest* **97**(8):1916-23.

Reid, M.B. (1998). "Role of nitric oxide in skeletal muscle: synthesis, distribution and functional importance." *Acta Physiol Scand* **162**(3):401-9.

Roberts, C.K., R.J. Barnard, R.K. Sindhu, M. Jurczak, A. Ehdaie and N.D. Vaziri (2005). "A high-fat, refined-carbohydrate diet induces endothelial dysfunction and oxidant/antioxidant imbalance and depresses NOS protein expression." *J Appl Physiol* **98**(1):203-10.

Rocchini, A.P. (2000). "Obesity hypertension, salt sensitivity and insulin resistance." *Nutr Metab Cardiovasc Dis* **10**(5):287-94.

Romanul, F.C.A. (1974). "Enzymes in muscle. I. Histochemical studies of enzymes in muscle fibers." *Arch Neurol* **11**:355-68.

Rosenkranz-Weiss, P., W.C. Sessa, S. Milstien, S. Kaufman, C.A. Watson and J.S. Pober (1994). "Regulation of nitric oxide synthesis by proinflammatory cytokines in umbilical vein endothelial cells." *J Clin Invest* **93**(5):2236-43.

Rothe, F., K. Langnaese and G. Wolfe (2005). "New aspects of the location of neuronal nitric oxide synthase in the skeletal muscle: a light and electron microscopic study." *Nitric Oxide* **13**(1):21-35.

Roy, B. and J. Garthwaite (2006). Nitric oxide activation of guanylyl cylcase in cell revisited." *Proc Natl Acad Sci USA* **103**(32):12185-90.

Ruetten, H., U. Zabel, W. Linz and H.H. Schmidt (1999). "Downregulation of soluble guanylyl cyclase in young and aging spontaneously hypertensive rats." *Circ Res* **85**(6):534-41.

Russwurm, M., S. Behrends, C. Harteneck and D. Koesling (1998). "Functional properties of a naturally occurring isoform of soluble guanylate cyclase." *Biochem J* **335**(Pt 1):125-30.

Sabino, B., M.A. Lessa, A. R. Nascimento, C.A.B. Rodrigues, M.G. Henriques, L.R. Garzoni, B.I. Levy and E. Tibiriçá (2008). "Effects of antihypertensive drugs on capillary rarefaction in spontaneously hypertensive rates: intravital microscopy and histologic analysis." *J Cardiovasc Pharmacol* **51**(4):402-9.

Said, H.M., C. Hagerman, J. Stojic, B. Schoemig, G.H. Vince, M. Flentje, K. Roosen and D. Vordermark (2007). "GAPDH is not regulated in human glioblastoma under hypoxic conditions." *BMC Mol Biol* **8**:55.

Sandrim, V.C., E.B. Coelho, F. Nobre, G.M. Arado, V.L. Lanchote and J.E. Tanus-Santos (2006). "Susceptible and protective eNOS haplotypes in hypertensive black and white subjects." *Atherosclerosis* **186**(2):428-32.

Sangrajrang, S., P. Denoulet, N.M. Laing, R. Tatoud, G. Millot, F. Calvo, K.D. Tew and A. Fellous (1998). "Association of estramustine resistance in human prostatic carcinoma cells with modified patterns of tubulin expression." *Biochem Pharmacol* **55**(3):325-31.

Sarafidis, P.A. and G.L. Bakris (2007). "Insulin and endothelium: an interplay contributing to hypertension development?" *J Clin Endocrinol Metab* **92**(2):379-85.

Schiaffino, S., L. Saggin, A. Viel and L. Gorza (1985). "Differentiation of fibre types in rat skeletal muscle visualized with monoclonal antimyosin antibodies." *J Muscle Res Cell Motil* **6**:60-1.

Schiaffino, S., S. Ausoni, L. Gorza, L. Saggin, K. Gundersen and T. Lømo (1988). "Myosin heavy chain isoforms and velocity of shortening of type 2 skeletal muscle fibres." *Acta Physiol Scand* **134**(4):575-6.

Schillaci, G., M. Pirro, G. Vaudo, F. Gemelli, S. Marchesi, C. Porcellati and E. Mannarineo (2004). "Prognostic value of the metabolic syndrome in essential hypertension." *J Am Coll Cardiol* **43**(10):1817-22.

Schulman, S.P., L.C. Becker, D.A. Kass, H.C. Champion, M.L. Terrin, S. Forman, K.V. Ernst, M.D. Kelemen, S.N. Townsend, A. Capriotti, J.M. Hare and G. Gerstenblith (2007). L-arginine therapy in acute myocardial infarction: the Vascular Interaction With Age in Myocardial Infarction (VINTAGE MI) randomized clinical trial." **295**(1):58-64.

Schulz, E., T. Jansen, P. Wenzel, A. Daiber and T. Münzel (2008). "Nitric oxide, tetrahydrobiopterin, oxidative stress, and endothelial dysfunction in hypertension." *Antioxid Redox Signal* **10**(6):1115-26.

Segal, S.S., S.E. Brett and W.C. Sessa (1999). "Codistribution of NOS and caveolin throughout peripheral vasculature and skeletal muscle of hamsters." *Am J Physiol* **277**(3 Pt 2):H1167-77.

Seidel, J.C. (1967). "Studies on myosin from red and white skeletal muscles of the rabbit. II. Inactivation of myosin from red muscles under mild alkaline conditions." *J Biol Chem* **242**(23):5623-9.

Sessa, W.C., K. Pritchard, N. Seyedi, J. Wang and T.H. Hintze (1994). "Chronic exercise in dogs increases coronary vascular nitric oxide production and endothelial cell nitric oxide synthase gene expression." *Circ Res* **74**(2):349-53.

Shah, D.I. and M. Singh (2006). "Activation of protein kinase A improves vascular endothelial dysfunction." *Endothelium* **13**(4):267-77

Shakibaei, M., G. Schulze-Tanzil, Y. Takada and B.B. Aggarwal (2005). "Redox regulation of apoptosis by members of the TNF superfamily." *Antioxid Redox Signal* **7**(3-4):482-96.

Shin, S., S. Mohan and H.L. Fung (2011). "Intracellular L-arginine concentration does not determine NO production in endothelial cells: implications on the "L-arginine paradox." **414**(4):660-3.

Shiva, S., Z. Huang, R. Grubina, J. Sun, L.A. Ringwood, P.H. MacArthur, X. Xu, E. Murphy, V.M. Darley-Usmar and M.T. Gladwin (2007). "Deoxyhemoglobin is a nitrite reductase that generates nitric oxide and regulates mitochondrial respiration." *Circ Res* **100**(5):654-61.

Sibmooh, N., B. Piknova, F. Rizzatti and A.N. Schechter (2007). "Nitrite generation in human erythrocytes from NO derivatives of hemoglobin by dehydroascorbic acid: Abstracts of Second International Meeting of the Role of Nitrite in Physiology." *Pathophysiol Therapeut* 69.

Silva, H.S., A. Kapela and N.M. Tsoukias (2007). "A mathematical model of plasma membrane electrophysiology and calcium dynamics in vascular endothelial cells." *Am J Physiol Cell Physiol* **293**(1):C277-93.

Silvagno, F., H. Xia and D.S. Bredt (1996). "Neuronal nitric-oxide synthase-mu, an alternatively spliced isoform expressed in differentiated skeletal muscle." *J Biol Chem* **271**(19):11204-8.

Simons, K. and E. Ikonen (1997). "Functional rafts in cell membranes." Nature **387**(6633):569-72.

Simons, K. and D. Toomre (2000). "Lipid rafts and signal transduction." *Nat Rev Mol Cell Biol* **1**(1):31-9.

Singel, D.J. and J.S. Stamler (2004). "Blood traffic control." *Nature* **430**(6997):297.

Singh, U., S. Devaraj, J. Vasquez-Vivar and I. Jialal (2007). "C-reactive protein decreases endothelial nitric oxide synthase activity via uncoupling." *J Mol Cell Cardiol* **43**(6):780-91.

Sjøgaard G. (1982). "Capillary supply and cross-sectional area of slow and fast twitch muscle fibres in man." *Histochemistry* **76**(4):547-55.

Skalak, T.C. and G.W. Schmid-Schöbein (1986). "The microvasculature in skeletal muscle. IV. A model of the capillary network." *Microvasc Res* 32(3):333-47

Smith, L.N., R.W. Barbee, K.R. Ward and R.N. Pittman (2004). "Prolonged tissue PO_2 reduction after contraction in spinotrapezius muscle of hypertensive rats." *Am J Physiol Heart Circ Physiol* **287**(1):H401-7.

Sonveaux, P., I.I. Lobysheva, O. Feron and T.J. McMahon (2006). "Transport and peripheral bioactivities of nitric oxides carried by red blood cell hemoglobin: role in oxygen delivery." *Physiology* Apr;**22**:97-112.

Sowers, J.R. (2004). "Insulin resistance and hypertension." *Am J Physiol Heart Circ Physiol* **286**(5):H1597-602.

Sréter, F.A., J.C. Seidel and J. Gergely (1966). "Studies on myosin from red and white skeletal muscles of the rabbit. I. Adenosine triphosphatase activity." *J Biol Chem* **241**(24):5772-6.

Srivastava, K., R. Narang, V. Sreenivas, S. Das, and N. Das (2008). "Association of eNOS Glu298Asp gene polymorphism with essential hypertension in Asian Indians." *Clin Chim Acta* **387**(1-2):80-3.

Stamler, J.S. and G. Meissner (2001). "Physiology of nitric oxide in skeletal muscle." *Physiological Reviews* **81**(1):209-37.

Stan, R.V. (2002). "Structure and function of endothelial caveolae." *Microvasc Res Tech* **57**(5):350-64.

Stone, J.R. and M.A. Marletta (1996). "Spectral and kinetic studies on the activation of soluble guanylate cyclase by nitric oxide." *Biochemistry* **35**(4):1093-9.

Stroes, E., J. Kastelein, F. Cosentino, D.W. Erkelens, R. Wever, H.A. Koomans, T. Lüscher and T. Rabelink (1997). "Tetrahydrobiopterin restores endothelial function in hypercholesterolemia." *J Clin Invest* **99**(1):41-6.

Su, Y., S. Edwards-Bennett, M.R. Bubb and E.R. Block (2003). "Regulation of endothelial nitric oxide synthase by the actin cytoskeleton." *Am J Physiol Cell Physiol* **284**(6):C1542-9.

Sullivan, S.M. and R.N. Pittman (1984). "In vitro O2 uptake and histochemical fiber type of resting hamster muscles. *J Apply Physiol* **57**(1):246-53.

Sunano, S., Z. Li-Bo, K. Matsuda, F. Sekiguchi, H. Wantanabe and K. Shimamura (1996). "Endothelium-dependent relaxation by alpha 2-adrenoceptor agonists in spontaneously hypertensive rat aorta." *J Cardiovasc Pharmacol* **27**(5):733-9.

Takanaka, T., H. Forster, A. De Micheli and M. Epstein (1992). "Impaired myogenic responsiveness of renal microvessels in Dahl salt-sensitive rats." *Circ Res* **71**(2):471-80.

Talmadge,T. and R.R. Roy (1993). "Electrophoretic separation of rat skeletal muscle myosin heavy-chain isoforms." *J Appl Physiol* **75**(5):2337-40.

Talukder, M.A.,T. Fujiki, K. Morikawa, M. Motoishi, H. Kubota, T. Morishita, M. Tsutsui, A. Takeshita and H. Shimokawa (2004). "Up-regulated neuronal nitric oxide synthase compensates coronary flow response to bradykinin in endothelial nitric oxide synthase-deficient mice." *J Cardiovasc Pharmacol* **44**(4):437-45.

Termin, A., R.S. Staron and D. Pette (1989). "Myosin heavy chain isoforms in histochemically defined fiber types of rat muscle." *Histochemistry* **92**(6):453-7.

Tesauro, M., W.C. Thompson, P. Rogliani, L. Qi, P.P. Chaudhary and J. Moss (2000). "Intracellular processing of endothelial nitric oxide synthase isoforms associated with differences in severity of cardiopulmonary diseases: cleavage of proteins with aspartate vs. glutamate at position 298." *Proc Natl Acad Sci USA* **97**(6):2832-5.

Thomson, L., M. Trujillo, R. Telleri and R. Radi (1995). "Kinetics of cytochrome c2+ oxidation by peroxynitrite: implications for superoxide measurements in nitric oxide-producing biological systems." *Arch Biochem Biophys* **319**(2):491-7.

Thöny, B., G. Auerbach and N. Blau (2000). "Tetrahydrobiopterin biosynthesis, regeneration and functions." *Biochem* **347**(Pt 1:1-16):9220-5.

Tiefenbacher, C.P. (2001). "Tetrahydrobiopterin: a critical cofactor for eNOS and a strategy in the treatment of endothelial dysfunction?" *Am J Physiol Heart Circ Physiol* **280**(6):H2484-8.

Topal, G., A. Brunet, L. Walch, J.L. Boucher, M. David-Dufilho (2007). "Mitochondrial arginase II modulates nitric-oxide synthesis through nonfreely exchangeable L-arginine pools in human endothelial cells." *J Pharmacol Exp Ther* **318**(3):1368-74.

Tsoukias, N.M., M. Kavdia and A.S. Popel (2004). "A theoretical model of nitric oxide transport in arterioles: frequency- vs. amplitude-dependent control of cGMP formation." *Am J Physiol Heart Circ Physiol* **286**(3):H1043-56.

Ushio-Fukai, M. and R.W. Alexander (2004). "Reactive oxygen species as mediators of angiogensis signaling: role of NAD(P)H oxidase." *Mol Cell Biochem* **264**(1-2):85-97.

Uwabo, J., M. Soma, T. Nakayama and K. Kanmatsuse (2000). "Association of a variable number of tandem repeats in the endothelial constitutive nitric oxide synthase gene with essential hypertension in Japanese." *Am J Hypertens* **11**(1 Pt 1):125-8.

Van de Poll, M.C.G., M.P.C. Siroen, P.A.M. van Leeuwen, P.B. Soeters, G.C. Melis, P.G. Boelens, N.E.P. Deutz and C.H.C. Dejong (2007). "Interorgan amino acid exchange in humans: consequences for arginine and citrulline metabolism." *Am J Clin Nutr* **85**(1):167-72.

Vasan, R., J.C. Evans, M.G. Larson, P.W.F. Wilson, J.B. Meigs, N. Rifai, E.J. Benjamin and D. Levy (2004). "Serum aldosterone and the incidence of hypertension in nonhypertensive persons." *N Eng J Med* **351**(1):33-41.

Vásquez-Vivar, J., B. Kalyanaraman, P. Martásek, N. Hogg, B.S. Masters, H. Karoui, P. Tordo and K.A. Pritchard Jr. (1998). "Superoxide generation by endothelial nitric oxide synthase: the influence of cofactors." *Proc Natl Acad Sci USA* **95**(16):9220-5.

Villanueva, C. and C. Giulivi (2010). "Subcellular and cellular locations of nitric oxide synthase isoforms as determinants of health and disease." *Free Radic Biol Med* **49**(3):307-16.

Wang, H.D., P.J. Pagano, Y. Du, A.J. Cayatte, M.T. Quinn, P. Brecher and R.A. Cohen (1998). "Superoxide anion from the adventitia of the rat thoracic aorta inactivates nitric oxide." *Circ Res* **82**(7):810-8.

Whitsett, J.A., J.C. Clark, J.R. Wispe and G.S. Pryhuber (1992). "Effects of TNF-alpha and phorbol ester on human surfactant protein and MnSOD gene transcription in vitro." *Am J Physiol* **262**(6 Pt 1):L688-93.

Witte, K., K. Jacke, R. Stahrenberg, G. Arlt, I. Reitenbach, L. Schilling and B. Lemmer (2002). "Dysfunction of soluble guanylyl cyclase in aorta and kidney of Goto-Kakizaki rats: influence of age and diabetic state." *Nitric Oxide* **6**(1):85-95.

World Health Organizaton (1999). "Definition, diagnosis and classification of diabetes mellitus and its complication. Part I: Diagnosis and classification of diabetes mellitus." *World Health Organization*, Geneva.

Wu G. and S.M. Morris Jr. (1998). "Arginine metabolism: nitric oxide and beyond." *Biochem J* **336**(Pt 1):1-17.

www.americanheart.org/presenter.jhtml?identifier=2114 – last accessed June 4, 2008

Xia, Y. and J.L. Zweier (1997). "Direct measurement of nitric oxide generation from nitric oxide synthase." *Proc Natl Acad Sci USA* **94**(23):12705-10.

Yanai, H., Y. Tomono, K. Ito, N. Furutani, H. Yoshida and N. Tada (2008). "The underlying mechanisms for development of hypertension in the metabolic syndrome." *Nutr J* Apr **17**;7:10.

Yang, B., T.N. Oo and V. Rizzo (2006). "Lipid rafts mediate H2O2 prosurvival effects in cultured endothelial cells." *FASEB J* **20**(9):1501-3.

Zani, B.G. and H.G. Bohlen (2005). "Transport of extracellular l-arginine via cationic amino acid transporter is required during in vivo endothelial nitric oxide production." *Am J Physiol Heart Circ Physiol* **289**(4):H1381-90.

Zhang, A.Y., F. Yi, G. Zhang, E. Gulbins and P.L. Li (2006). "Lipid raft clustering and redox signaling platform in coronary arterial endothelial cells." *Hypertension* **47**(1):74-80.

Zhang, D.X., A.P. Zou and P.L. Li (2003). "Ceramide-induced activation of NADPH oxidase and endothelial dysfunction in small coronary arteries." *Am J Physiol Heart Circ Physiol* **284**(2):H605-12.

Zhang, D.X., F.X. Yi, A.P. Zou and P.L. Li (2002). "Role of ceramide in TNF-alpha-induced impairment of endothelium-dependent vasorelaxation in coronary arteries." *Am J Physiol Heart Circ Physiol* **283**(5):H1785-94.

Zhang, J., J.M. Patel, Y.D. Li and E.R. Block (1997). "Proinflammatory cytokines downregulate gene expression and activity of constitutive nitric oxide synthase in porcine pulmonary artery endothelial cells." *Res Commun Mol Pathol Pharmacol* **96**(1):71-87.

Zhao, Y., P.E. Brandish, D.P. Ballou and M.A. Marletta (1999). "A molecular basis for nitric oxide sensing by soluble guanylate cyclase." *Proc Natl Acad Sci USA* **96**(26):14753-8.

Zharikov, S.I. and E.R. Block (1998). "Characterization of L-arginine uptake by plasma membrane vesicles isolated from cultured pulmonary artery endothelial cells." *Biochim Biophys Acta* **1369**(1):173-83.

Zou, M.H., C. Shi and R.A. Cohen (2002). "Oxidation of the zinc-thiolate complex and uncoupling of endothelial nitric oxide synthase by peroxynitrite." *J Clin Invest* **109**(6):817-26.

Zuo, L., M. Ushio-Fukai, S. Ikeda, L. Hilenski, N. Patrushev and R.W. Alexander (2005). "Caveolin-1 is essential for activation of Rac1 and NAD(P)H oxidase after angiotensin II type I receptor stimulation in vascular smooth muscle cells: role in redox signaling and vascular hypertrophy." *Arterioscler Thromb Vasc Biol* **25**(9):1824-30.

Zweier, J.L., A. Samouilov and P. Kuppusamy (1999). "Non-enzymatic nitric oxide synthesis in biological systems." *Biochim Biophys Acta* **1411**(2-3):250-62.

APPENDIX A

Image Grading Instruction Sheet

Name:_____

IMAGE GRADING INSRUCTIONS

- There are three (3) practice slides and 14 experimental slides.
- Total time to grade all slides, including the practice slides, should be about 30 minutes. Although you may take as much time as you require, please try to grade all slides in ~30 minutes.
- You can advance to a new slide or review a previous slide by clicking the "**I<**" and "**>I**" buttons. ***DO NOT*** use the scrolling wheel on the mouse! This will change the image size and magnification.
- Grade *only* fibers that have a corresponding line on that slide's score sheet.

For example:

Slide 3

0 = absent 1 = light 2 = intermediate 3 = dark

Fiber #	NOS1 Staining Grade			
1	0	1	2	3
2	0	1	2	3
3	0	1	2	3
4	0	1	2	3
5	0	1	2	3
7	0	1	2	3

**Note the gap between fiber #5 and #7!

- You may change your staining grade for any fiber at any time.
- If you cannot determine a particular fiber's boundary, please do not hesitate to ask for assistance.

- All images have been filtered, processed and equalized; however, *DO NOT compare slides to one another.* Grade fibers based on what you see *just in that slide.*

- Consider the *entire fiber* when deciding on a staining score.

APPENDIX B

Mean NOS 1 / Type I Fiber Numeric Staining Scores by Observer in Practice (WKY) subjects ($\alpha = 0.05$). The means were compared using the unequal variance *F*-test and not found to be significantly different. [($F(6, 34.1) = 1.55$, *p*-value = 0.19)

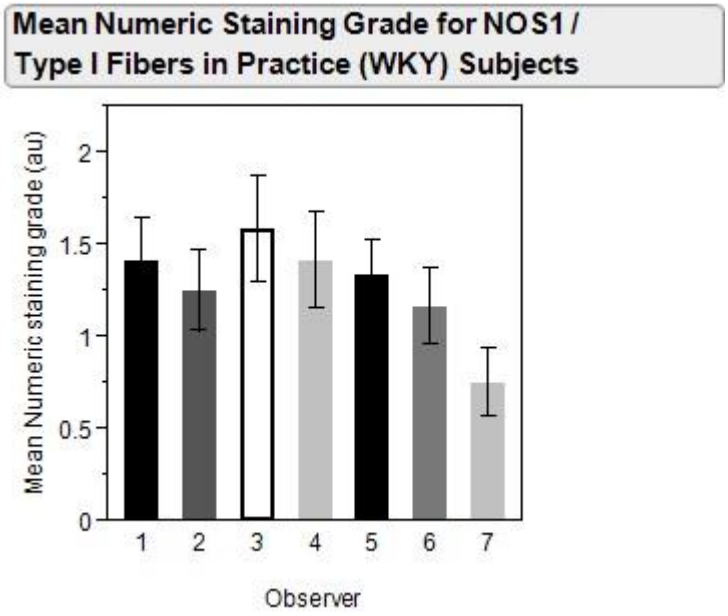

APPENDIX C

Summary Statistics for Practice Numeric Staining Grades

Observer	Number of Fibers Graded	Mean Score ± SE
1	12	1.42 ± 0.23
2	12	1.25 ± 0.22
3	12	1.58 ± 0.29
4	12	1.42 ± 0.26
5	12	1.33 ± 0.19
6	12	1.17 ± 0.21
7	12	0.75 ± 0.18

No statistically significant differences between observers' scores was detected ($\alpha = 0.05$).

VITA

Andrew T. Yannaccone was born on February 19th, 1979 in Lewisburg, Pennsylvania, USA. He is a U.S. citizen. After graduating from Warrior Run High School in 1997, he attended College Misericordia (now Misericordia University), graduating in May 2002 with a Bachelor of Science in Health Science and Master of Science in Physical Therapy.

After passing the National Physical Therapy Examination in July of 2002, Andrew practiced full-time as a staff physical therapist in acute and sub-acute rehabilitation settings until August of 2006 when he enrolled in the Doctor of Philosophy Program in Physiology at Virginia Commonwealth University, School of Medicine.

Upon completion of his degree, Andrew will join the Department of Physical Therapy in the College of Health Professions and Social Work at Temple University in Philadelphia, Pennsylvania as an Assistant Professor.